JARÐFEINGI
FAROESE GEOLOGICAL SURVEY

The high-resolution marine seismic survey 2020

The Suðuroyar subsea tunnel: Seismic processing report

Report to Landsverk

Uni K. Petersen

December 2020

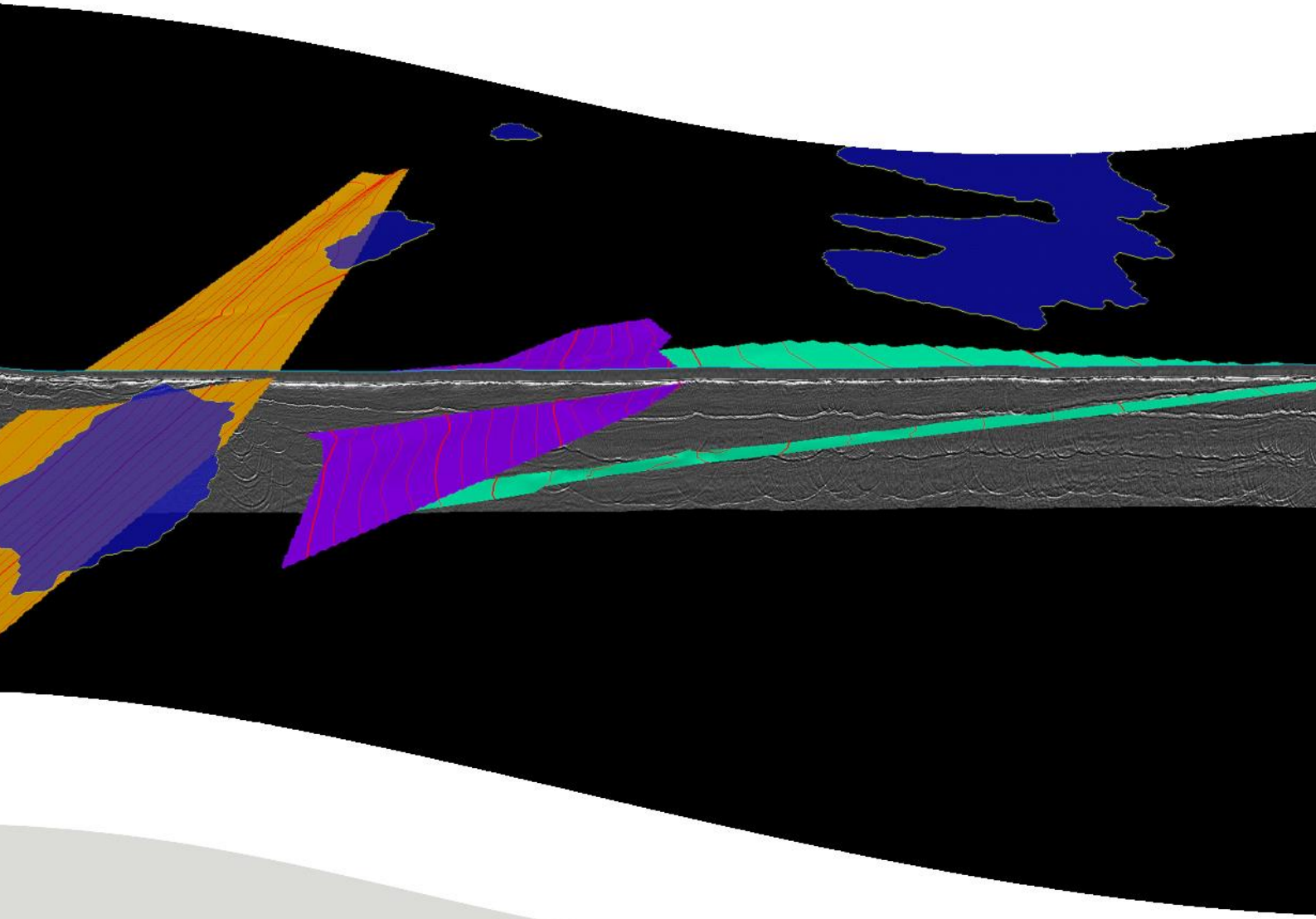

JF-J-2020-13

Table of Contents

Introduction

This report documents the analysis and processing of the high-resolution marine seismic data acquired in connection with the planning of the Suðuroyar tunnel. The survey utilizes the same method that was used in the planning of the Skálafjarðar and Sandoy subsea tunnels (Petersen, 2015, 2016).

As part of the preparation of the Skálafjarðar and Sandoy subsea tunnels, high-resolution marine seismic data were acquired with a 600 m long streamer and with airgun source. Refraction seismic velocity analysis was used to obtain a detailed velocity model of the subsurface, and processing to stacked seismic profiles generated profiles for interpretation of layering.

The seismic profiles provided means for tying geology at different locations, from onshore observations and information from drillholes, and extrapolate these across the entire profile of the tunnel. Especially, the ties between locations situated on different islands were of great importance. Furthermore, the reflection seismic profiles clearly imaged the sedimentary basin in Tangafjørð, and with the very good constraint on the velocities obtained, it was possible to give a good estimate of the depth to the bedrock, placing it higher than previously estimated. This resulted in that the final outline of the tunnel was shallower than initially planned in Tangafjørð thus resulting in a shorter tunnel. The initial deepest point at 220 m depth was reduced to 189 m depth making it 31 m shallower, and this allowed the total length of the tunnel to be shortened by 600 m.

The planning of the seismic survey for the Suðuroyartunnel started early in 2020. It was planned to take place in the summer and arrangements were made with Aarhus University and Havstovan regarding equipment and research vessel. Tidal current is a severe problem in the Suðuroyarfjørð area considering the 600 m long streamer. Therefore, the only time possible to perform the acquisition was during 13 – 15 July since this was the only time during the summer with very week tidal current. The acquisition went very well with perfect weather conditions, resulting in high quality data very well suited for the analysis and processing.

This report marks the completion of the analysis and processing of the data. The stacked profiles produce good images of the basalts down to the first seabed multiple. A few strong reflections can even be interpreted below the first seabed multiple. Furthermore, the data show an unexpected relatively deep sedimentary basin between Sandoy and Skúvoy. The velocity models from refraction seismic velocity analysis give detailed velocity information in the uppermost about 100 m below seabed.

Acquisition

Acquisition setup

Navigation System Details

Software:	NaviPac ver 4.2.3
Datum:	WGS84
Projection:	UTM north, Zone 29

Recording System Details

System Type:	Geometrics GeoEel controller ver 5.844
Highcut filter:	anti-alias
Low Cut:	Out
Sample rate:	1 ms
Record length:	3 sec
Reference point:	Midship transom
GPS antenna x position:	2.6 m
GPS antenna y position:	21 m
Airgun tow-point x:	2.6 m (SB)
Airgun tow-point y:	0 m
Airgun tow-length:	-32 m
Streamer tow-point x:	-2.6 m (PS)
Streamer tow-point y:	0 m
Streamer tow-length:	-52 m
Nearfield hydrophone:	Aux 2
Data format:	Seg-D
Byte position of navigation:	starts at 142. Airgun x, y at 148, 158.

Energy Source Details

Source type:	Sercel GI Gun
Source size:	45 cu. in.
Source depth:	3 m
Air pressure:	120 bar
Source firing delay:	50 ms
Shot point interval:	12.5 m

Streamer Details

Streamer type:	Geometrics GeoEel
Hydrophone type:	Geopoint
Tow section:	30 m
Live section:	50 m
No. of live sections:	12
No. of channels/live section:	8
Channel interval:	6.25 m
Planned depth:	3 m
Stretch section:	25 m
Length from Tail GPS to last ch.:	25 m

Seismic profiles

The seismic profiles are planned such, that there is a threefold coverage with about 100 m offset along the current tunnel location for the Sandoy–Skúvoy leg and with about 200 m offset for the Skúvoy–Suðuroy leg. There are several crossing profiles. These have a direction that is preferably perpendicular to the strike of the basalt flows. This is to better distinguish coherent noise from primary signal. In addition, a few long profiles to aid the geological overview of the area were planned as a second priority.

Due to good planning of the acquisition sequence, and to very good conditions during acquisition, we managed to acquire all planned seismic profiles. Table 1 lists the seismic profiles and figures 1, 2, and 3 show the location of the seismic profiles.

Table 1. List of all seismic profiles. See Figure 1 for location.

Profiles	Velocity model	Comments
SUT2020_LinjaH	model04layer03a	Tunnel Sandoy–Skúvoy
SUT2020_LinjaB	model04layer03a	Tunnel Sandoy–Skúvoy
SUT2020_LinjaI	model04layer03a	Tunnel Sandoy–Skúvoy
SUT2020_LinjaK	model05	Tunnel Skúvoy–Suðuroy
SUT2020_LinjaJ	model05	Tunnel Skúvoy–Suðuroy
SUT2020_LinjaM	model05	Tunnel Skúvoy–Suðuroy
SUT2020_LinjaO1	model07layer04a	
SUT2020_LinjaU1	model05layer03a	
SUT2020_LinjaT1	model05	
SUT2020_LinjaS1	model05	
SUT2020_LinjaL	model05layer01a2	
SUT2020_LinjaA	model04	
SUT2020_LinjaC1	model04layer05edita	
SUT2020_LinjaD	model03layer06ba	
SUT2020_LinjaP	model04layer05a	
SUT2020_LinjaF	model05layer02a2	
SUT2020_LinjaG1	model09layer01a	
SUT2020_LinjaQ	model08layer01a2	
SUT2020_LinjaR	model04	

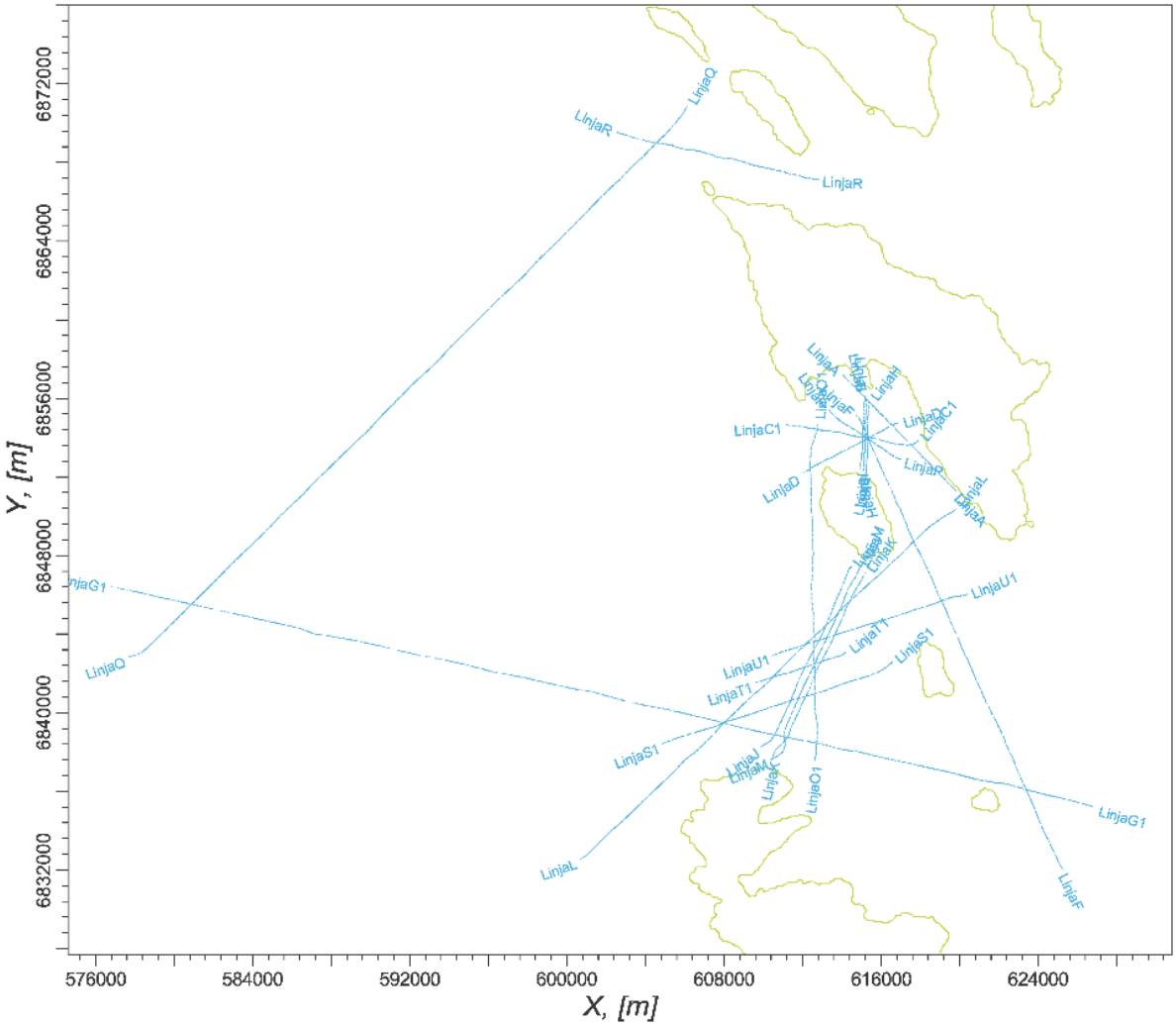

Figure 1. All seismic profiles with navigation of processed data. Coordinates are in WGS84, UTM29.

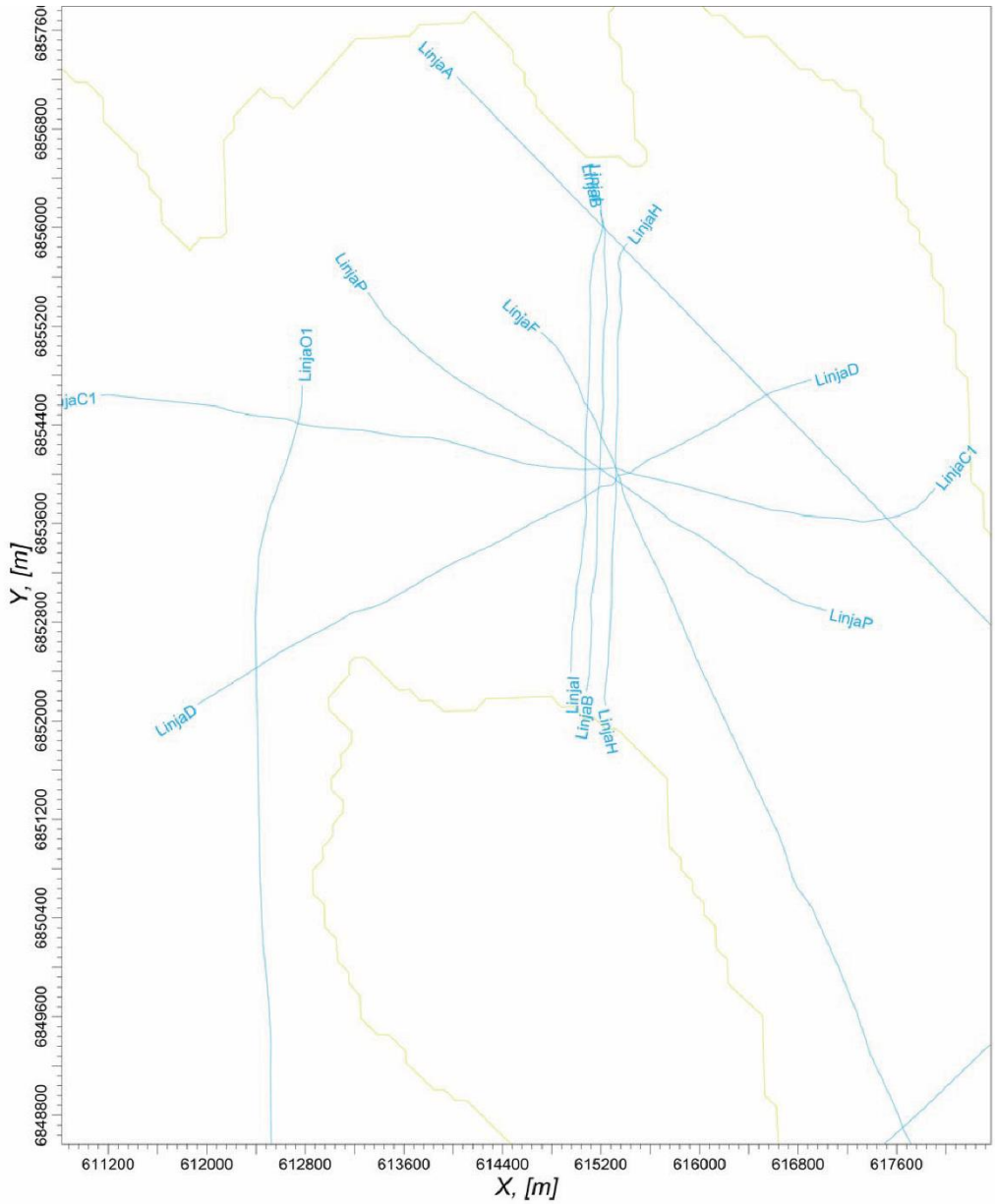

Figure 2. The seismic profiles between Sandoy and Skúvoy.

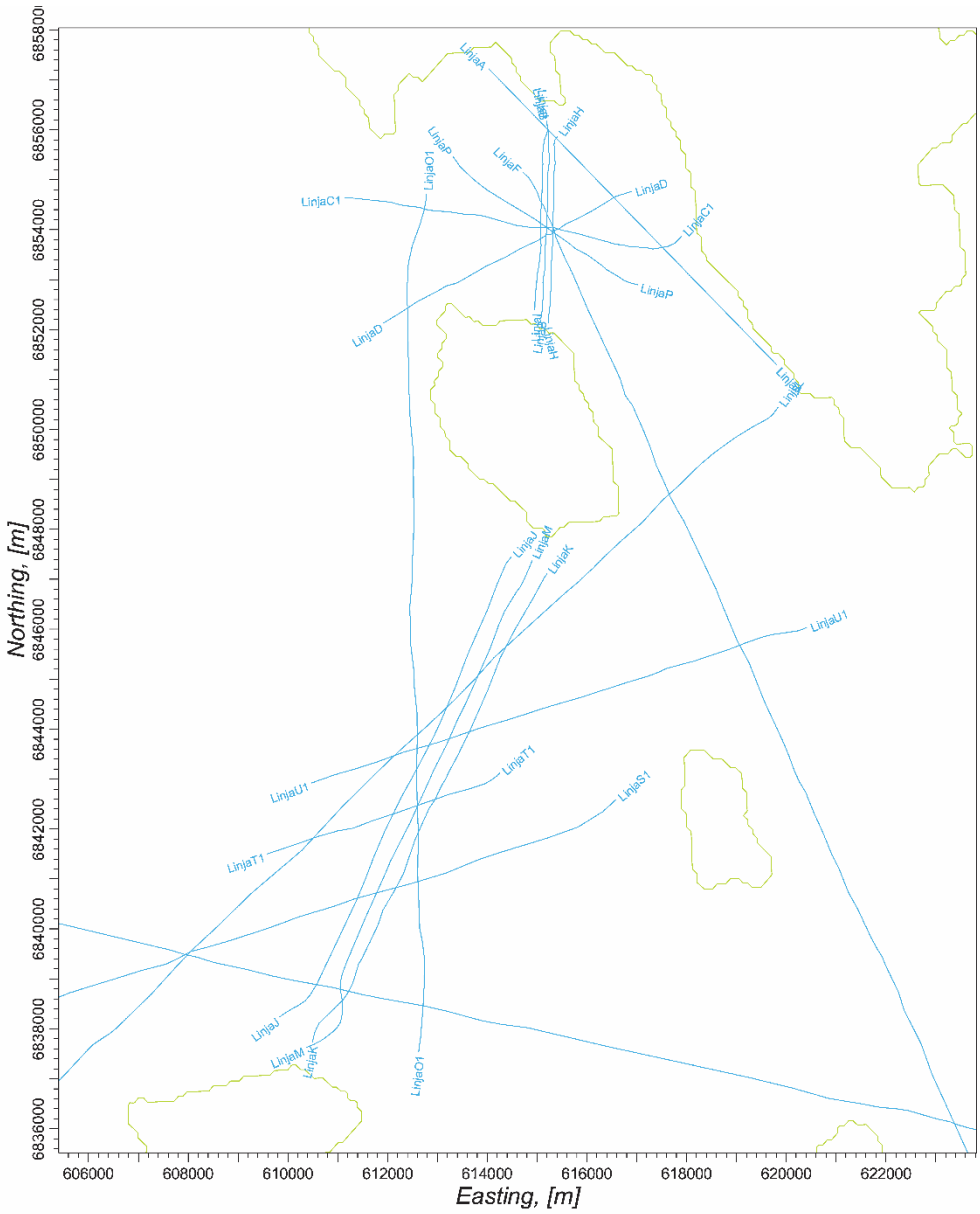

Figure 3. The seismic profiles between Suðuroy and Skúvoy.

Preparation of data

Preparation, and the subsequent processing of data, was performed with the software packages Seismic Unix, Matlab®, and WARRPI (e.g. Petersen, 2011). The combined use of Seismic Unix and Matlab was used to assigning geometry and processing to stack, while WARRPI was used for velocity analysis.

The seismic field data are in SEGD format with shot number as filenames. Data were read with *segdread* with following parameters:
segdread tape=$file use_stdio=1 ns=4000 verbose=1 > SUT2020.$profile.pos$name.ch1.su.

Navigation is supplied in navigation files and in SEGD headers. The navigation in SEGD headers is used for the preparation. Reading of SEGD headers is done with Matlab based on the following functions:

```
tmp=fread(fid,9*2,'ubit4','ieee-be');%ShipposX
function string1=headervalue(tmp)
 string1='';
   for i=1:length(tmp)*0.5;
      st1=dec2hex(tmp(i*2-1));
      st1=[st1,dec2hex(tmp(i*2))];
      string1=[string1,char(hex2dec(st1))];
   end
end
```

Some shot-gathers had corrupted headers. For these gathers the position was taken as the average of the positions before and after.

The geometry is based on endpoints of a 2D profile that is defined for each seismic profile. The end points are chosen such that the 2D profile closely resembles the shot-point for that profile. Common Depth Point's (CDP) are defined on that 2D profile. Shot positions are projected onto the 2D profile and CDP location of each trace is determined from the offset and shot position. Figure 4 shows an example of a 2D profile used for the geometry of the SUT2020_LinjaD seismic profile.

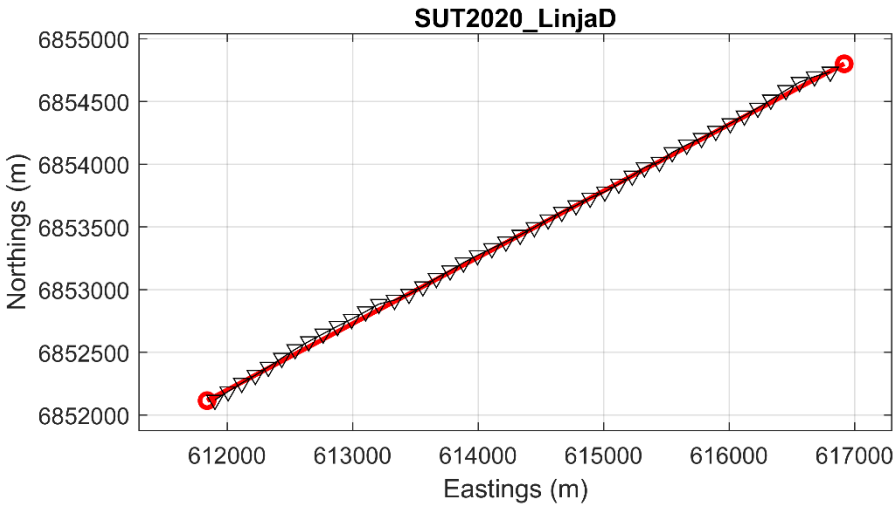

Figure 4. Black line shows shot-points with every 10th shot-point annotated as triangles. Red line with circles as endpoints shows the 2D profile that closely resamples the shot-point locations.

Offset from airgun to first channel is from the difference between tow-length of airgun and of streamer: 52 m - 32 m=20 m. Further analysis on traveltimes of the seismic signal leads to determining the offset to the first channel to be 41 m. See Appendix A for field notes of acquisition setup.

Initially, the recording length of the streamer was 600 m. However, during testing, after deployment of the streamer, the signal from the 3 last sections was not good, so the recording length was reduced with 3 sections to 450 m corresponding to 72 channels, which was used for LinjaO1, LinjaK, and LinjaU1. At this point the bad section of the streamer was removed, which recovered the 2 other sections, so from this point the streamer was recording on 550 m corresponding to 88 channels.

Ideally, the combination of 12.5-m shot spacing and 6.25-m receiver spacing gives a CDP-interval of 3.125 m. However, shallow water and high velocities just below seabed result in that coherent noise was not stacked out. Testing of different CDP intervals resulted in the choice of a 12.5-m CDP-interval.

Zero time of gathers was set at the first upward zero crossing. This resulted in a 5-ms time shift upwards.

Refraction seismic analysis and processing to stack

The main effort as to the processing parameters, was put into producing reliable velocity models for stacking, thus obtaining optimal focusing of the primary energy. Due to the generally high scattering of the signal, conventional velocity analysis on CDP-gathers, analysing the traveltimes of primary reflections, is in not at all possible. Therefore, refraction seismic analysis is used for the velocity models.

Furthermore, due to the high scattering of the seismic signal, it was considered useful only to use a wide bandpass filter and otherwise avoid additional filtering of data. This approach has previously been shown to give the best seismic images under similar conditions (Petersen, 2014; Petersen et al., 2015). Coherent noise, mainly seabed multiples and noise from the airgun, must then be identified on the stacked data during interpretation of data.

The main coherent noise relates to seabed multiples, bedrock multiples, and to a delayed airgun signal with a delay of 0.047 s as measured on the shot gathers, the origin of which is not known.

Velocity inversion

The velocities used for Normal Move Out (NMO) correction and depth migration are from velocity models derived from refraction seismic analysis. The process is iterative, starting with a *brutestack* (Figure 5) picking the seabed. The initial velocity model is 2-layer with seabed as interface (Figure 6). Velocity of 1480 m/s was assigned in the water column above seabed, and in the basalt column below the seabed, a vertical velocity gradient, with velocities in the range 3000 – 4500 m/s, was used (Figure 6). The 3000 – 4500 m/s interval is based on the Glyvursnes seismic experiments (e.g. Petersen et al., 2013).

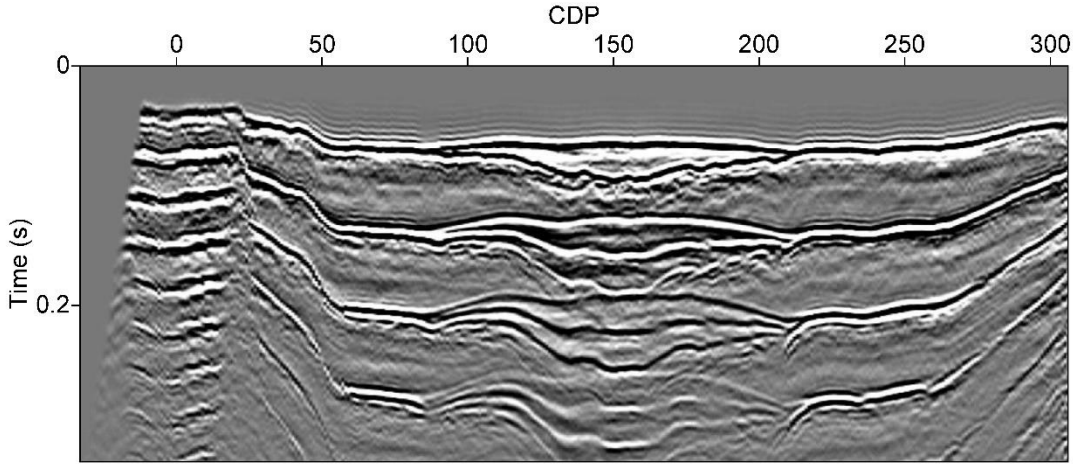

Figure 5. Brutestack for the Linjal profile

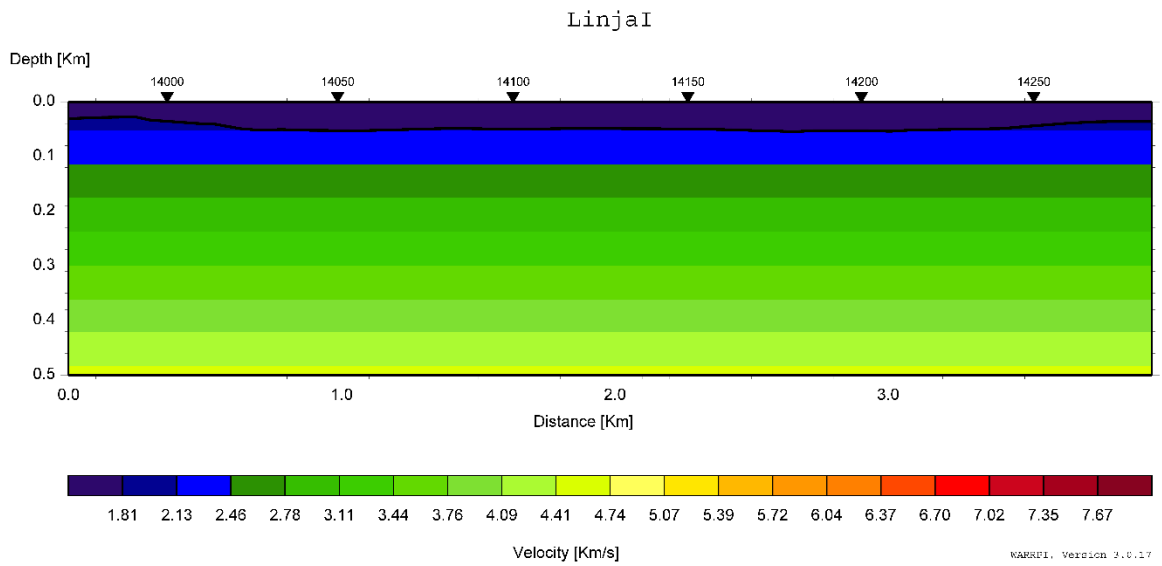

Figure 6. Initial velocity model for LinjaI. Position of every 50th shot point is annotated.

For each profile, an initial model was designed. The models for the seismic profiles between Sandoy and Skúvoy are 500 m deep and for the rest of the seismic profiles they are 1000 m deep.

Quality control of seabed is done by inspection of reflections from the seabed (Figure 7). Traveltime of the direct wave verifies the velocity in water.

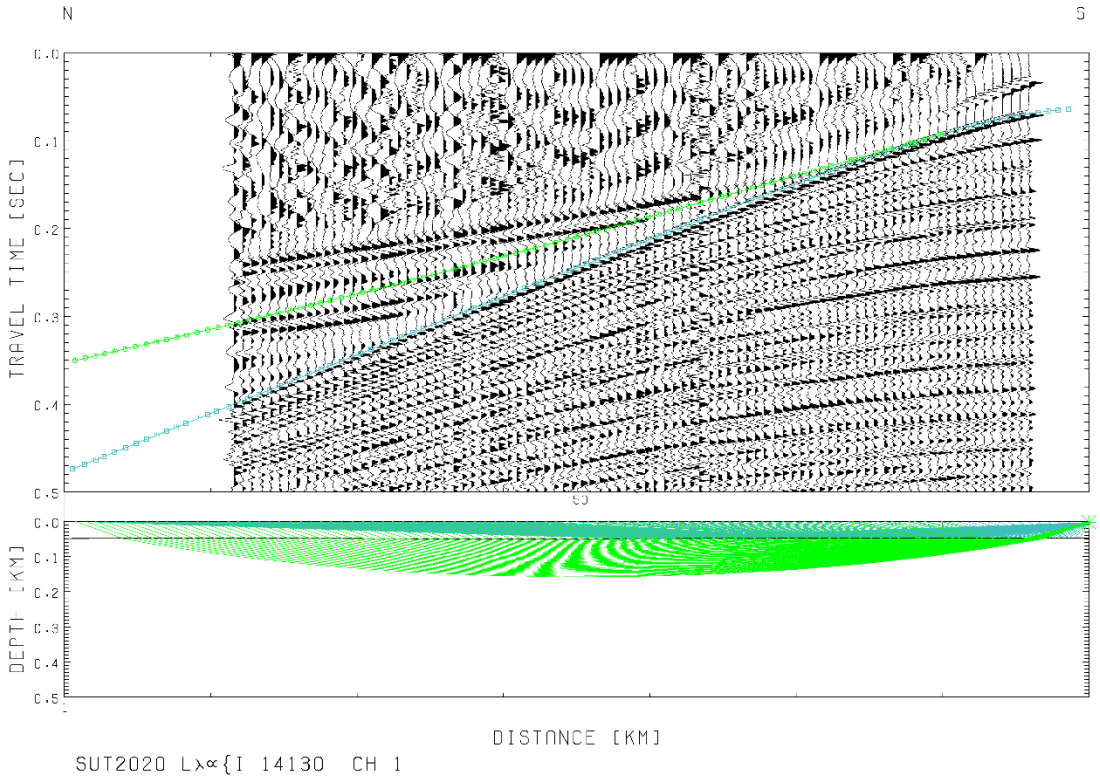

Figure 7. Example of traveltimes of initial velocity model (Figure 6). Upper: Traveltimes of the reflection from seabed and for the refracted seismic wave below seabed of the initial model. Crosses mark the first breaks used for velocity inversion. Lower: Ray paths.

WARRPI is used for the inversion to derive a velocity model that complies to traveltimes of picks of first breaks as described in Petersen et al. (2013). For all models, the grid was 100 × 10

grid points horizontally and vertical, respectively. The horizontal grid is equally spaced while the vertical grid has exponential increasing grid interval.

In the velocity analysis, every 10th shot-gather was used for 500-m deep models, and every 20th shot-gather was used for the 1000-m deep models. Table 1 lists the names of final velocity models that were used in the final processing and depth migration iteration.

Figure 8 shows the result of the inversion for the 2-layer model in Figure 6.

For all profiles, the calculated traveltimes of the first breaks converge towards the picked traveltimes with a Root-Mean-Square (RMS) deviation between picked and modelled traveltimes of only about 4 ms. Figure 9 is a typical example with the traveltimes coinciding with picked traveltimes.

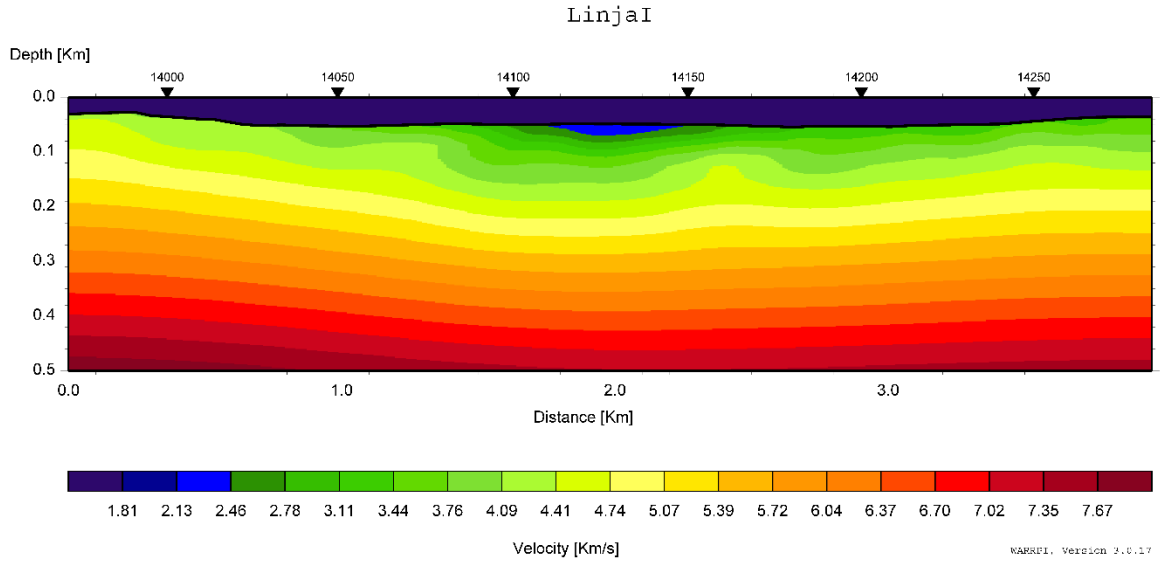

Figure 8. Two-layer velocity model for LinjaI. Model version: Model04. Position of every 50th shot point is annotated.

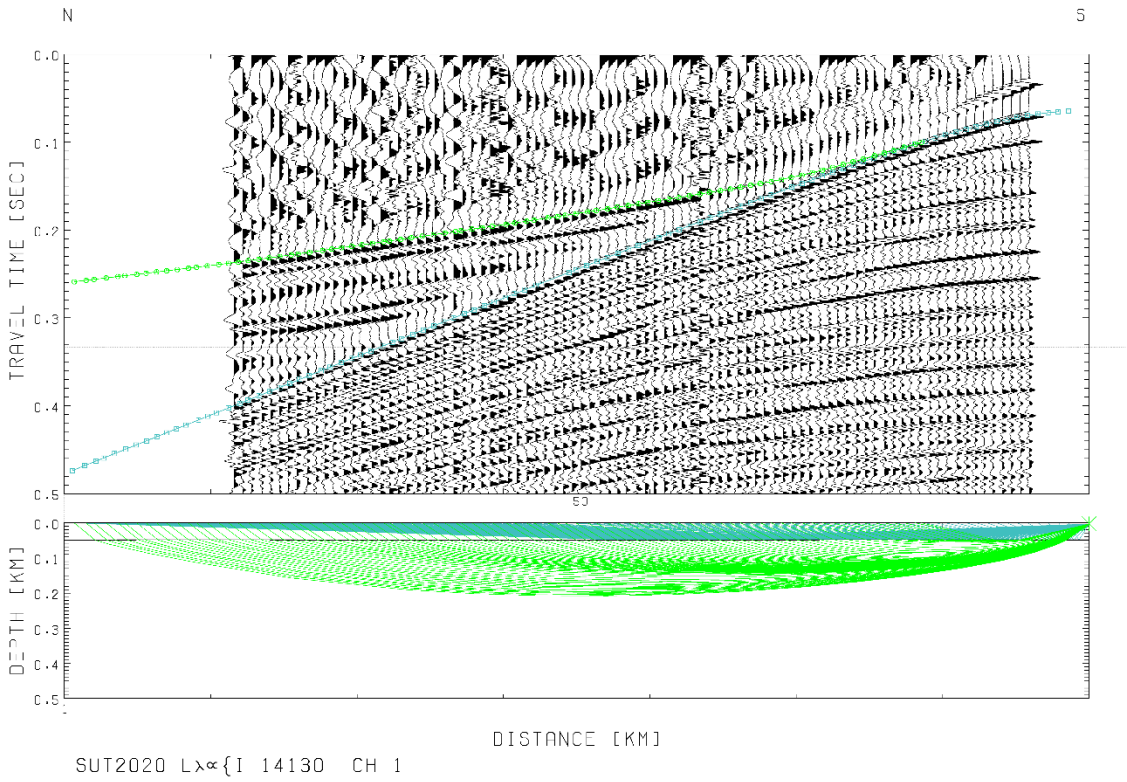

Figure 9. Traveltimes of inverted velocity model (Figure 8). Upper: Example of traveltimes of the reflection from seabed and for the refracted seismic wave below seabed of the initial model. Lower: Ray paths.

Processing to stack

The processing to stack sequence is as follows:

- Geometry: projection onto a 2D profile.
- CDP sorting
- Gain: Tpow=1 (Correction for spherical divergence)
- Mute bad traces
- Bandpass filter: Low pass=12Hz, high pass=600 Hz
- NMO correction, smute=1.3 (stretch mute).
- Stack data
- Median filter: Using the two adjacent traces weighted 0.5 (only applied to final models)
- Post stack depth migration
- CDP positions of 2D profile are projected back onto shot-point navigation.

Notice that the deeper section of the velocity model is without data coverage and that the velocities are unrealistic high (Figure 8). Therefore, for all velocity model's to be used for NMO correction and depth migration, unrealistic velocities above 5500 m/s are set to 5500 m/s.

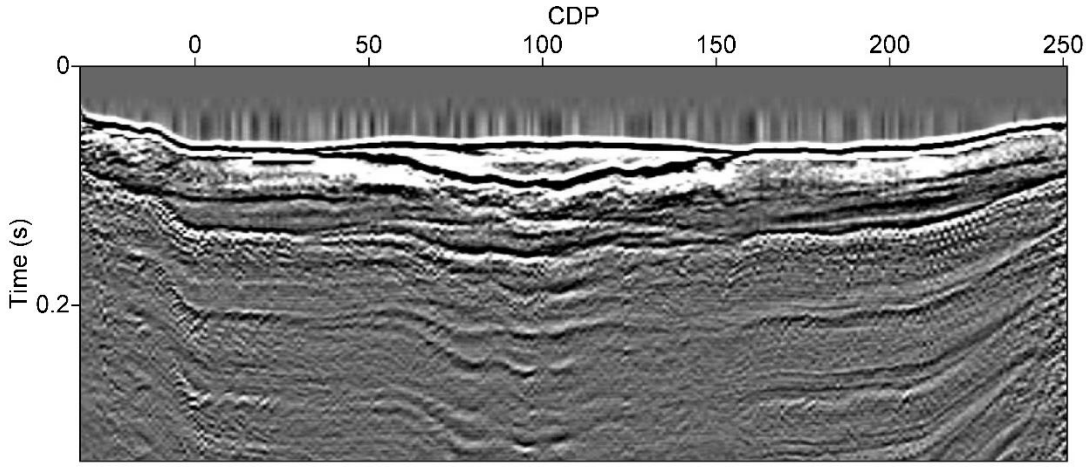

Figure 10. LinjaI stack with velocities from Model04

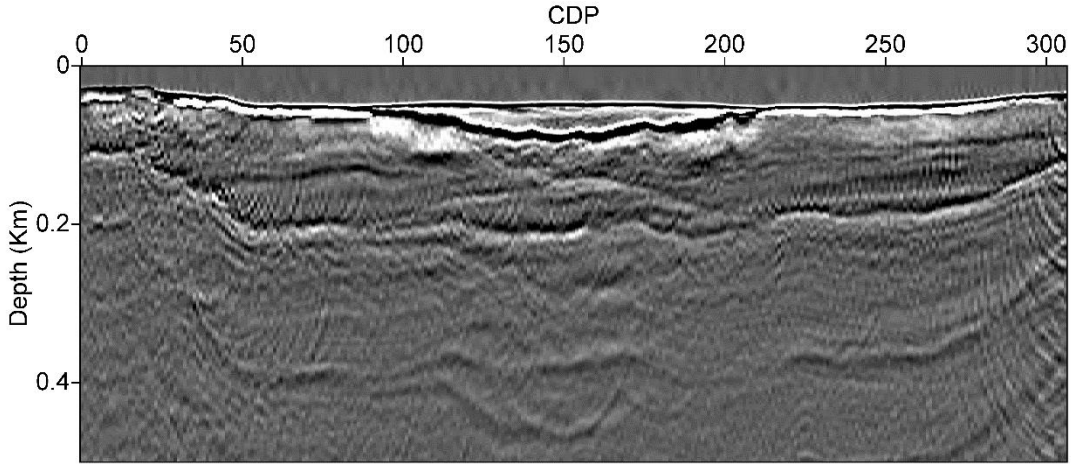

Figure 11. LinjaI depth migration velocities from Model04

The stacked profile (Figure 10 and 11), clearly shows a sedimentary basin. The next level model is thus defined as a 3-layer model with one interface for the seabed and one for the base of the sedimentary basin (Figure 12).

The interface of base sediment basin is from picks on depth migrated data. Velocity analysis on shot-gathers estimate the sediment velocity to be about 1800 m/s. Figure 13 shows shot point 14130 as an example of traveltimes of the reflections from the base of the sedimentary basin with sediment velocities set to 1800 m/s.

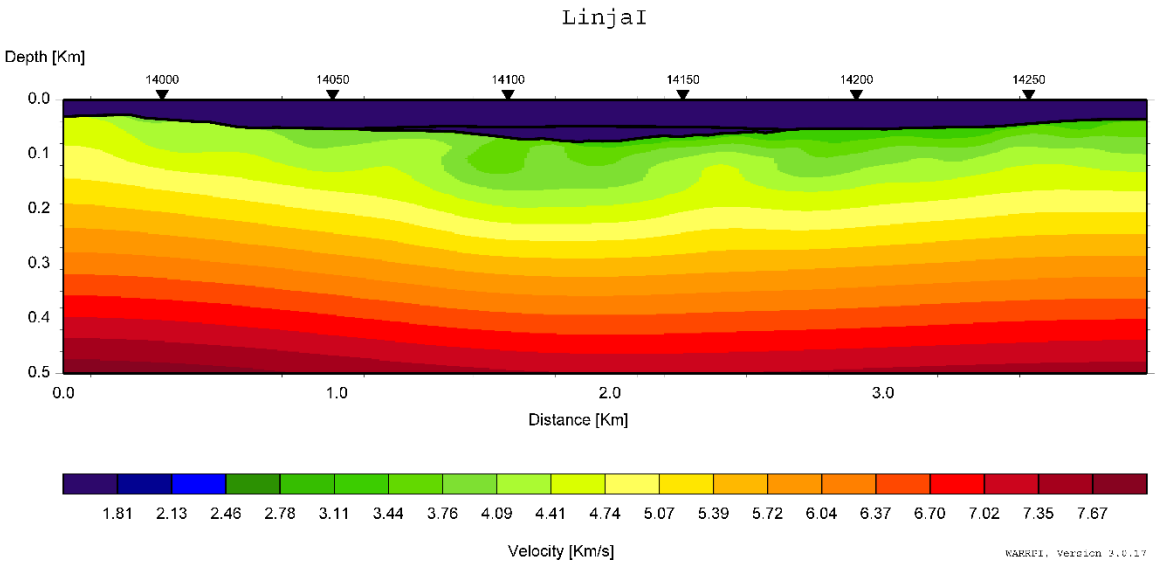

Figure 12. The inverted 3-layer model. Version: Model04layer01a2. Position of every 50th shot point is annotated.

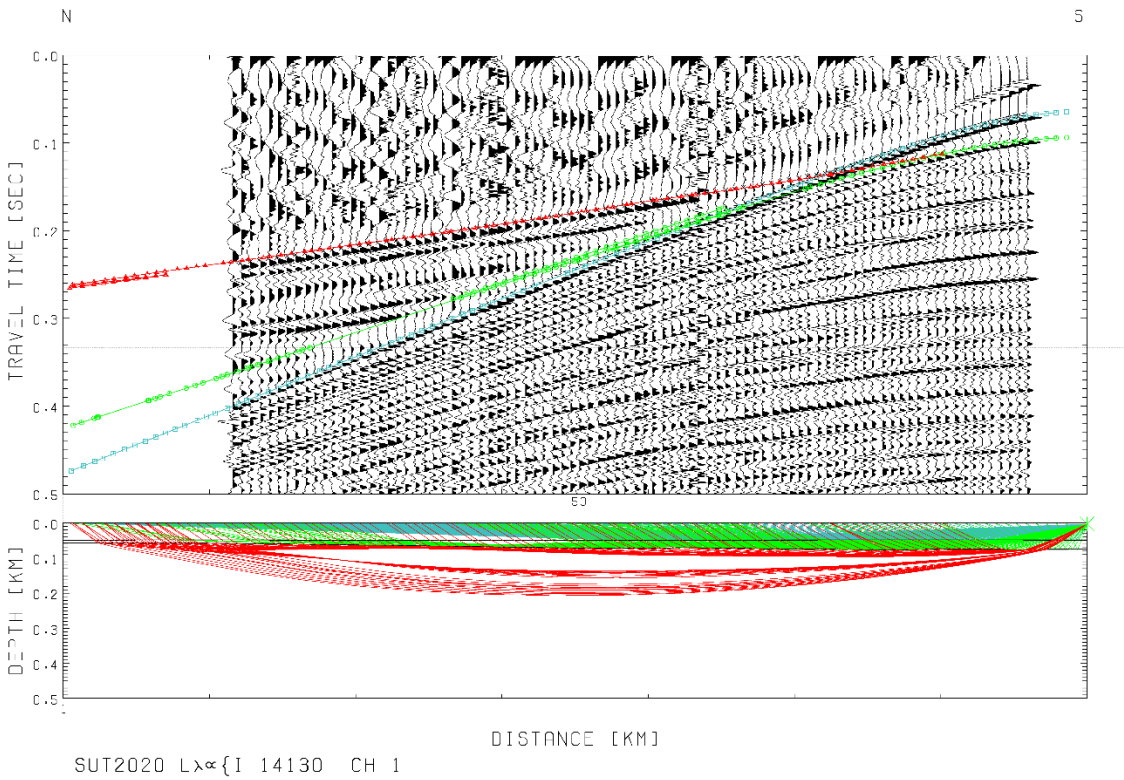

Figure 13. Traveltimes of inverted 3-layer model (Figure 12). Upper: Example of traveltimes of the reflection from seabed, from base sediment basin, and for the refracted seismic wave below seabed of the initial model. Lower: Ray paths.

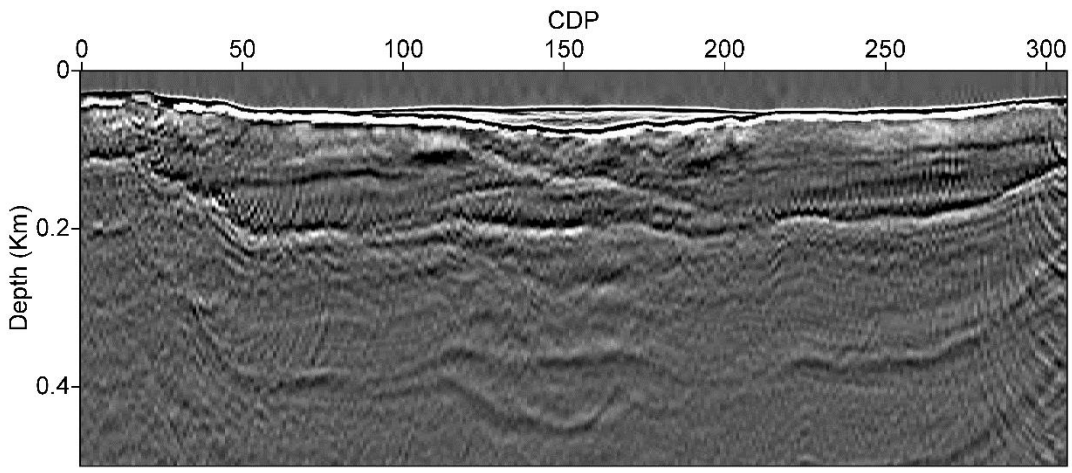

Figure 14. Depth migrated Linjal. Version: model04layer01a2.

For better constraint on the depth of the base of the sedimentary basin, a few iterations were done to improve the depth migration thus giving a more accurate depth when picking the sedimentary basin (Figure 14).

Forward modelling

For selected profiles forward modelling was attempted in order to model deeper reflectors. Figure 15 shows forward modelling of LinjaI to a 5-layer model. In addition to the sedimentary basin, there are three layers below the sedimentary basin. The second layer below the sedimentary basin represents a velocity inversion, that is, going from a layer with higher velocity above to a layer with lower velocity below. Interfaces and the velocity of the second layer are from forward modelling, adjusting the parameters to give the best fit of traveltimes of reflections for all gathers. Figure 16 and 17 show examples of traveltimes for this model.

Velocity inversions are bad for surface seismic data because they diverge the seismic energy away from the surface, especially when the velocity inversion occurs in a shallow layer. This could be an explanation for some of the profiles with section of bad imaging. There are indications that these sections coincide with velocity inversions.

Forward modelling was primarily attempted for the profiles between Sandoy and Skúvoy to try to enhance sections of the profiles where the stacked data did not show a clear image due to noise from multiples and to difficult imaging due to the nature of the basalts. Clearly, there is information to gain from this approach, however it was not completed in detail due to time restrictions of the project.

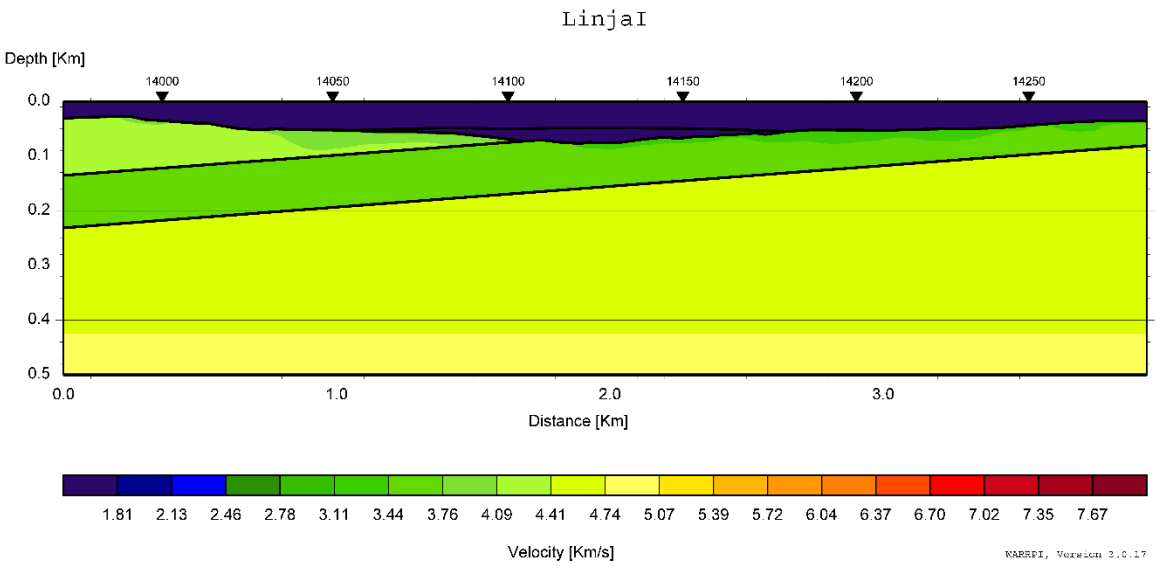

Figure 15. Forward modelling 5-layer model. Version model04layer03a. Position of every 50th shot point is annotated.

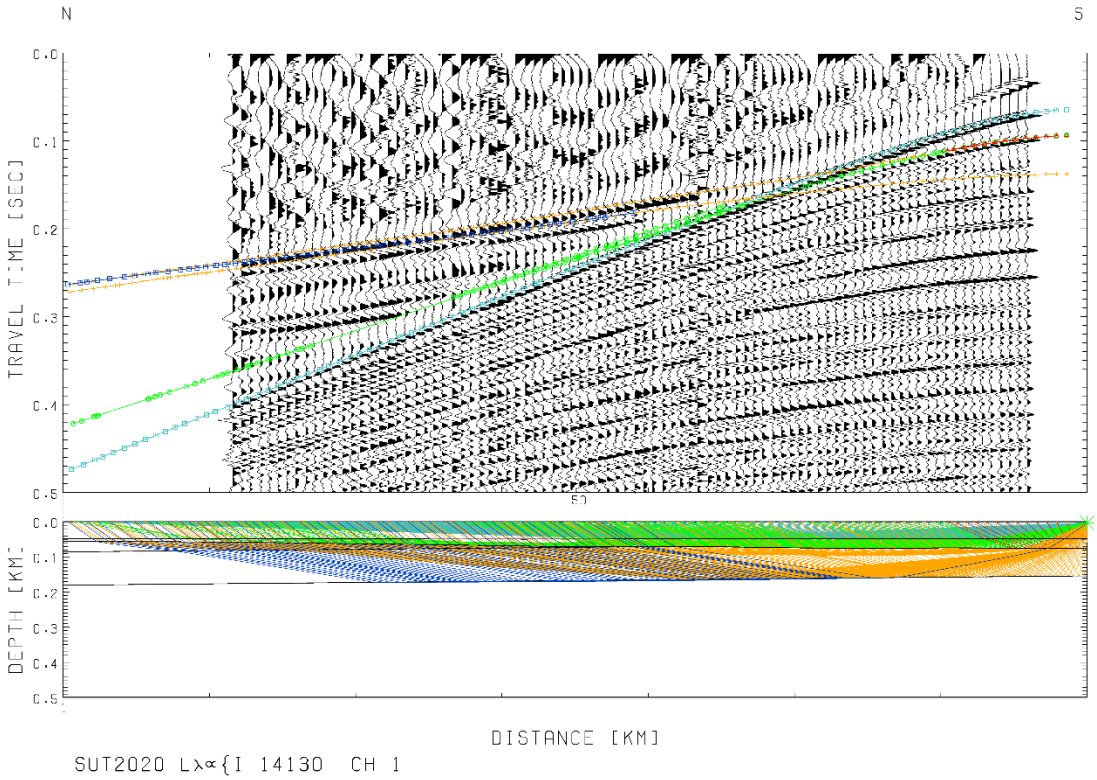

Figure 16. Traveltimes of forward modelling 5-layer model (Figure 15Figure 12). Upper: Example of traveltimes of the reflection from seabed, base sediment basin, 4th interface, refractions from sediments, low-velocity layer. Lower: Ray paths

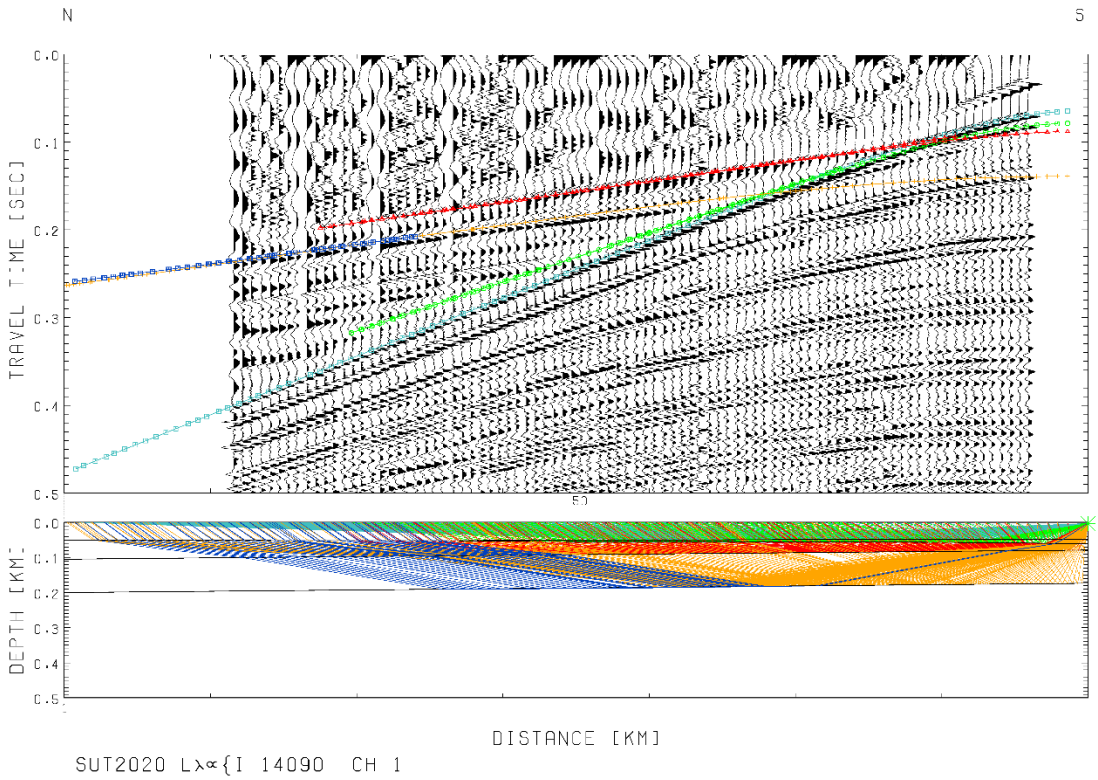

Figure 17. Traveltimes of forward modelling 5-layer model (Figure 15Figure 12). Shot position is moved 500 m to the left in order to better show the effect of the low-velocity layer. Upper: Example of traveltimes of the reflection from seabed, base sediment basin, 3rd and 4th interfaces, refractions from sediments, 1st and 2nd bellow sediments. Lower: Ray paths

Results

Coherent noise

In the processing, in order to preserve most of the signal, no means have been the taken to remove coherent noise, except from the effect of stacking data. Therefore, in the interpretation, special care must be taken to identify the coherent noise to aid the interpretation. Figure 18 and 19 show examples of how the noise appears on the stacked profiles. Notice, that the noise is best identified in the time domain.

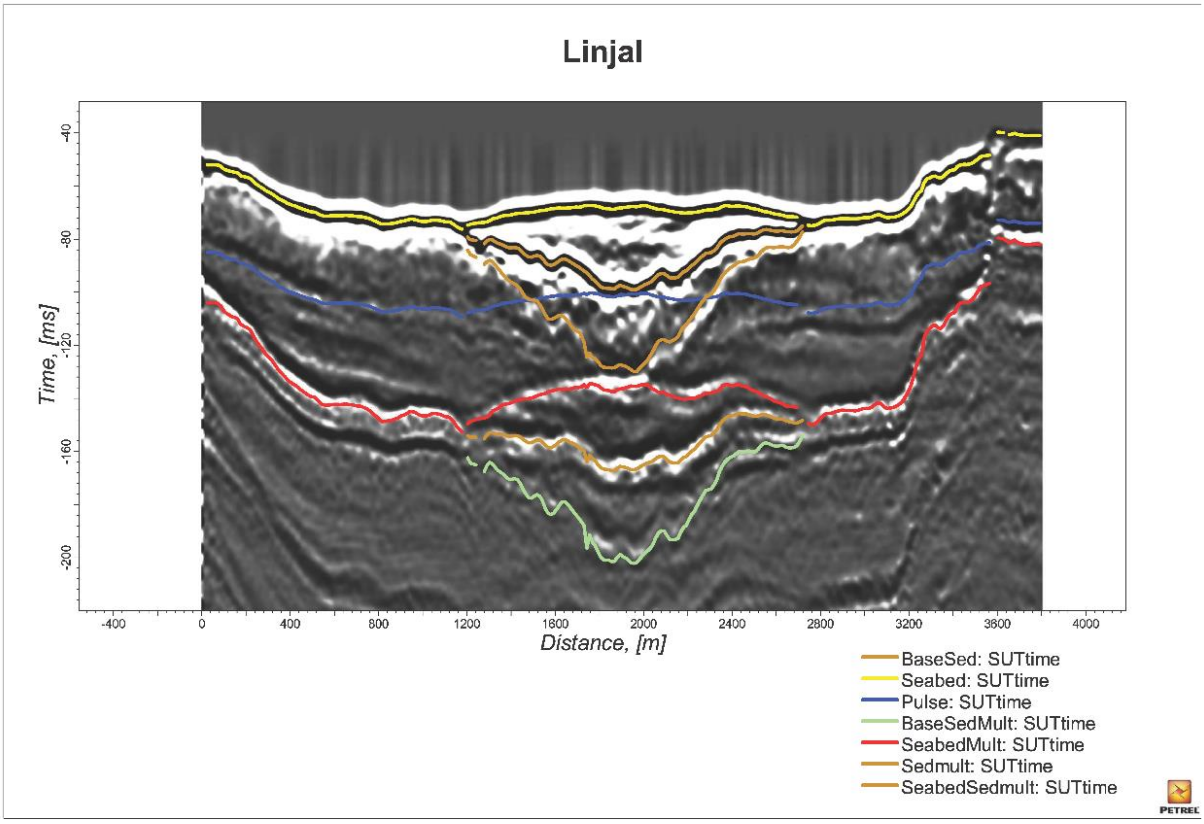

Figure 18. Linjal with annotated seabed and bedrock reflection and examples of multiple reflections from these. ***BaseSed****: reflection from bedrock in sedimentary basin,* ***Seabed****: reflection from seabed,* ***Pulse****: delayed pulse from airgun,* ***BaseSedMult****: Multiple of BaseSed,* ***SeabedMult****: Multiple of Seadbed,* ***Sedmult****: Multiple between seabed and bedrock in sedimentary basin,* ***SeabedSedmult****: Multiple of seabed + multiple between seabed and bedrock in sedimentary basin.*

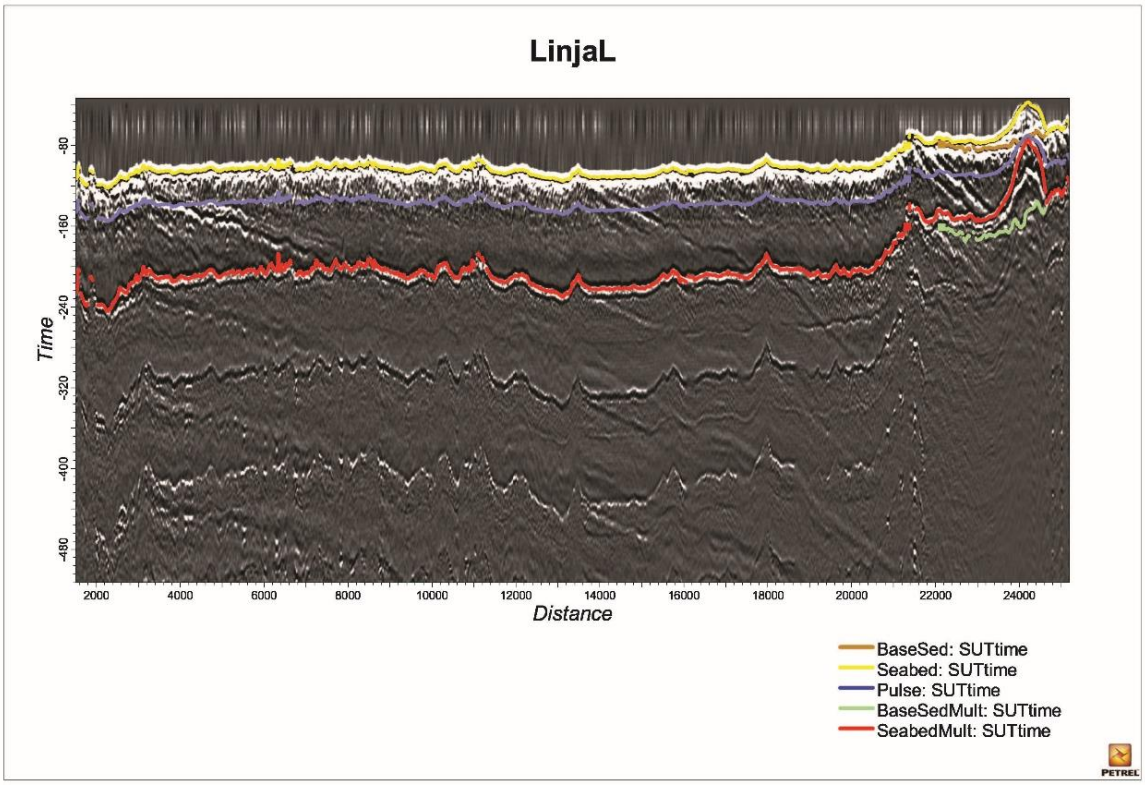

*Figure 19. LinjaL with annotated seabed and bedrock reflections and examples of coherent noise. **BaseSed**: reflection from bedrock in sedimentary basin, **Seabed**: reflection from seabed, **Pulse**: delayed pulse from airgun, **BaseSedMult**: Multiple of BaseSed, **SeabedMult**: Multiple of Seadbed.*

Processed data and velocity models

Below, the analysed and processed data are presented for all profiles. Each profile is presented with the following figures:

1. Final stacked data
2. Depth migration. Depth sampling is 0.5 m. Notice that depth of 1 km compares to approximately 0.45 s in the time domaine.
3. Velocity models used for the processing. For orientation some shot positions are marked as triangles on the surface of the model.
4. Ray coverage of refracted waves. The colour bar shows number of rays crossing each grid element. Line thickness of the bedrock interface shows number of rays crossing the bedrock.
5. One example of traveltimes and ray paths. Upper: Traveltimes of the reflection from seabed and for the refracted seismic wave below seabed of the initial model. Crosses mark the first breaks used for velocity inversion. Lower: Ray paths.

LinjaL

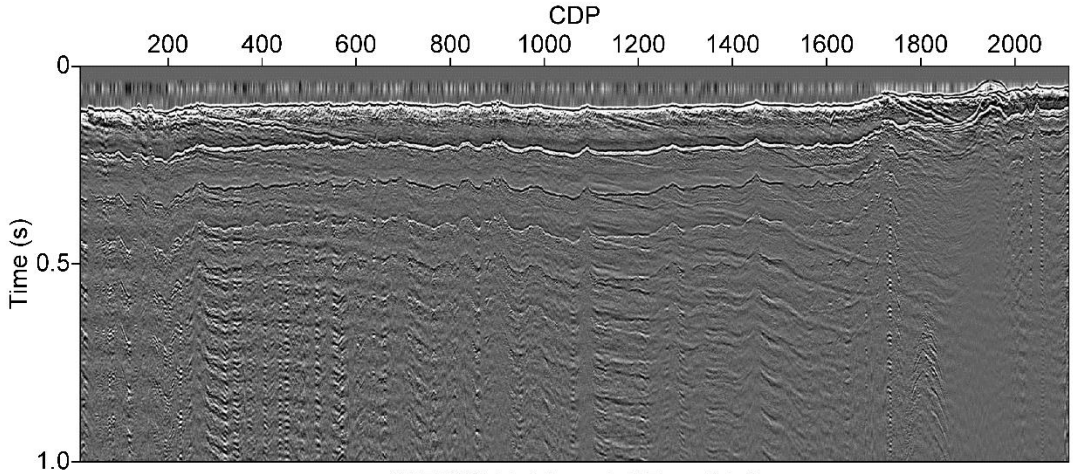

SUT2020_LinjaL model05layer01a2

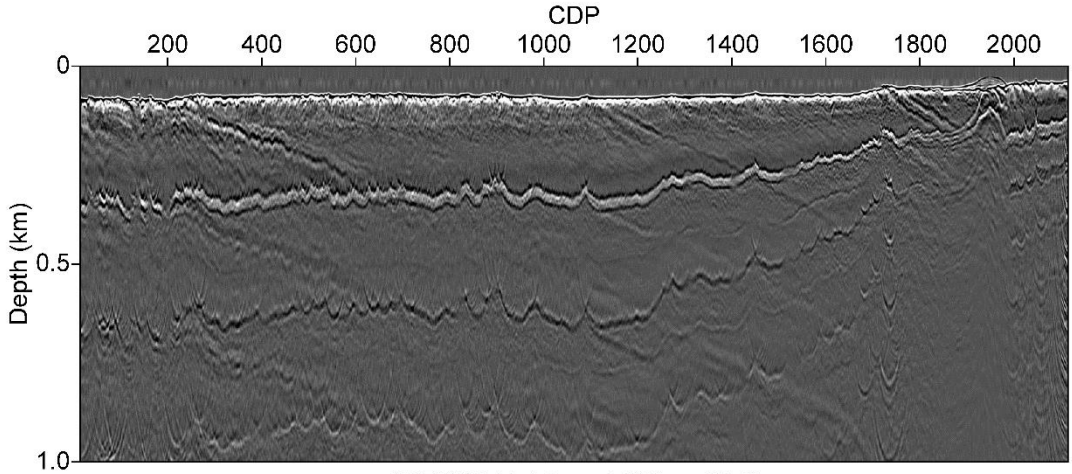

SUT2020_LinjaL model05layer01a2

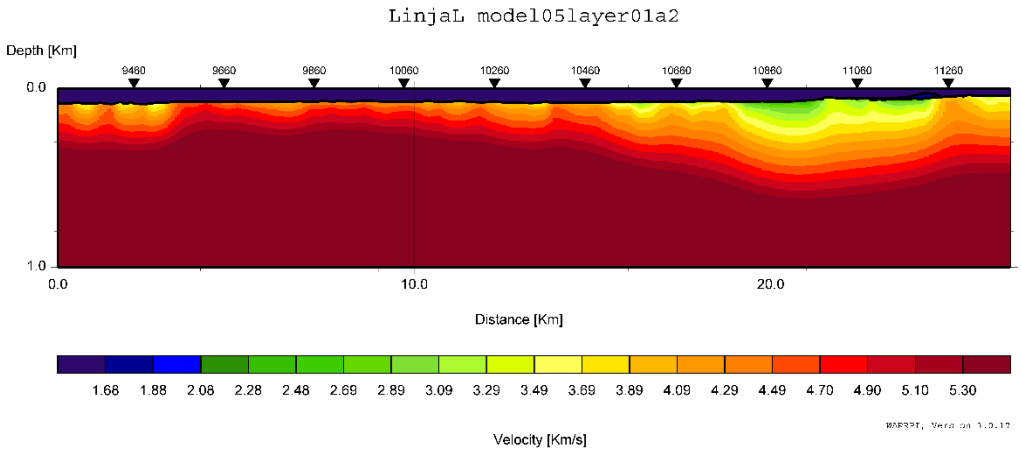

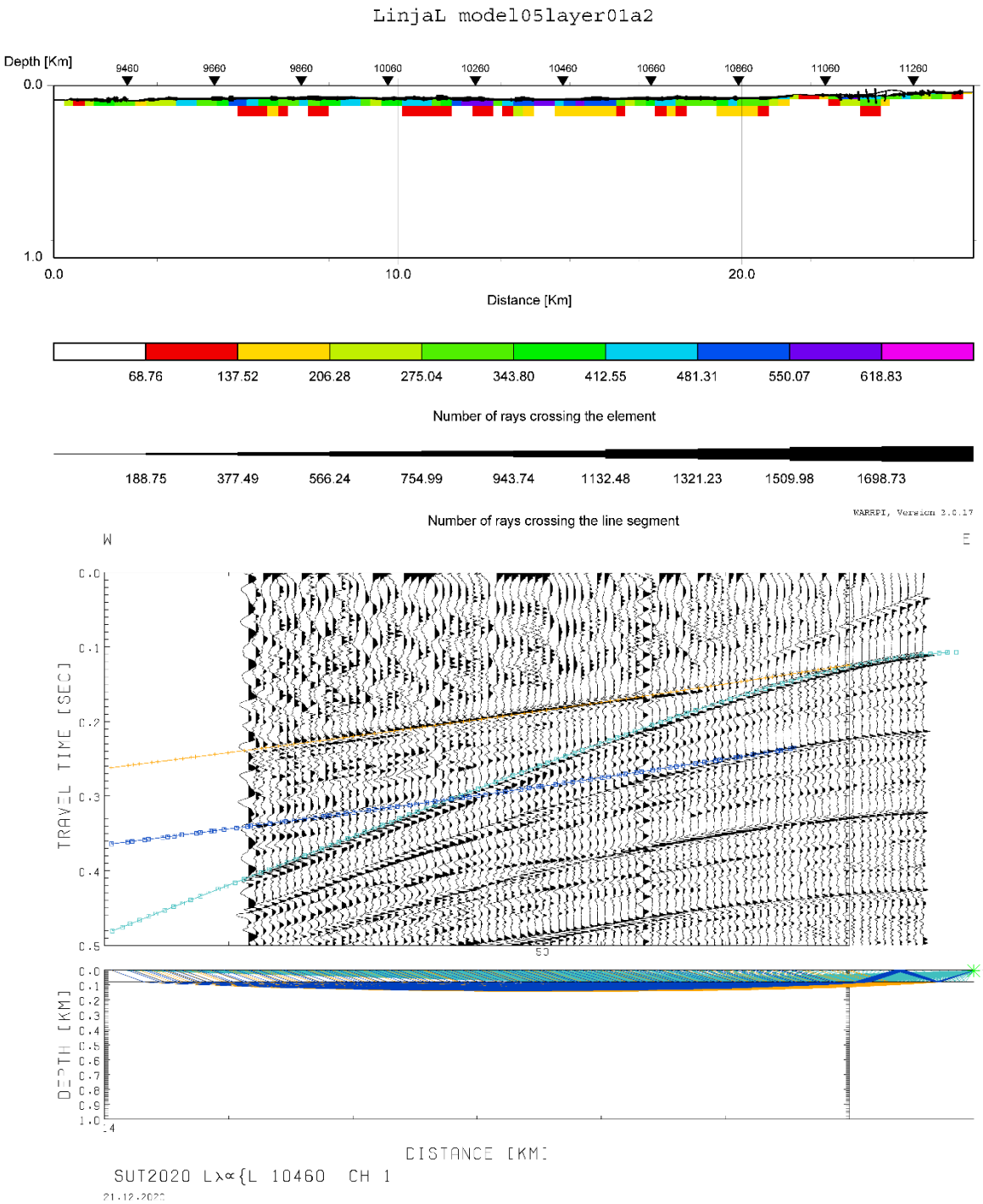
LinjaL model05layer01a2
Depth [Km]
9460
9660
9860
10060
10260
10460
10660
10860
11060
11260
0.0
1.0
0.0
10.0
20.0
Distance [Km]
68.76
137.52
206.28
275.04
343.80
412.55
481.31
550.07
618.83
Number of rays crossing the element
188.75
377.49
566.24
754.99
943.74
1132.48
1321.23
1509.98
1698.73
Number of rays crossing the line segment
W
E
TRAVEL TIME [SEC]
DEPTH [KM]
DISTANCE [KM]
SUT2020 L λ∝{L 10460 CH 1

LinjaF

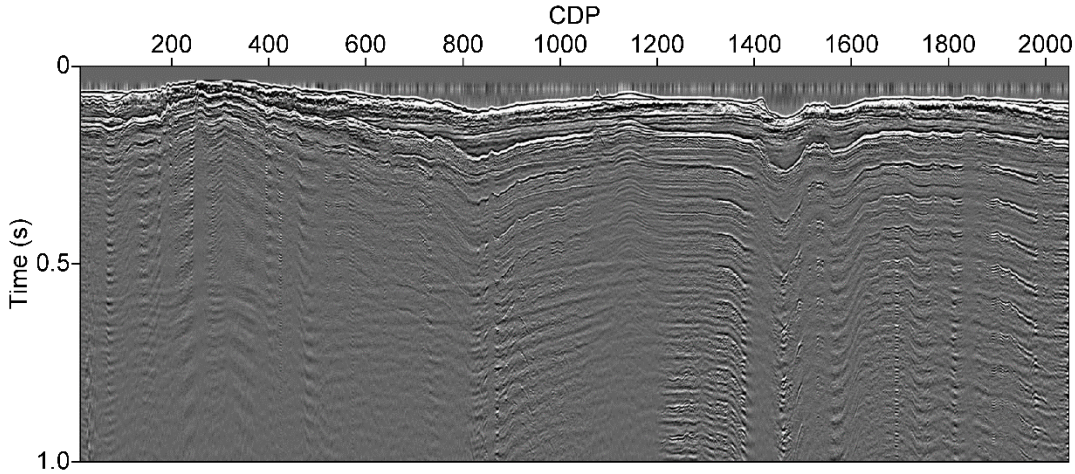

SUT2020_LinjaF model05layer02a2

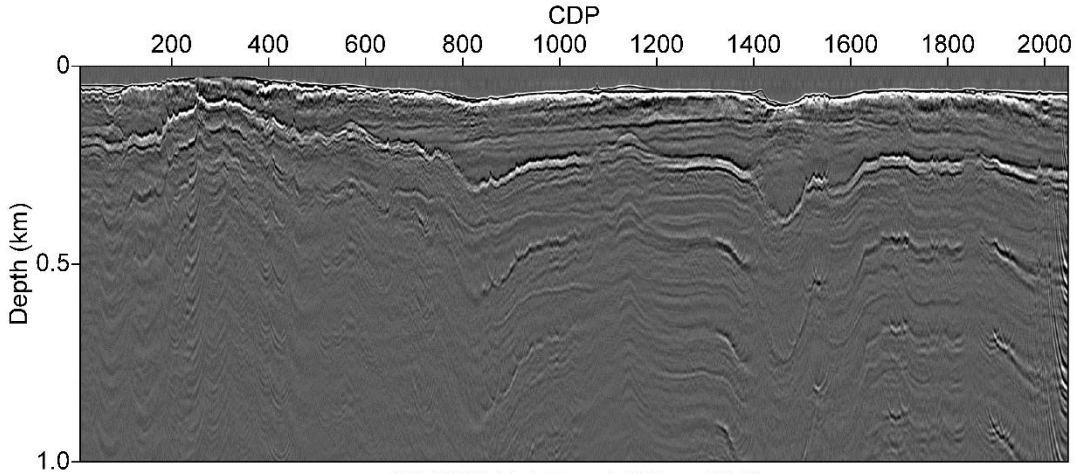

SUT2020_LinjaF model05layer02a2

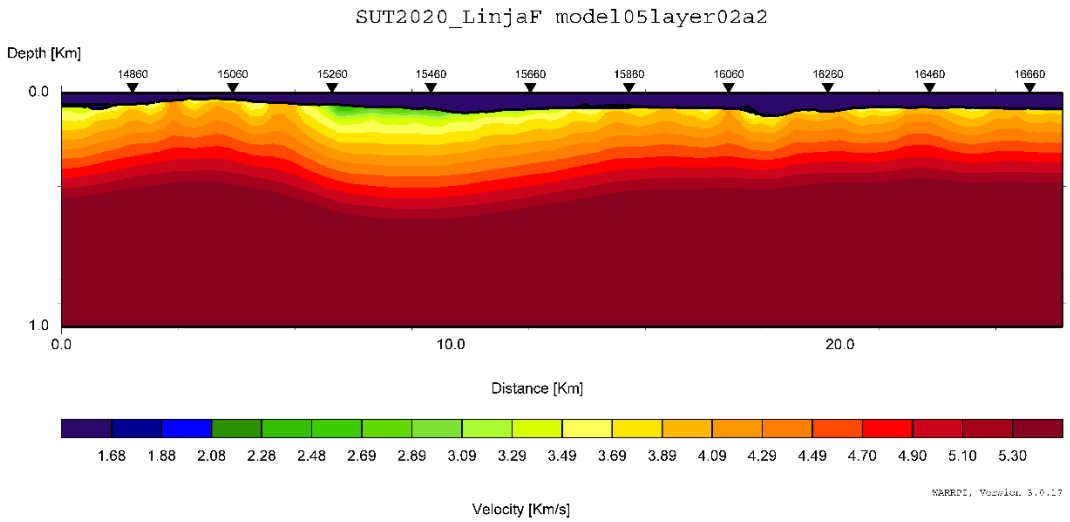

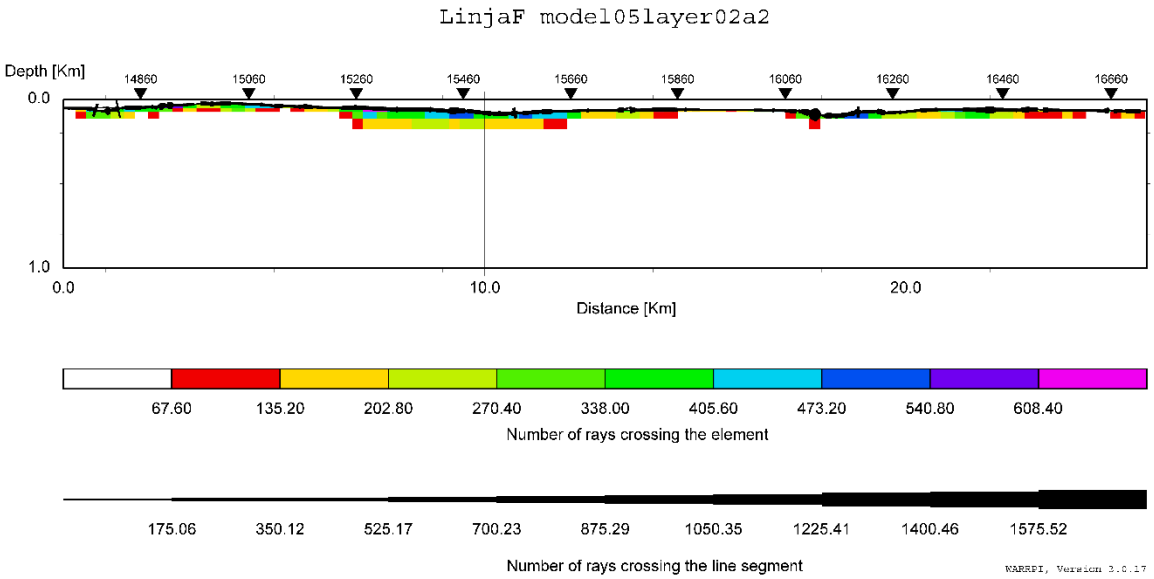
LinjaF model05layer02a2
Depth [Km]
14860
15060
15260
15460
15660
15860
16060
16260
16460
16660
0.0
1.0
0.0
10.0
20.0
Distance [Km]
67.60
135.20
202.80
270.40
338.00
405.60
473.20
540.80
608.40
Number of rays crossing the element
175.06
350.12
525.17
700.23
875.29
1050.35
1225.41
1400.46
1575.52
Number of rays crossing the line segment
WARRPI, Version 3.0.17

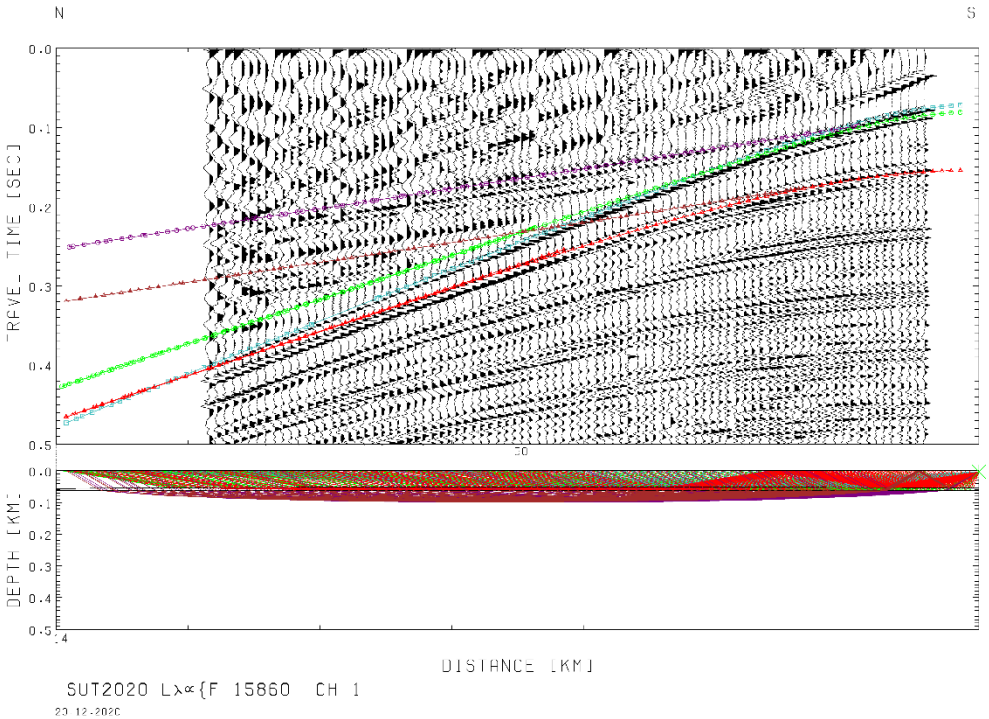
N
S
TRAVEL TIME [SEC]
0.0
0.1
0.2
0.3
0.4
0.5
30
DEPTH [KM]
0.0
0.1
0.2
0.3
0.4
0.5
DISTANCE [KM]
SUT2020 LinjaF 15860 CH 1
20.12.2020

LinjaI

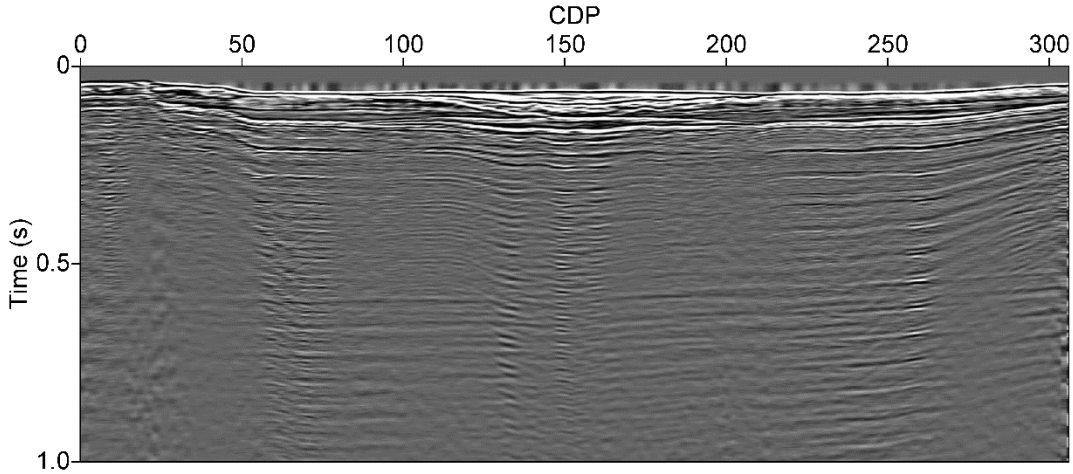

SUT2020_Linjal model04layer03a

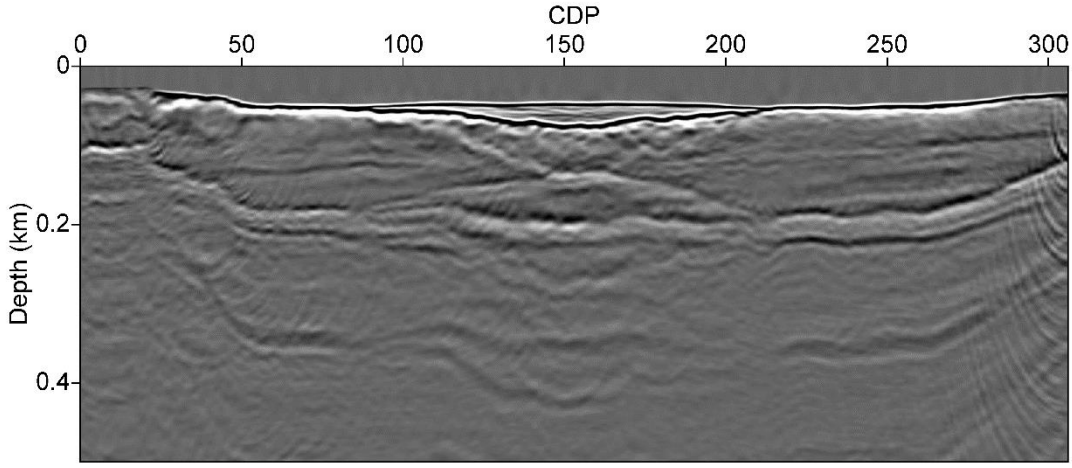

SUT2020_Linjal model04layer03a

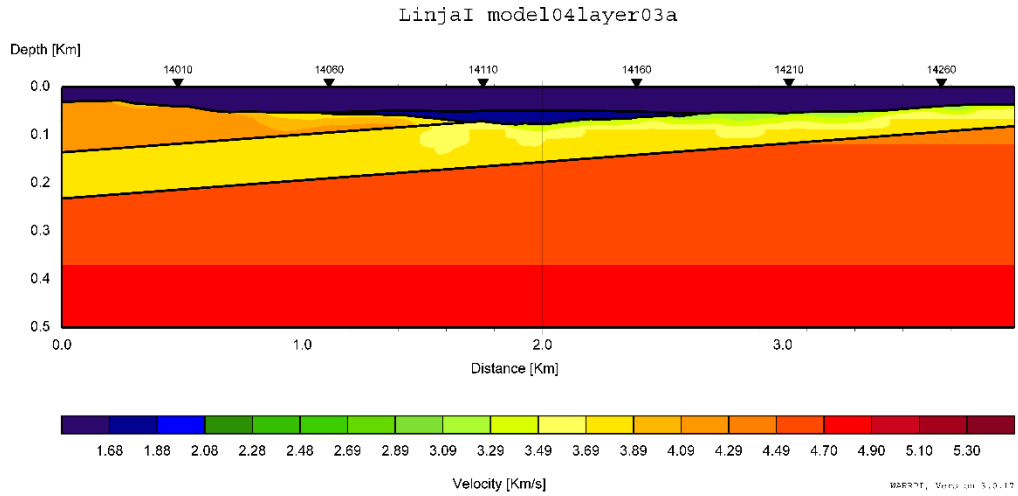

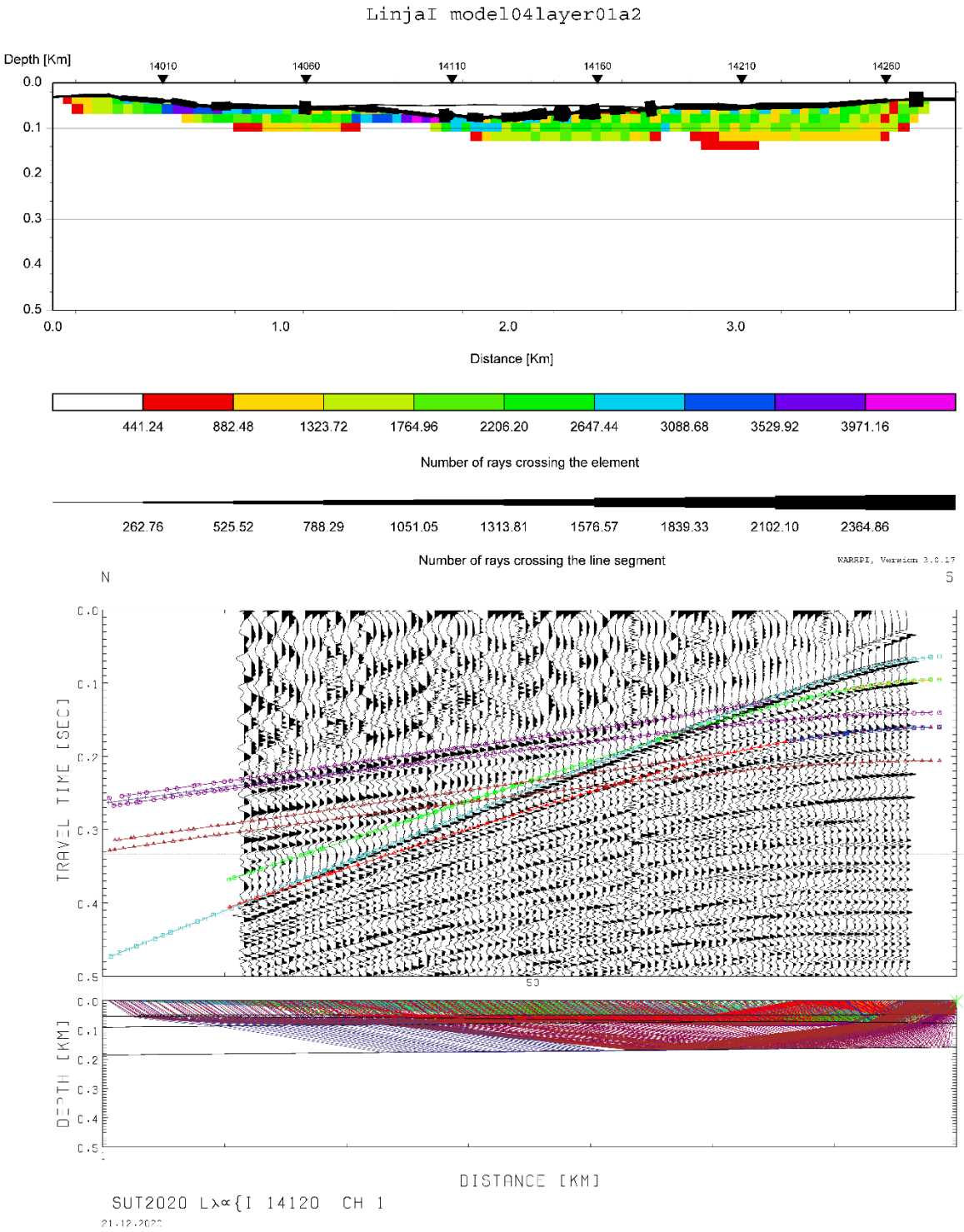
LinjaI model04layer01a2
Depth [Km]
14010
14060
14110
14160
14210
14260
0.0
0.1
0.2
0.3
0.4
0.5
0.0
1.0
2.0
3.0
Distance [Km]
441.24
882.48
1323.72
1764.96
2206.20
2647.44
3088.68
3529.92
3971.16
Number of rays crossing the element
262.76
525.52
788.29
1051.05
1313.81
1576.57
1839.33
2102.10
2364.86
Number of rays crossing the line segment
N
S
TRAVEL TIME [SEC]
DEPTH [KM]
DISTANCE [KM]
SUT2020 L λ∝{I 14120 CH 1

LinjaB

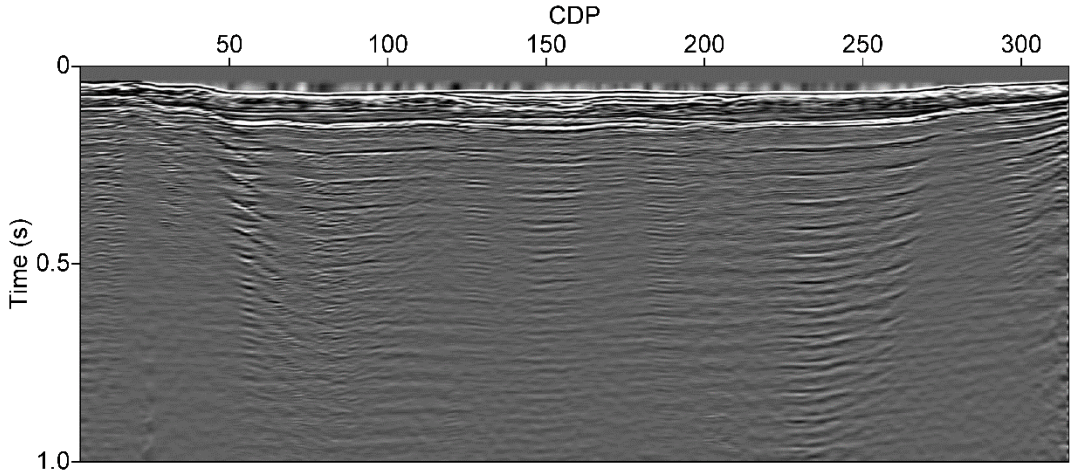

SUT2020_LinjaB model04layer03a

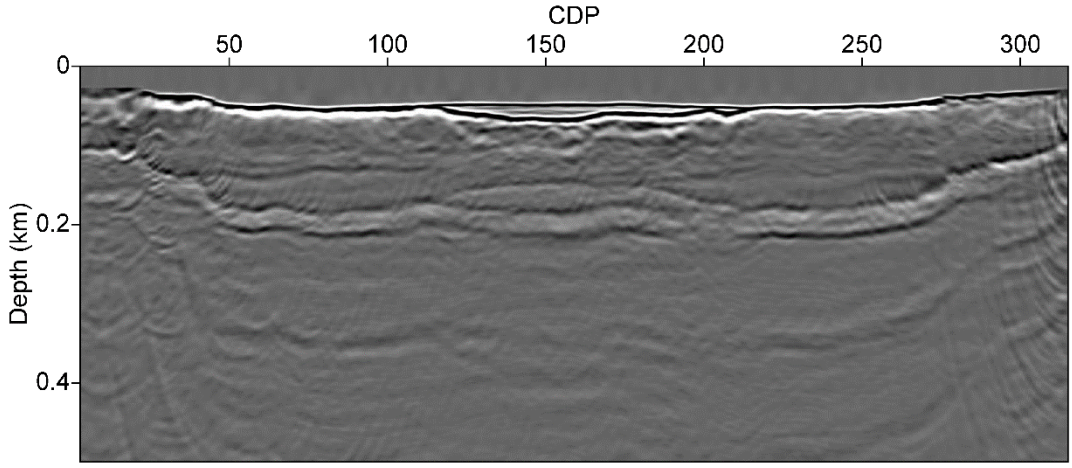

SUT2020_LinjaB model04layer03a

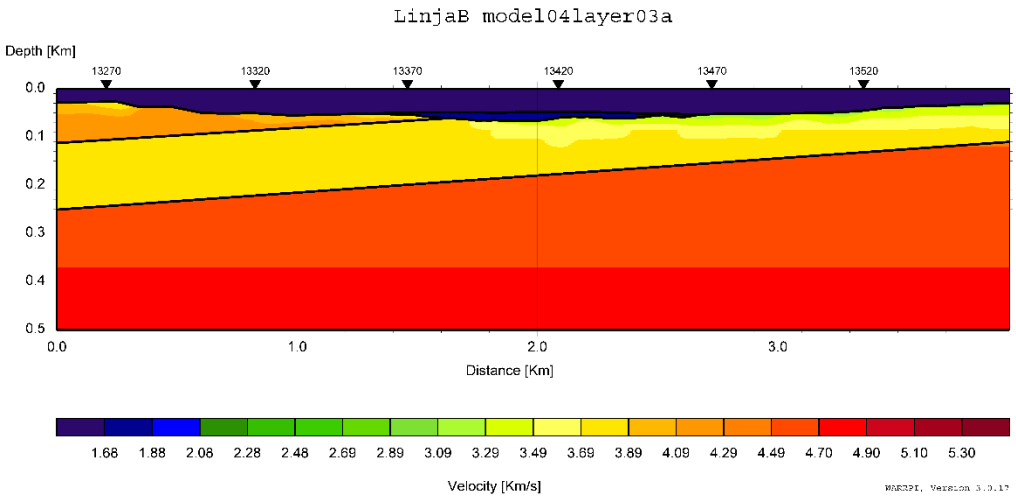

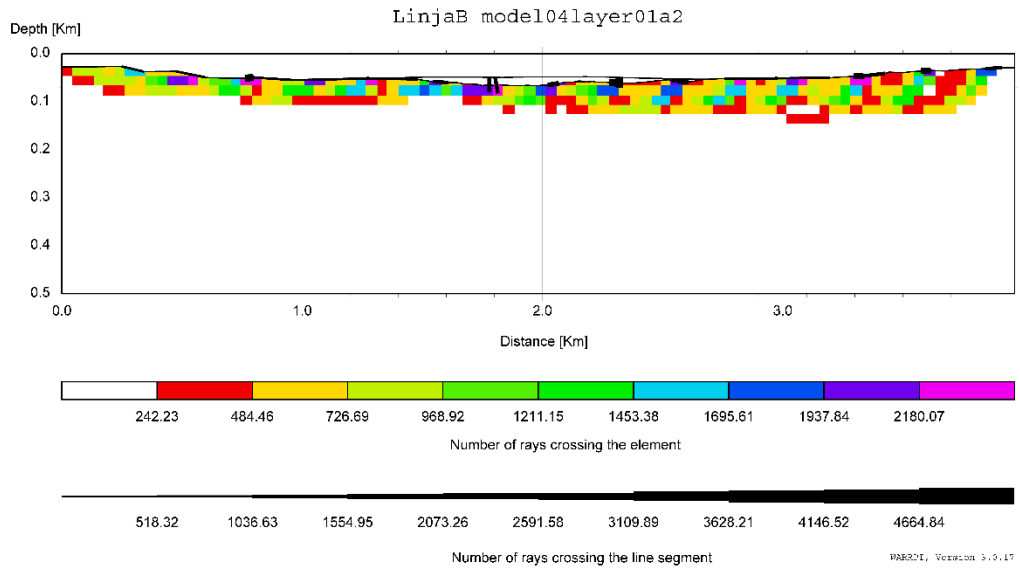
LinjaB model04layer01a2
Depth [Km]
0.0
0.1
0.2
0.3
0.4
0.5
0.0
1.0
2.0
3.0
Distance [Km]
242.23
484.46
726.69
968.92
1211.15
1453.38
1695.61
1937.84
2180.07
Number of rays crossing the element
518.32
1036.63
1554.95
2073.26
2591.58
3109.89
3628.21
4146.52
4664.84
Number of rays crossing the line segment

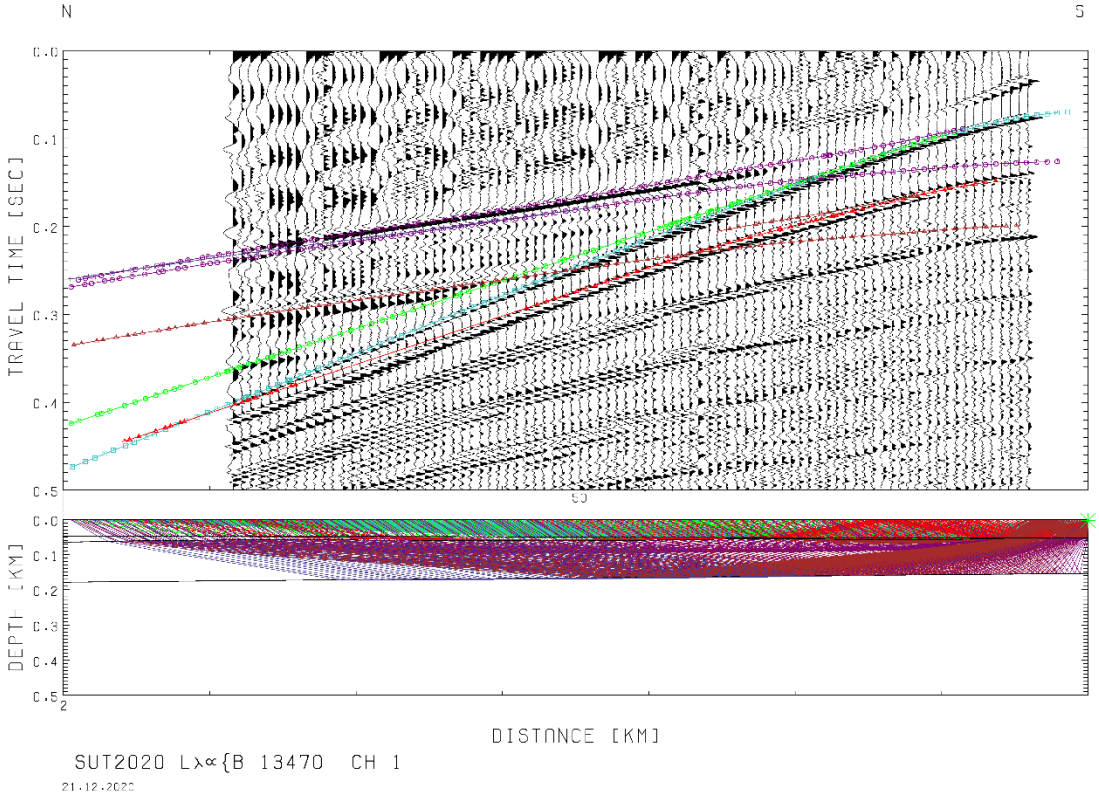
N
S
TRAVEL TIME [SEC]
0.0
0.1
0.2
0.3
0.4
0.5
DEPTH [KM]
DISTANCE [KM]
SUT2020 LλαB 13470 CH 1

LinjaH

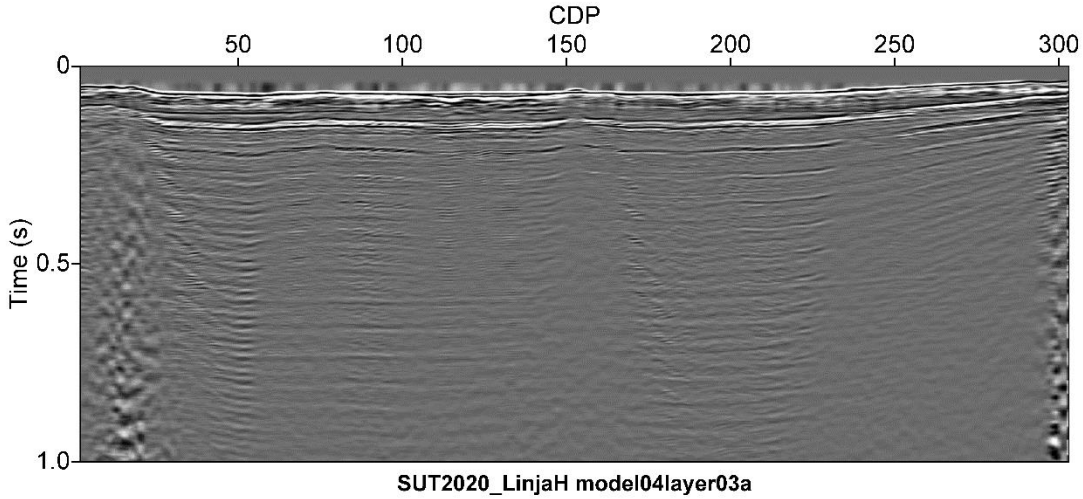
CDP
50
100
150
200
250
300
0
0.5
1.0
Time (s)
SUT2020_LinjaH model04layer03a

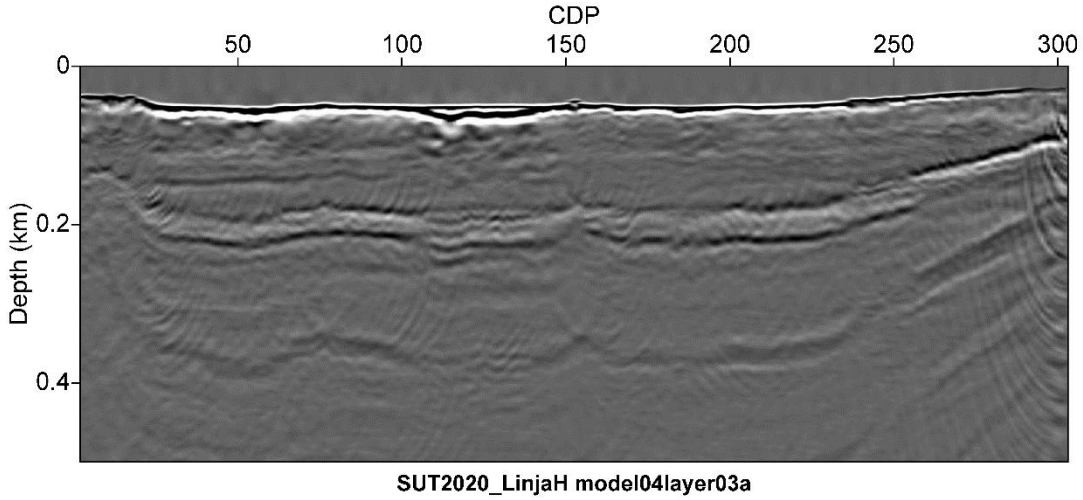
CDP
50
100
150
200
250
300
0
0.2
0.4
Depth (km)
SUT2020_LinjaH model04layer03a

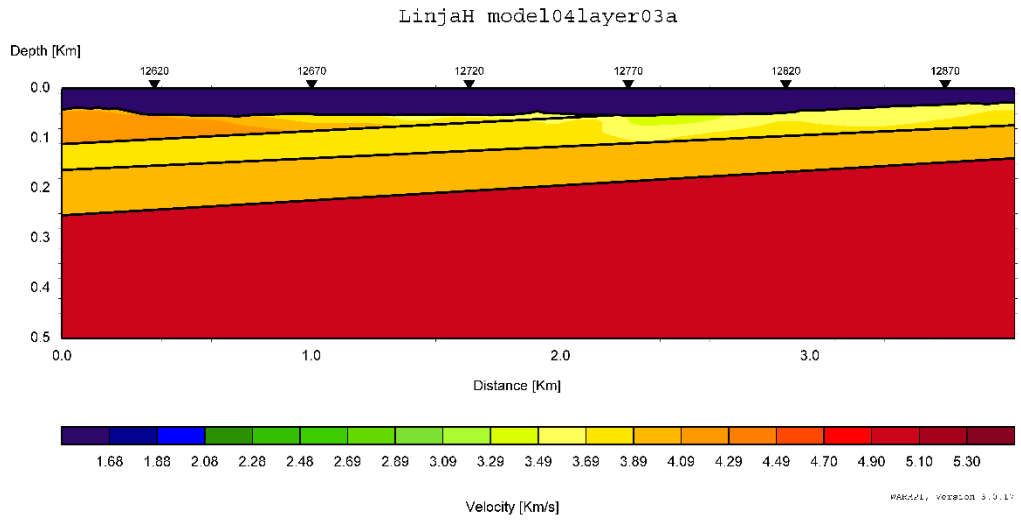
LinjaH model04layer03a
Depth [Km]
12620
12670
12720
12770
12820
12870
0.0
0.1
0.2
0.3
0.4
0.5
0.0
1.0
2.0
3.0
Distance [Km]
1.68
1.88
2.08
2.28
2.48
2.69
2.89
3.09
3.29
3.49
3.69
3.89
4.09
4.29
4.49
4.70
4.90
5.10
5.30
Velocity [Km/s]

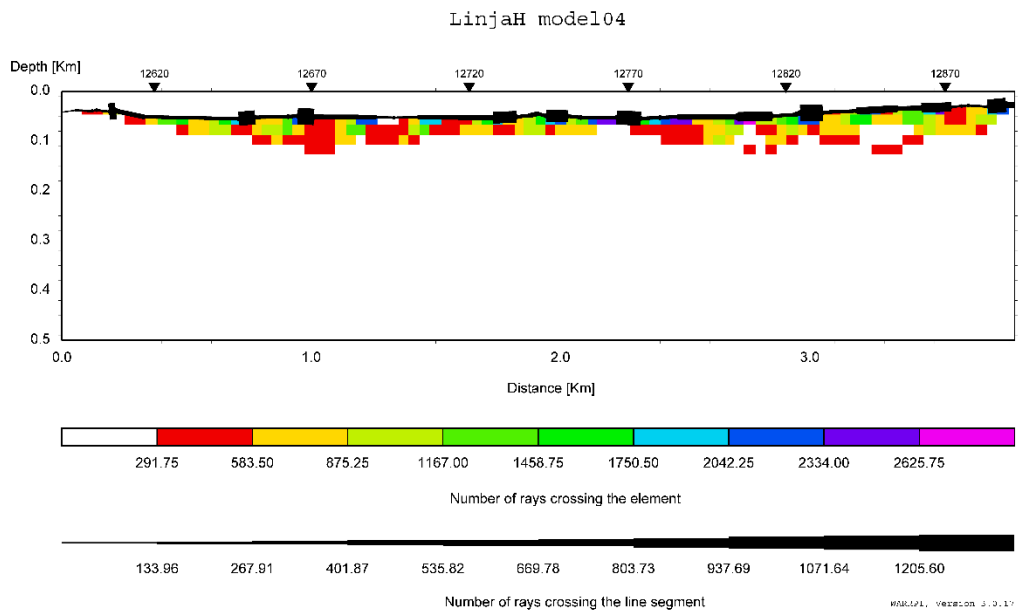
LinjaH model04
Depth [Km]
12620
12670
12720
12770
12820
12870
0.0
0.1
0.2
0.3
0.4
0.5
0.0
1.0
2.0
3.0
Distance [Km]
291.75
583.50
875.25
1167.00
1458.75
1750.50
2042.25
2334.00
2625.75
Number of rays crossing the element
133.96
267.91
401.87
535.82
669.78
803.73
937.69
1071.64
1205.60
Number of rays crossing the line segment

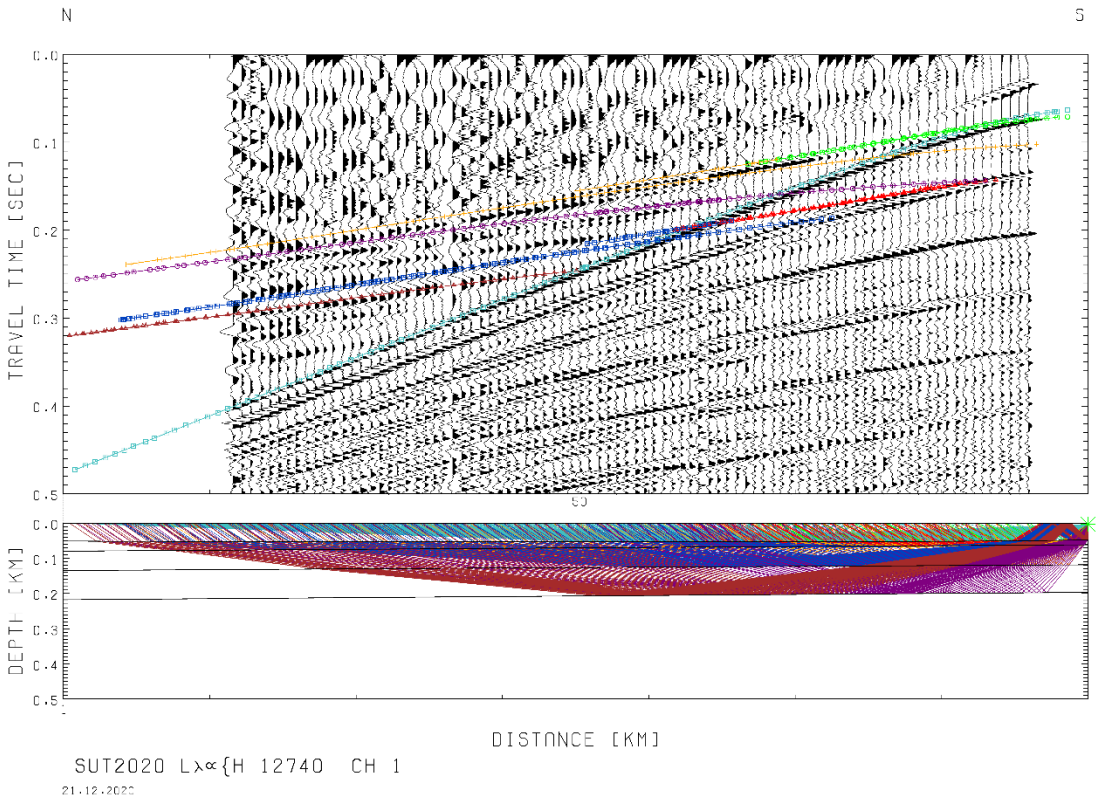
N
S
TRAVEL TIME [SEC]
DEPTH [KM]
DISTANCE [KM]
SUT2020 LλαΣH 12740 CH 1

LinjaP

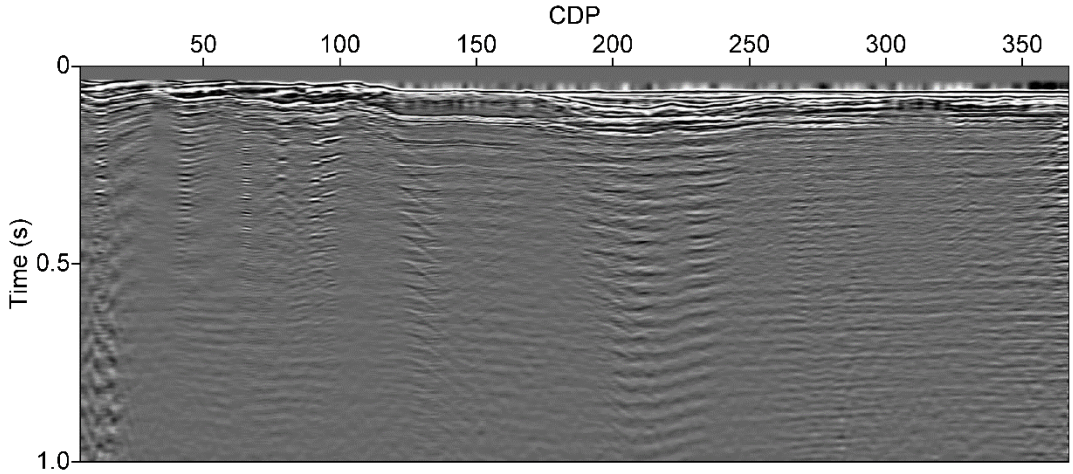

SUT2020_LinjaP model04layer05a

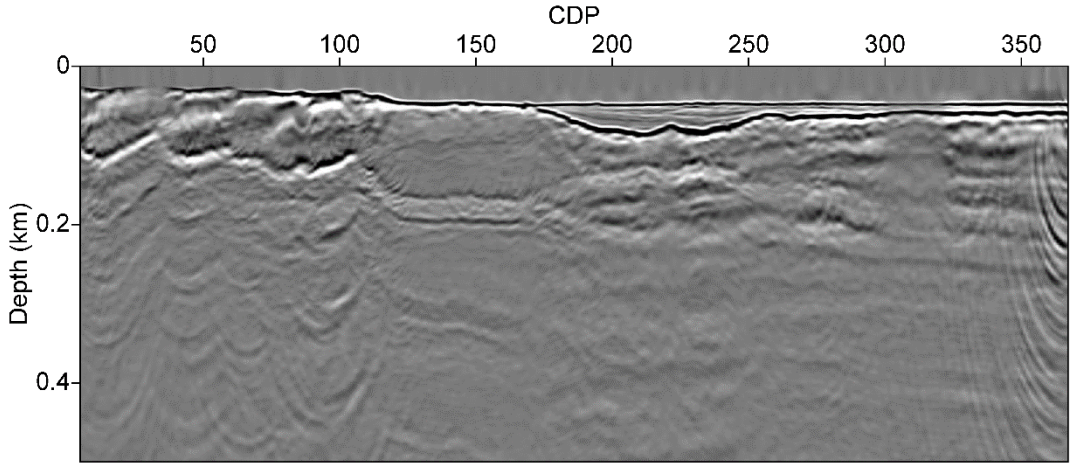

SUT2020_LinjaP model04layer05a

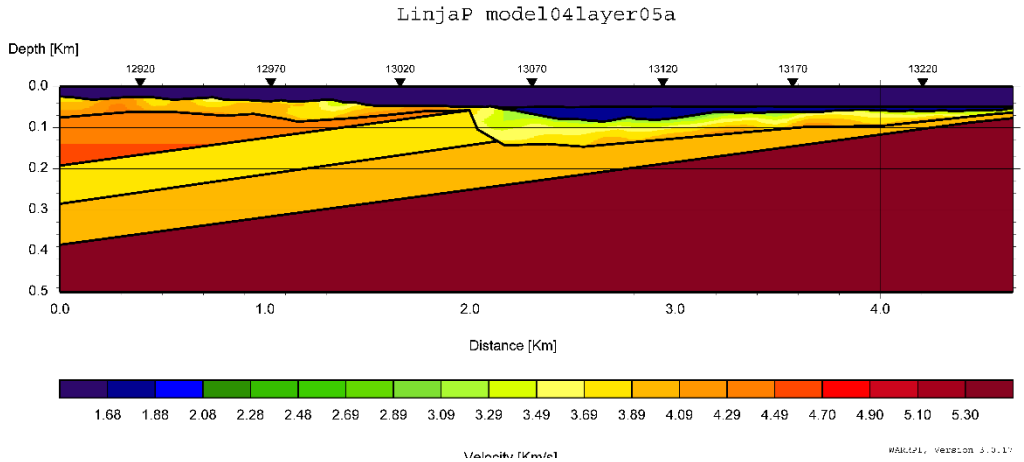

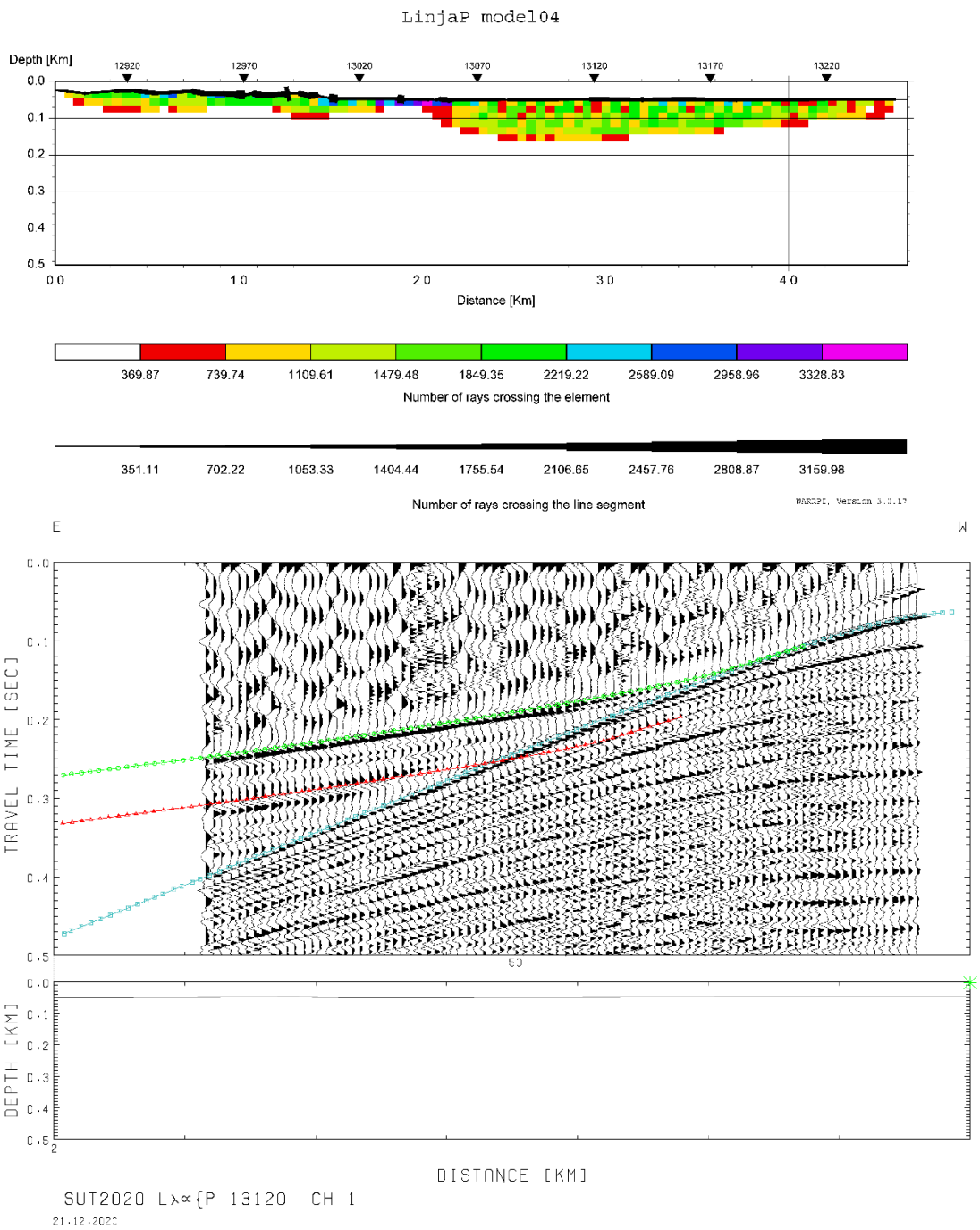
LinjaP model04
Depth [Km]
12920
12970
13020
13070
13120
13170
13220
0.0
0.1
0.2
0.3
0.4
0.5
0.0
1.0
2.0
3.0
4.0
Distance [Km]
369.87
739.74
1109.61
1479.48
1849.35
2219.22
2589.09
2958.96
3328.83
Number of rays crossing the element
351.11
702.22
1053.33
1404.44
1755.54
2106.65
2457.76
2808.87
3159.98
Number of rays crossing the line segment
TRAVEL TIME [SEC]
DEPTH [KM]
DISTANCE [KM]
SUT2020 LJ{P 13120 CH 1

LinjaC1

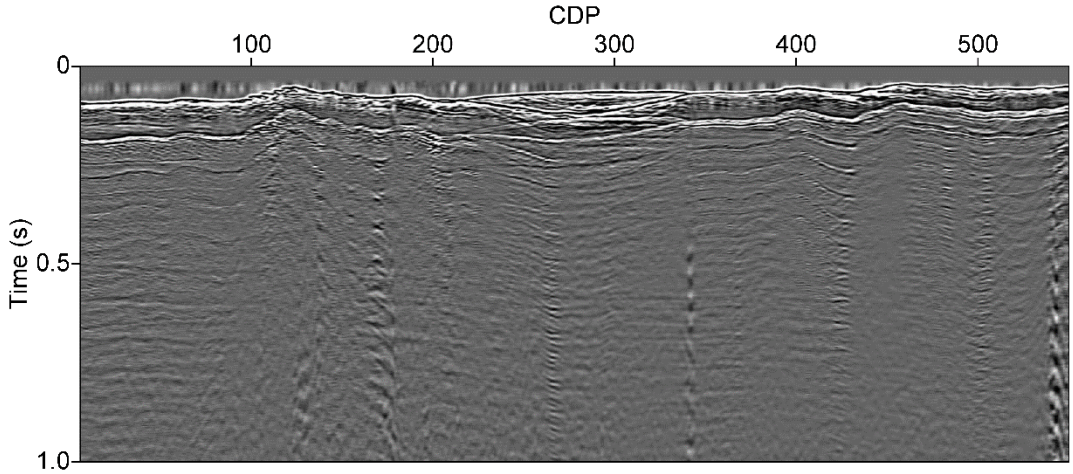

SUT2020_LinjaC1 model04layer05edita

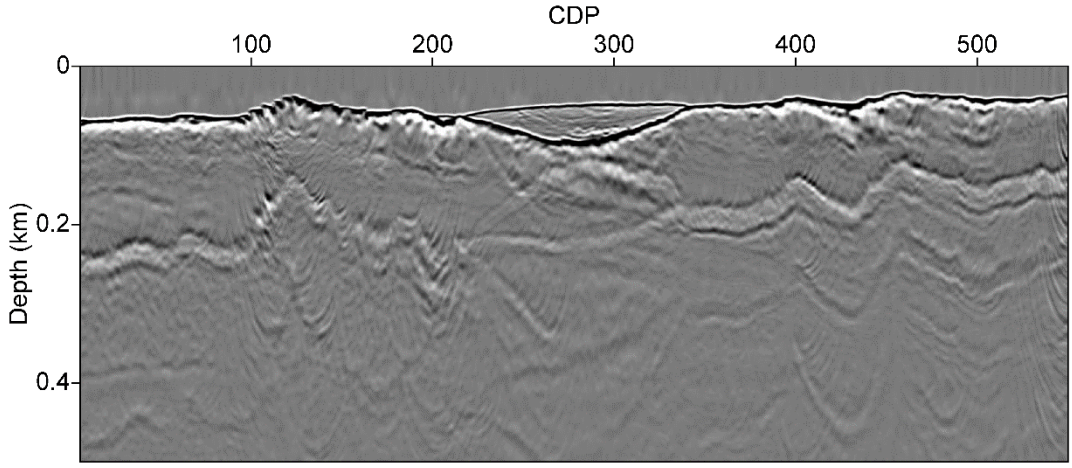

SUT2020_LinjaC1 model04layer05edita

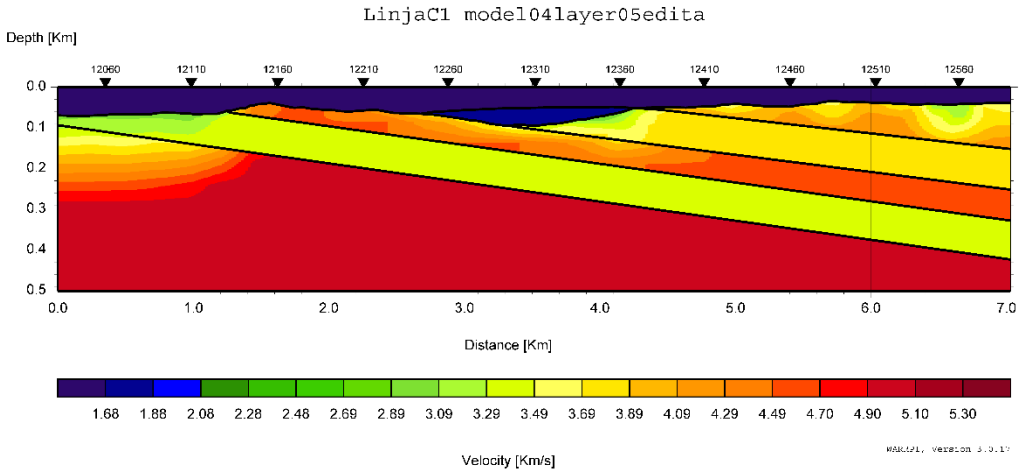

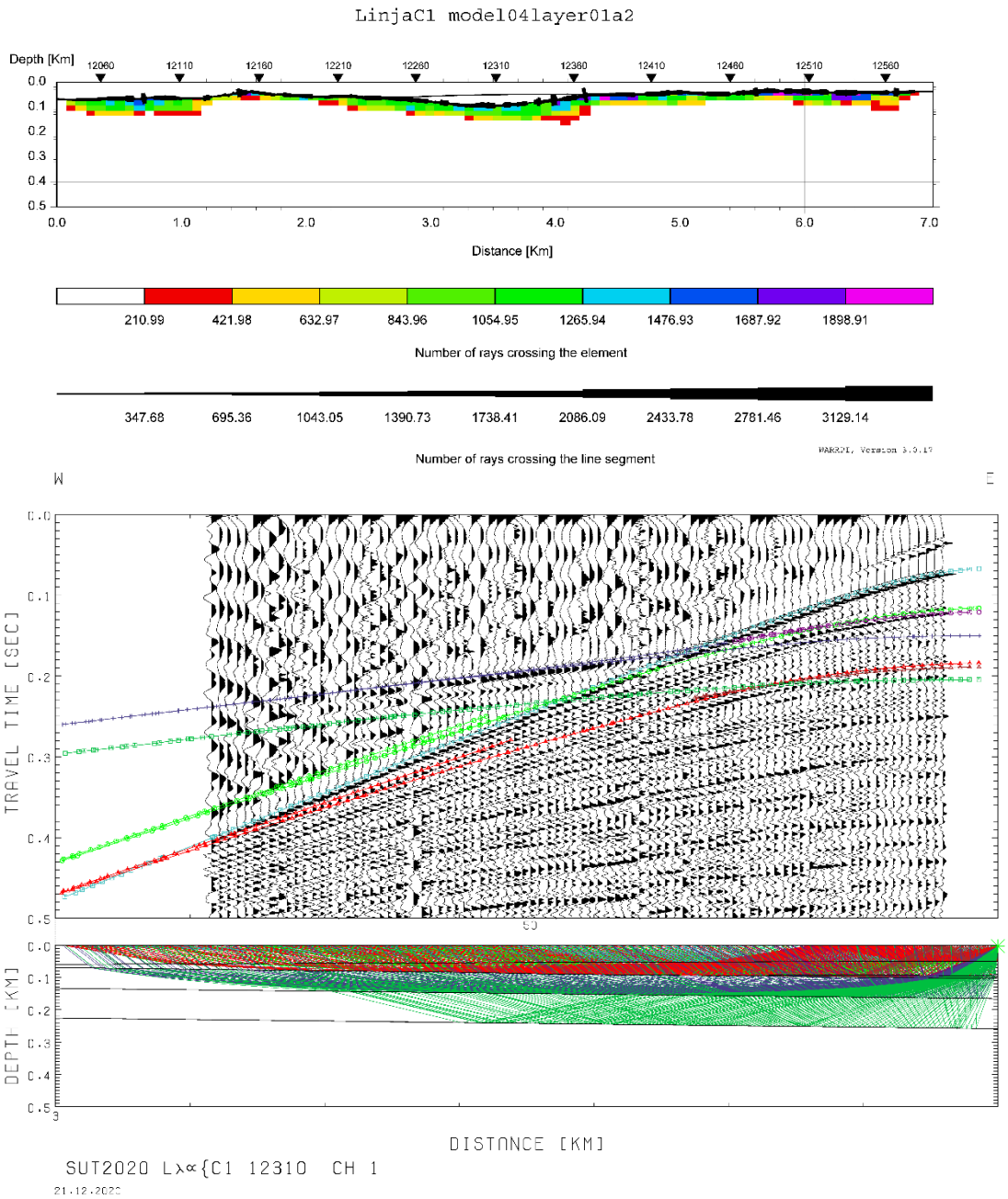
LinjaC1 model04layer01a2
Depth [Km]
12060
12110
12160
12210
12260
12310
12360
12410
12460
12510
12560
0.0
0.1
0.2
0.3
0.4
0.5
0.0
1.0
2.0
3.0
4.0
5.0
6.0
7.0
Distance [Km]
210.99
421.98
632.97
843.96
1054.95
1265.94
1476.93
1687.92
1898.91
Number of rays crossing the element
347.68
695.36
1043.05
1390.73
1738.41
2086.09
2433.78
2781.46
3129.14
Number of rays crossing the line segment
W
E
TRAVEL TIME [SEC]
DEPTH [KM]
DISTANCE [KM]
SUT2020 Lλα{C1 12310 CH 1

LinjaD

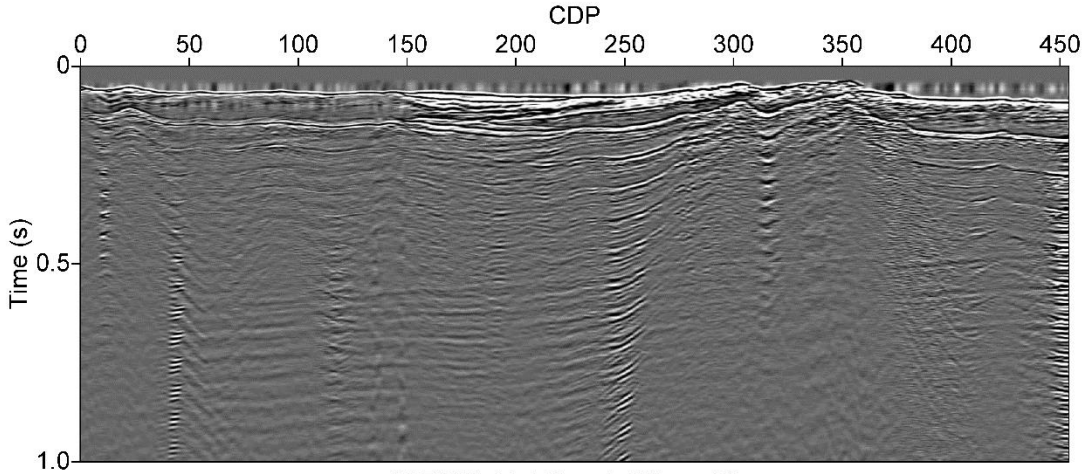

SUT2020_LinjaD model03layer06ba

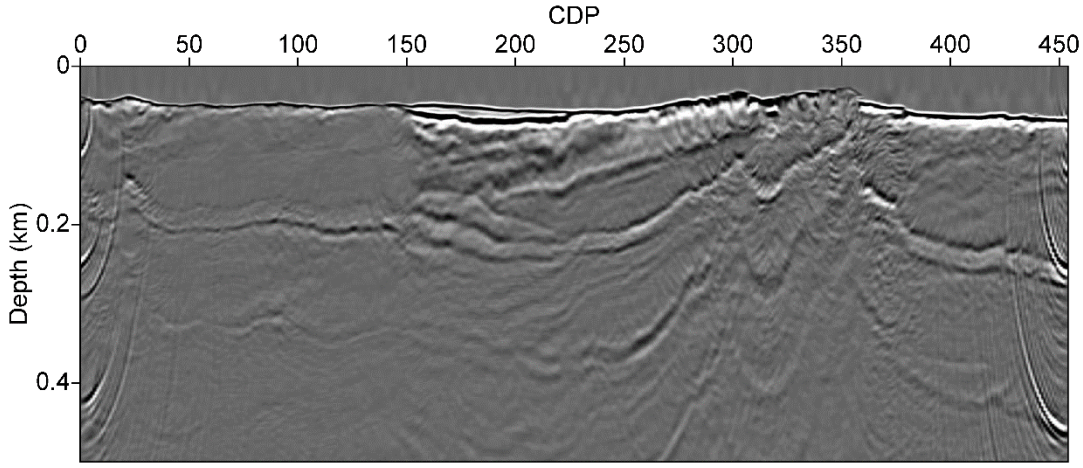

SUT2020_LinjaD model03layer06ba

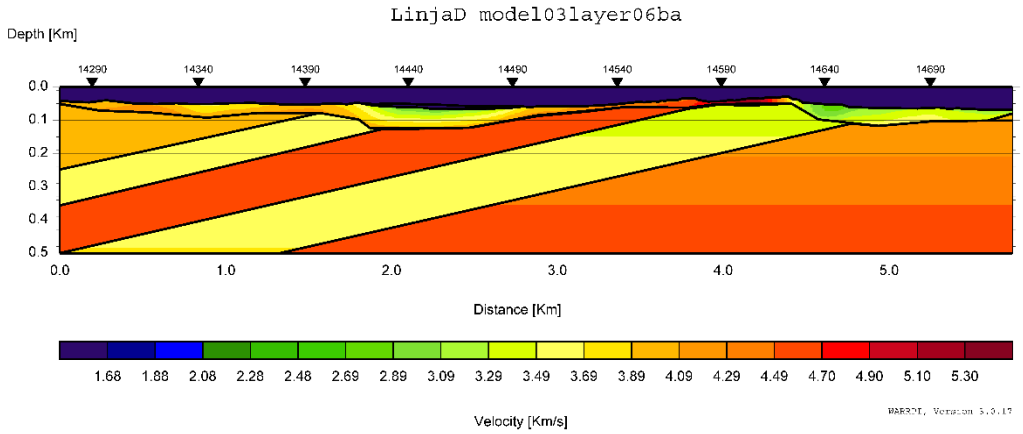

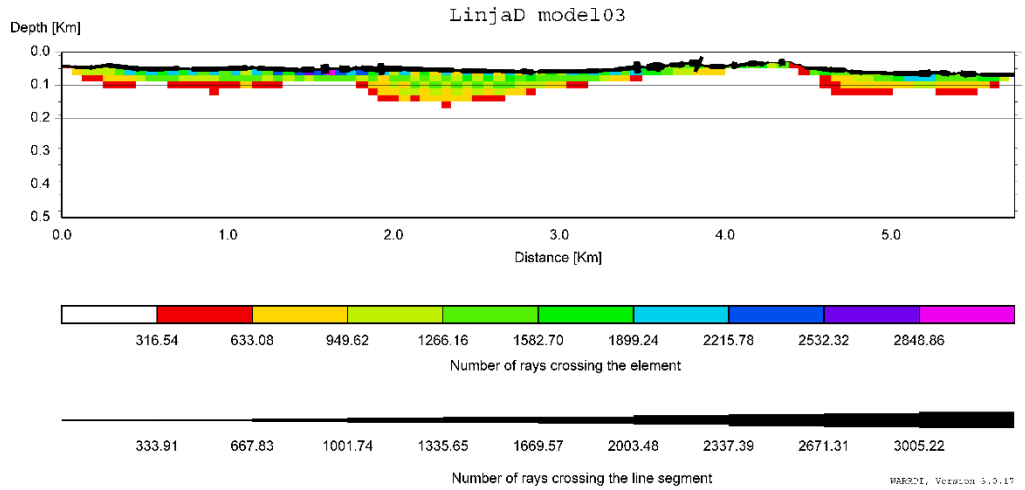
LinjaD model03
Depth [Km]
0.0
0.1
0.2
0.3
0.4
0.5
0.0
1.0
2.0
3.0
4.0
5.0
Distance [Km]
316.54
633.08
949.62
1266.16
1582.70
1899.24
2215.78
2532.32
2848.86
Number of rays crossing the element
333.91
667.83
1001.74
1335.65
1669.57
2003.48
2337.39
2671.31
3005.22
Number of rays crossing the line segment

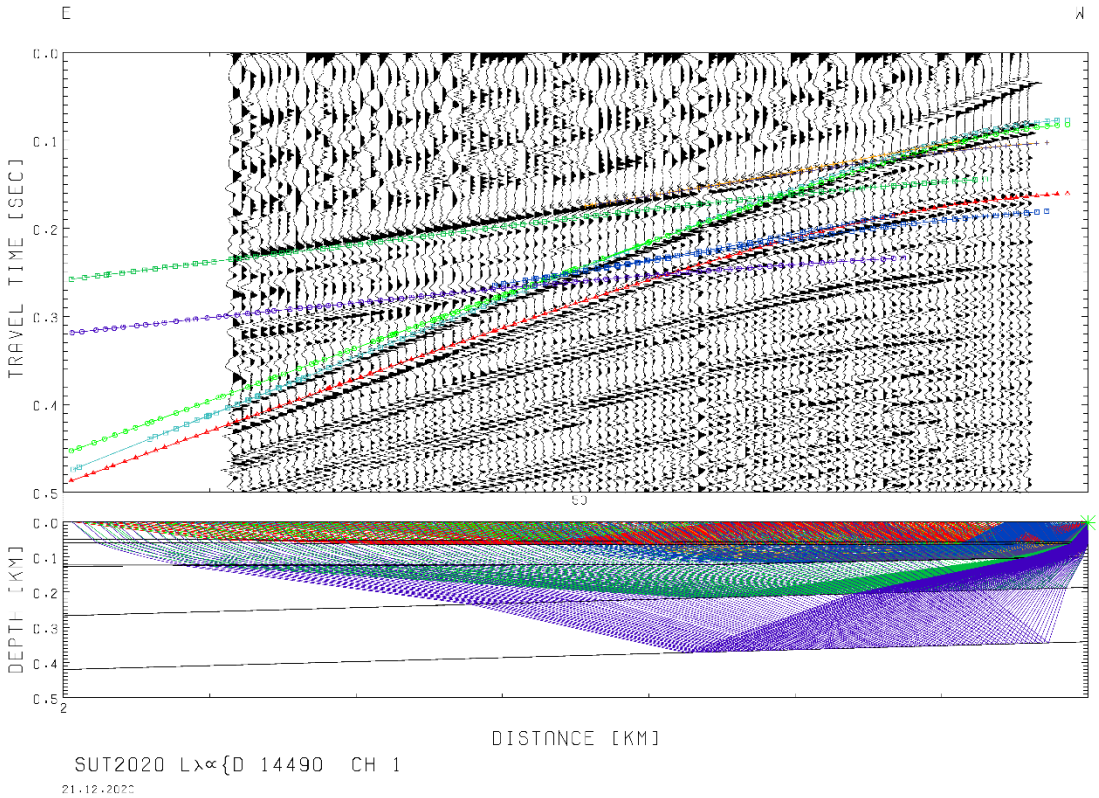
TRAVEL TIME [SEC]
DEPTH [KM]
DISTANCE [KM]
SUT2020 L{D 14490 CH 1

LinjaA

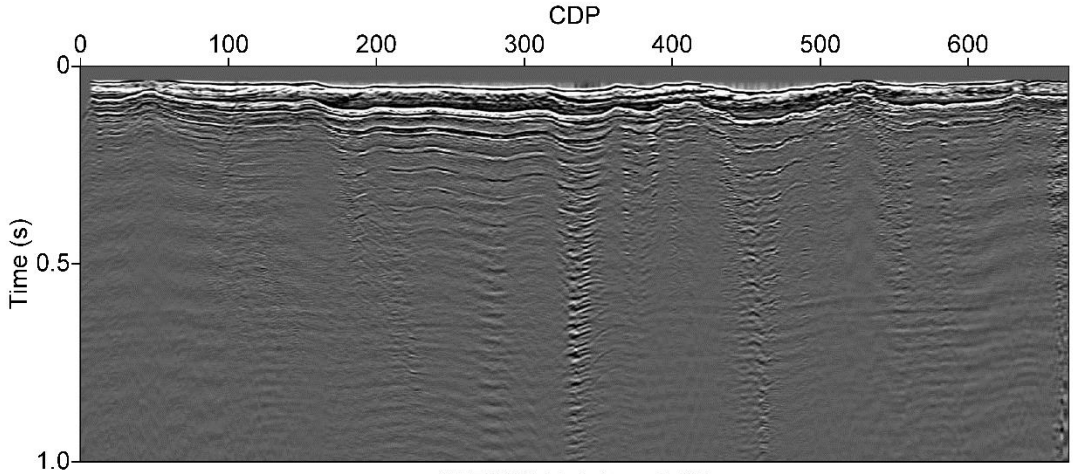

SUT2020_LinjaA model04

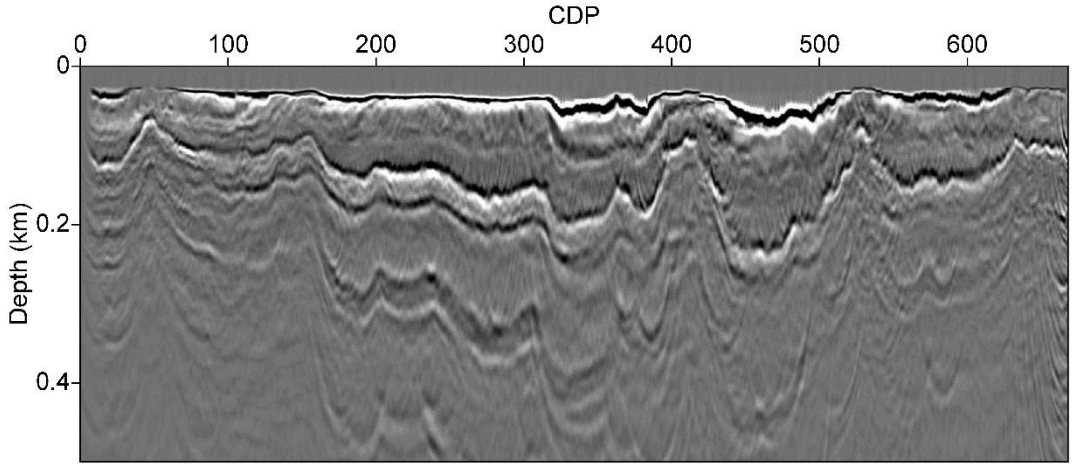

SUT2020_LinjaA model04

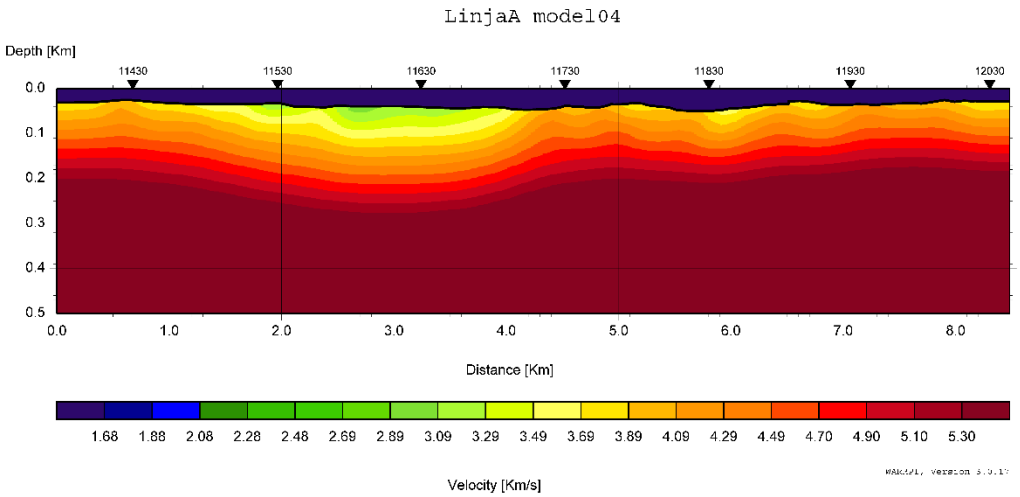

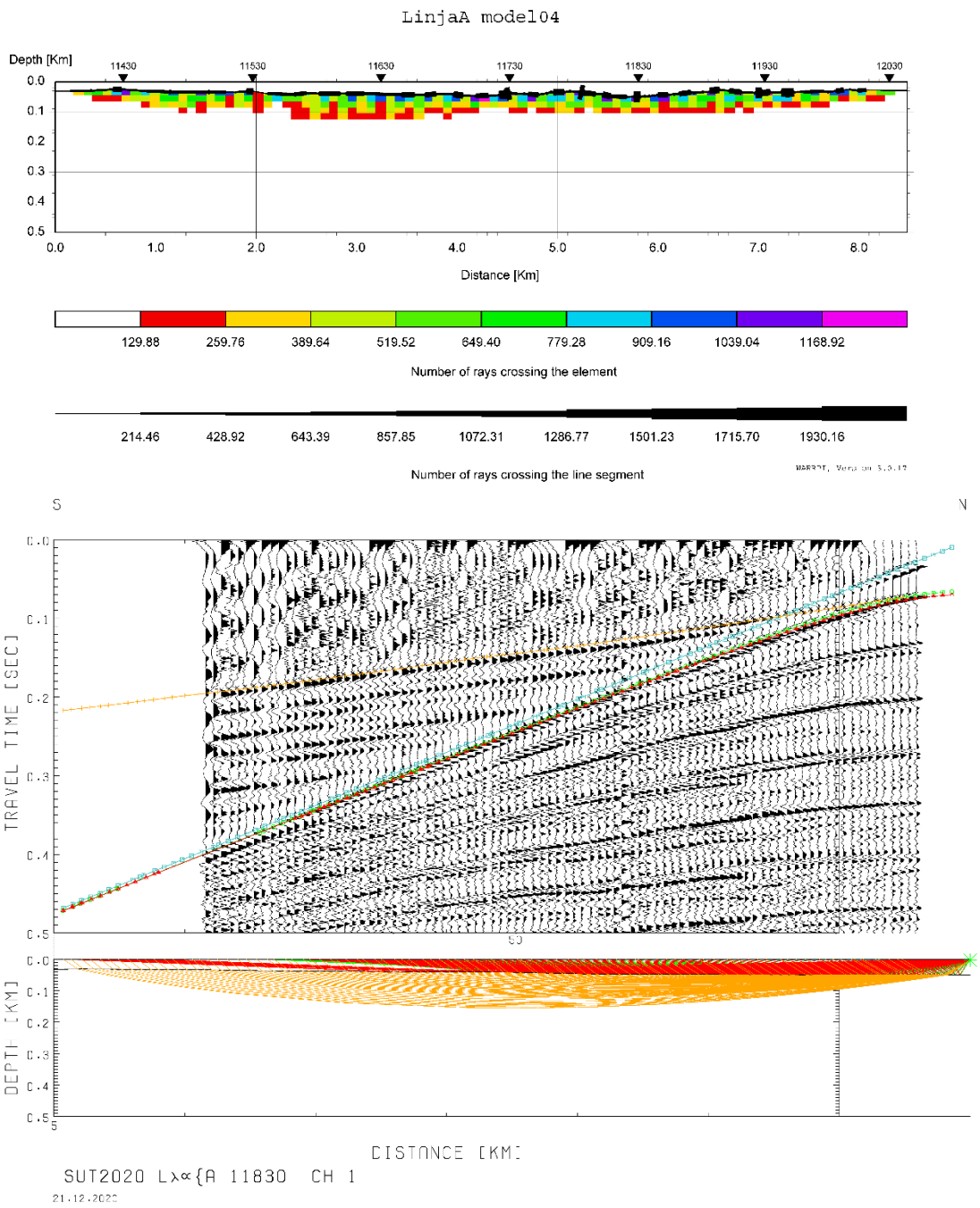
LinjaA model04
Depth [Km]
11430
11530
11630
11730
11830
11930
12030
Distance [Km]
129.88
259.76
389.64
519.52
649.40
779.28
909.16
1039.04
1168.92
Number of rays crossing the element
214.46
428.92
643.39
857.85
1072.31
1286.77
1501.23
1715.70
1930.16
Number of rays crossing the line segment
S
N
TRAVEL TIME [SEC]
DEPTH [KM]
DISTANCE [KM]
SUT2020 LλαΘA 11830 CH 1
21.12.2020

LinjaJ

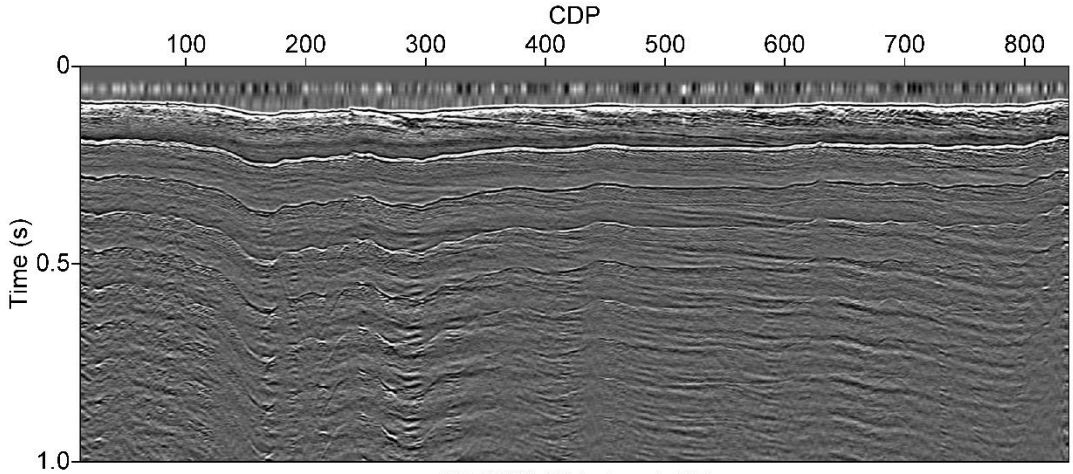

SUT2020_LinjaJ model05

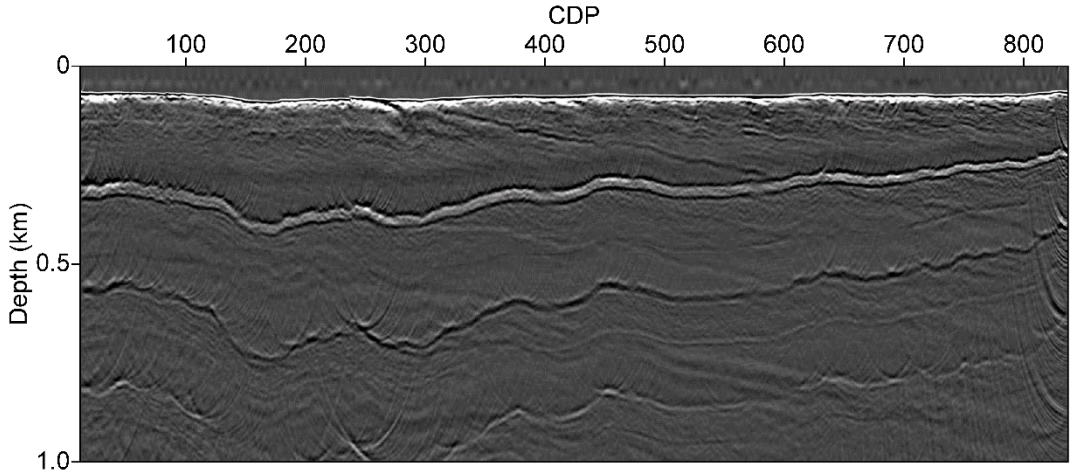

SUT2020_LinjaJ model05

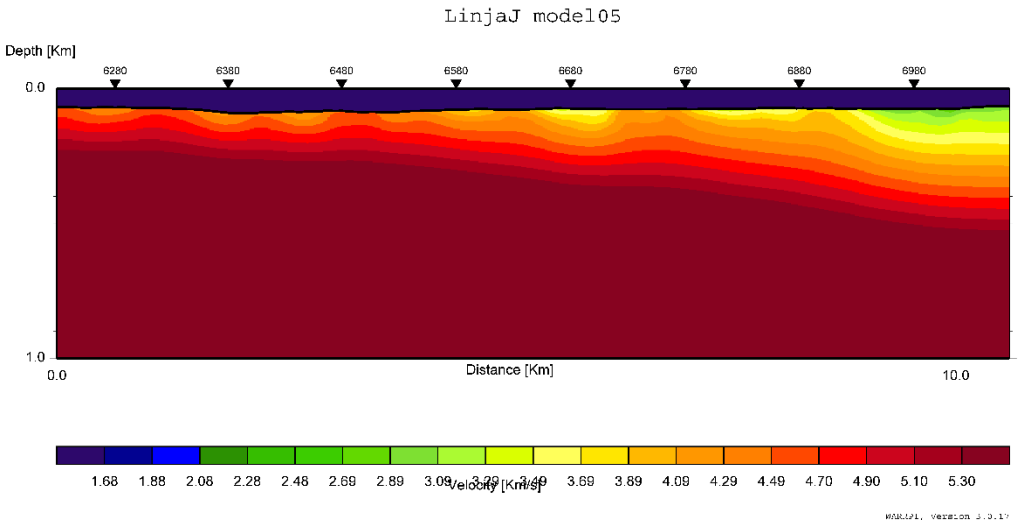

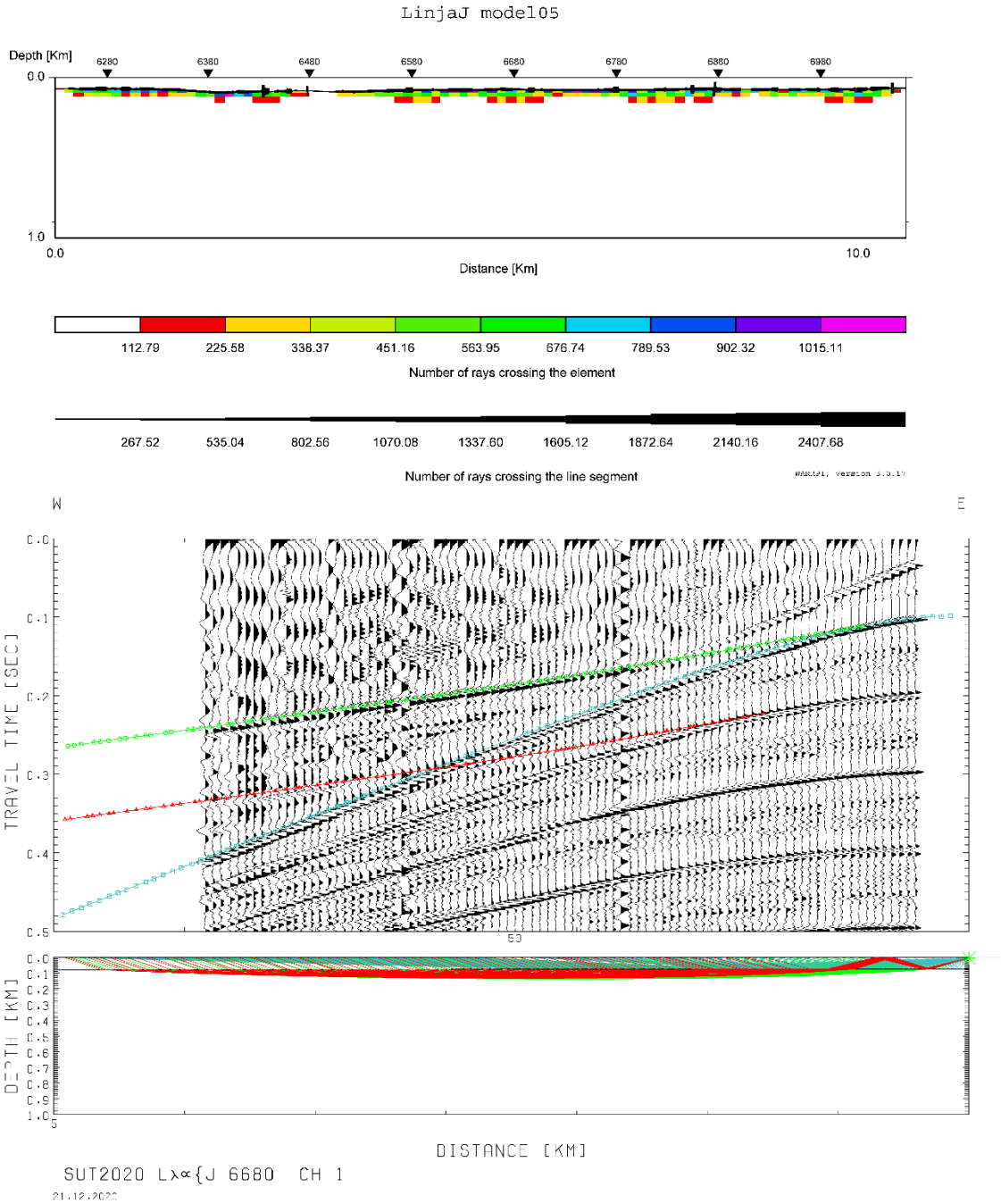
LinjaJ model05
Depth [Km]
6280
6380
6480
6580
6680
6780
6880
6980
0.0
1.0
0.0
10.0
Distance [Km]
112.79
225.58
338.37
451.16
563.95
676.74
789.53
902.32
1015.11
Number of rays crossing the element
267.52
535.04
802.56
1070.08
1337.60
1605.12
1872.64
2140.16
2407.68
Number of rays crossing the line segment
W
E
TRAVEL TIME [SEC]
DEPTH [KM]
DISTANCE [KM]
SUT2020 Lλα{J 6680 CH 1

LinjaM

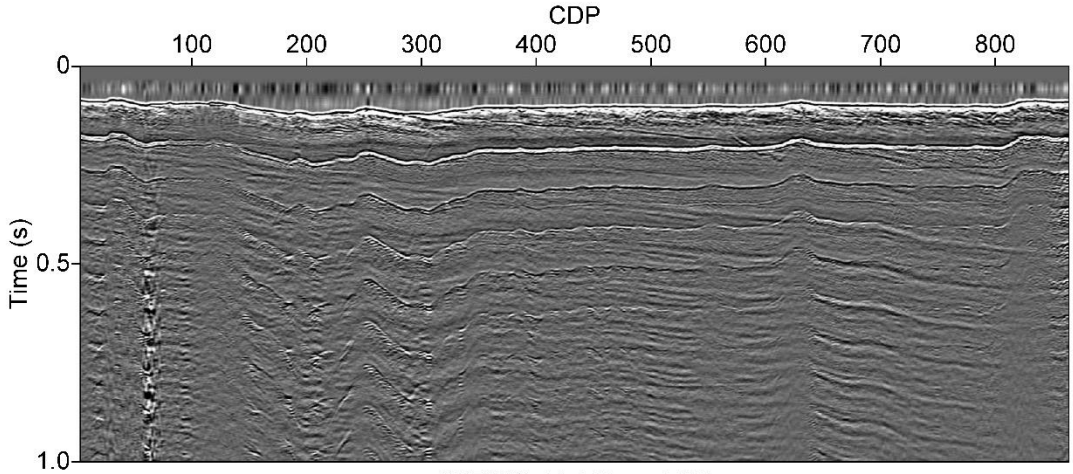

SUT2020_LinjaM model05

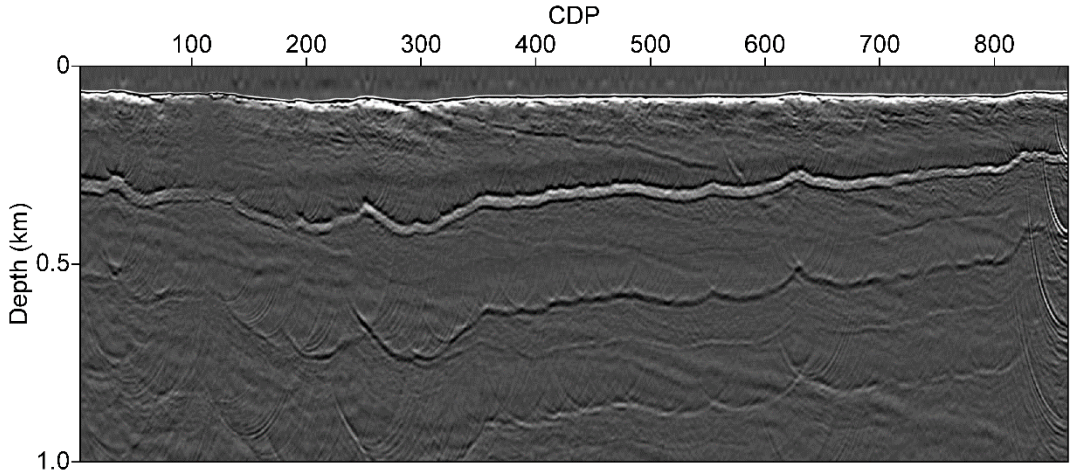

SUT2020_LinjaM model05

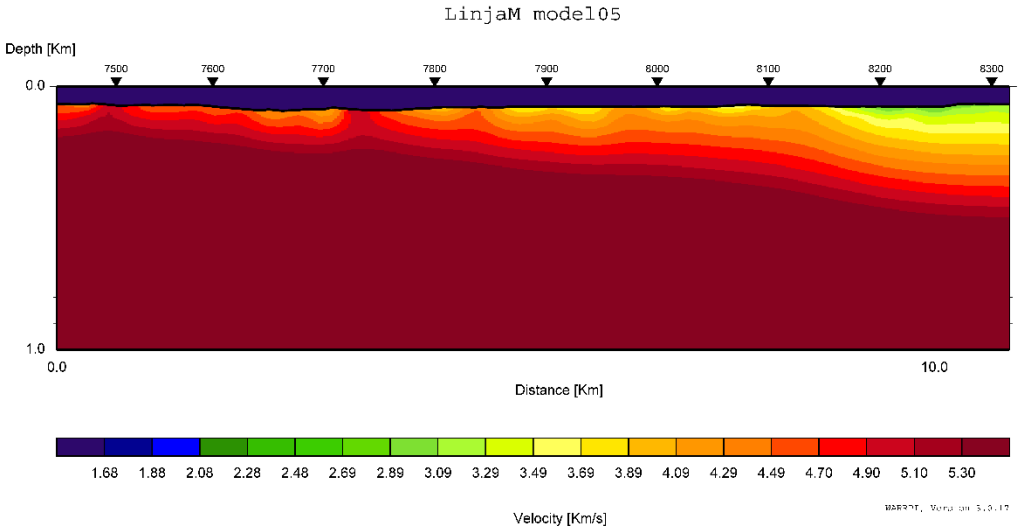

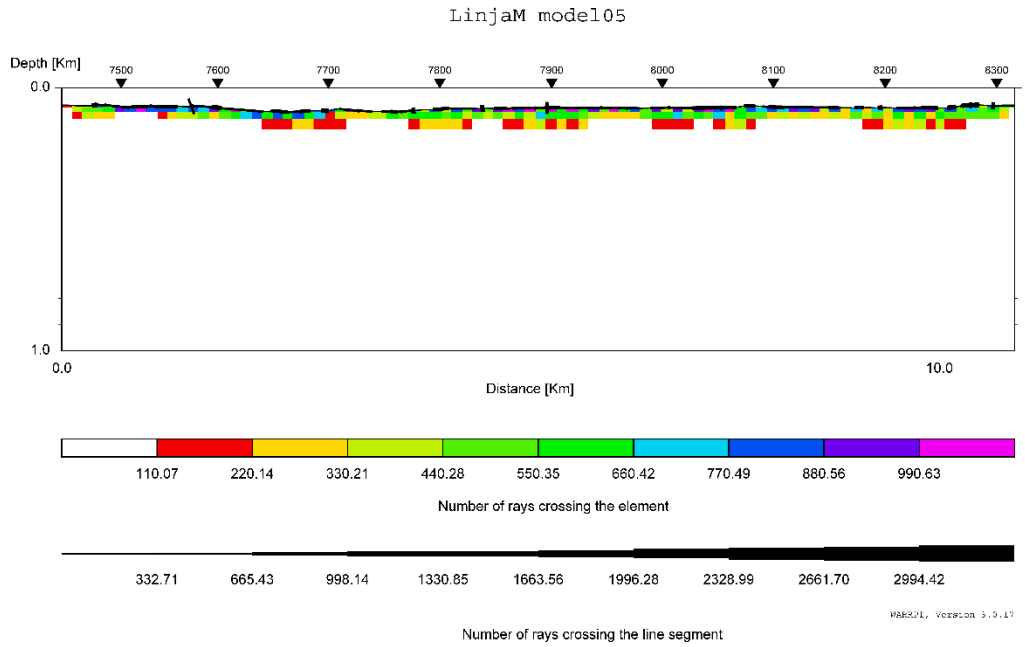
LinjaM model05
Depth [Km]
7500
7600
7700
7800
7900
8000
8100
8200
8300
0.0
1.0
0.0
10.0
Distance [Km]
110.07
220.14
330.21
440.28
550.35
660.42
770.49
880.56
990.63
Number of rays crossing the element
332.71
665.43
998.14
1330.85
1663.56
1996.28
2328.99
2661.70
2994.42
Number of rays crossing the line segment

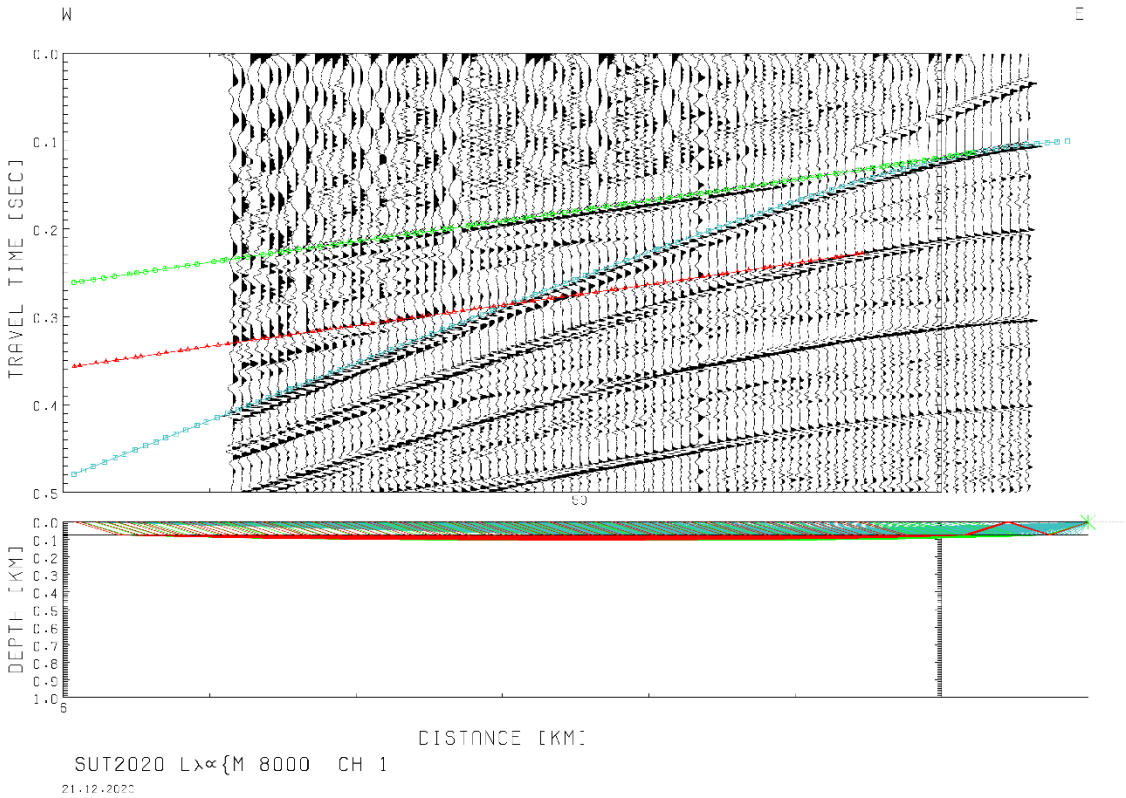
W
E
TRAVEL TIME [SEC]
DEPTH [KM]
DISTANCE [KM]
SUT2020 LJ{M 8000 CH 1
21.12.2020

LinjaK

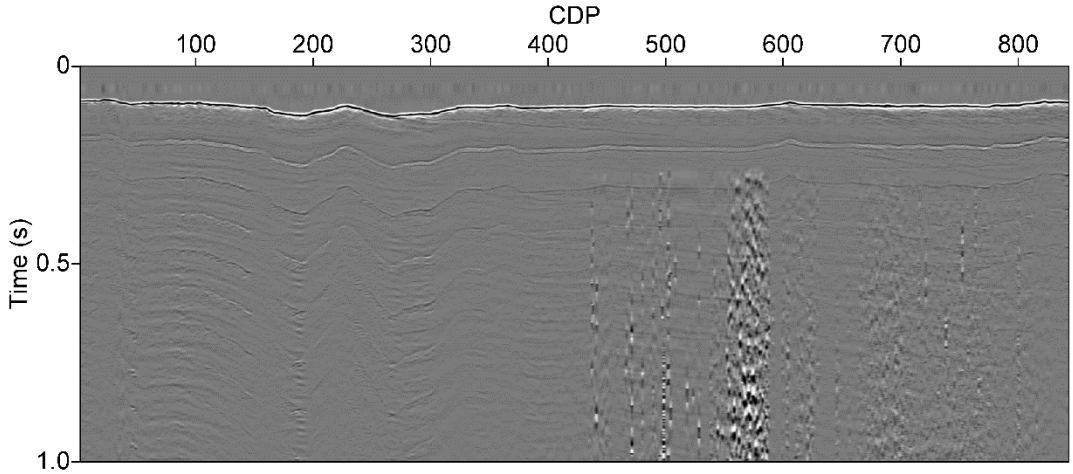

SUT2020_LinjaK model05

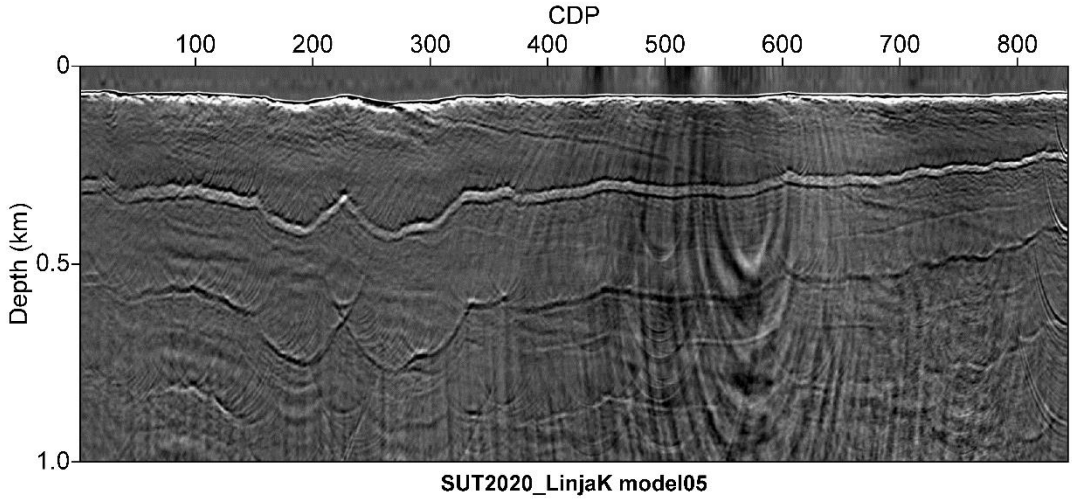

SUT2020_LinjaK model05

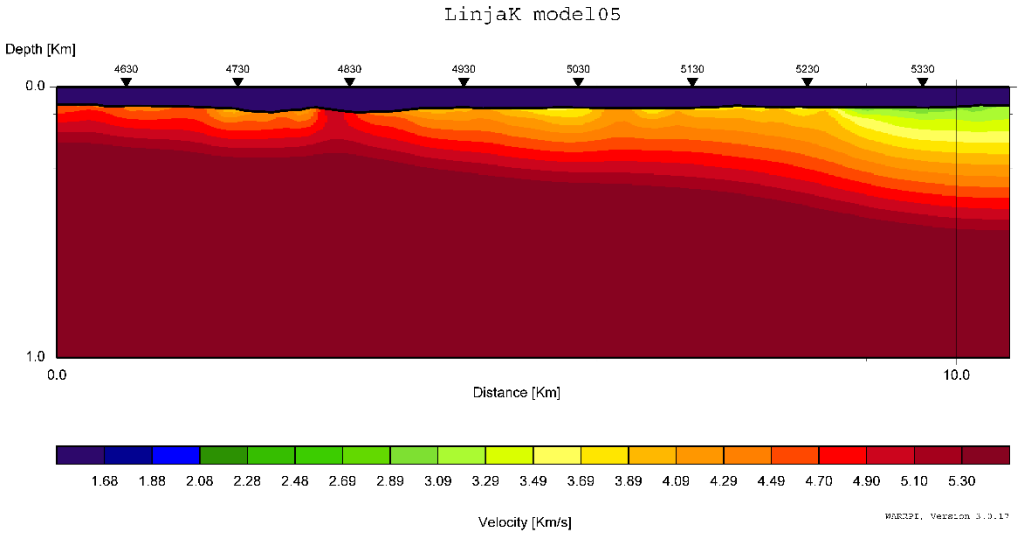

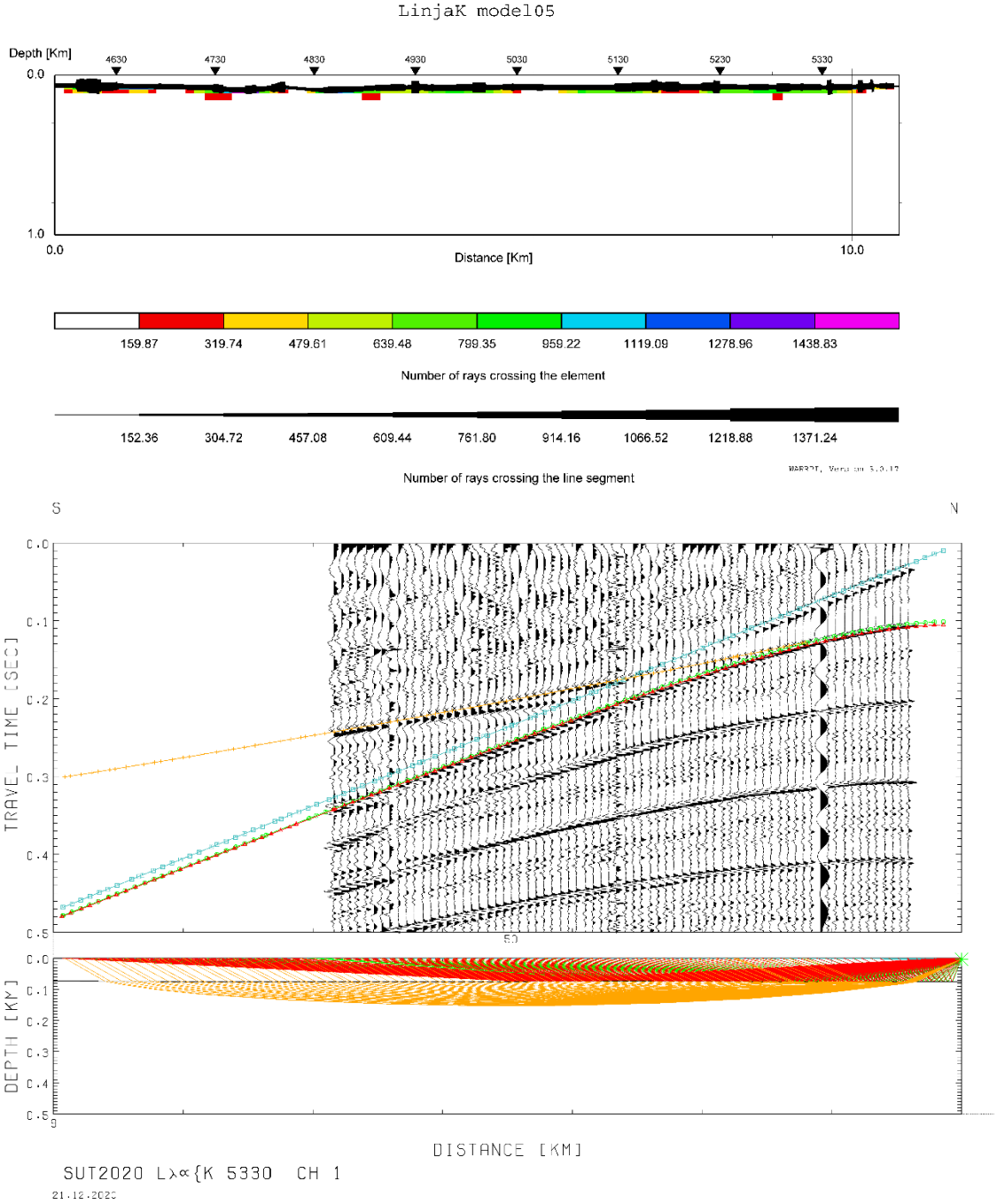
LinjaK model05
Depth [Km]
4630
4730
4830
4930
5030
5130
5230
5330
0.0
1.0
0.0
10.0
Distance [Km]
159.87
319.74
479.61
639.48
799.35
959.22
1119.09
1278.96
1438.83
Number of rays crossing the element
152.36
304.72
457.08
609.44
761.80
914.16
1066.52
1218.88
1371.24
Number of rays crossing the line segment
S
N
TRAVEL TIME [SEC]
DEPTH [KM]
DISTANCE [KM]
SUT2020 LJ{K 5330 CH 1

LinjaU1

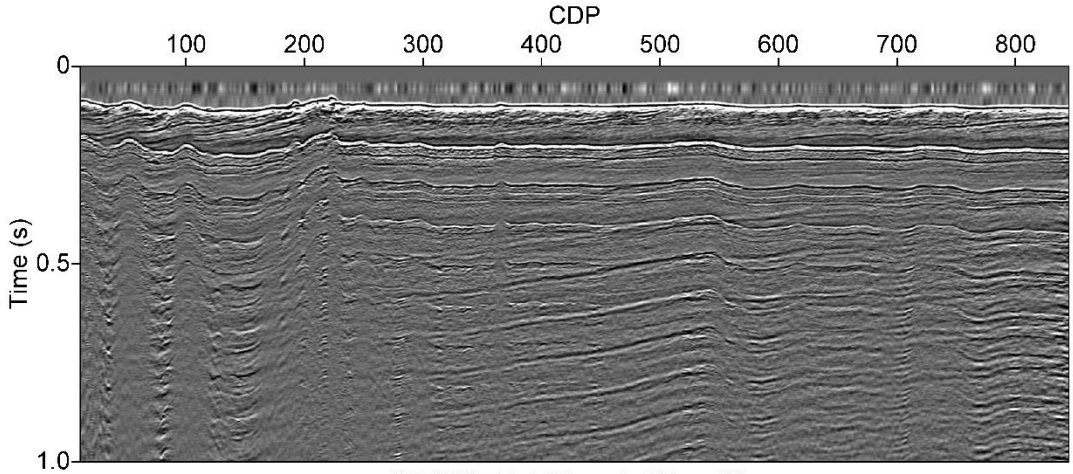

SUT2020_LinjaU1 model05layer03a

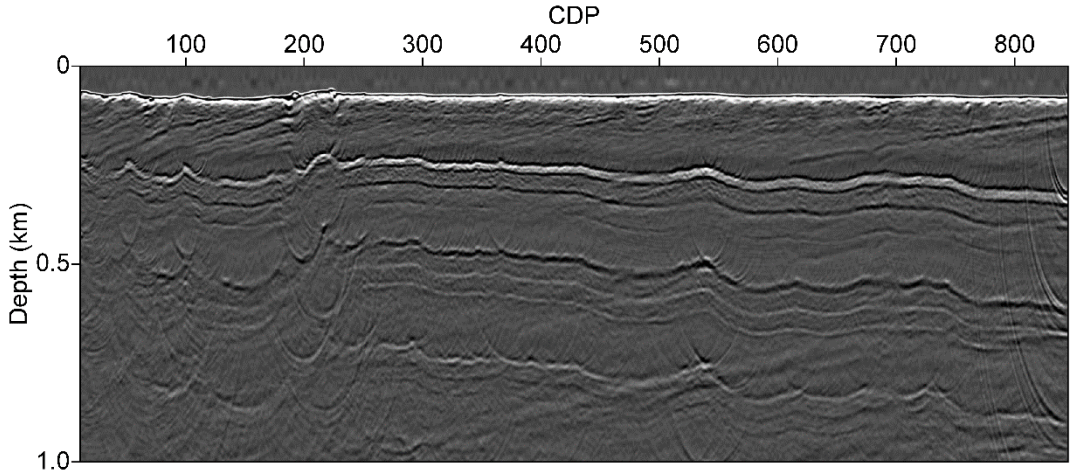

SUT2020_LinjaU1 model05layer03a

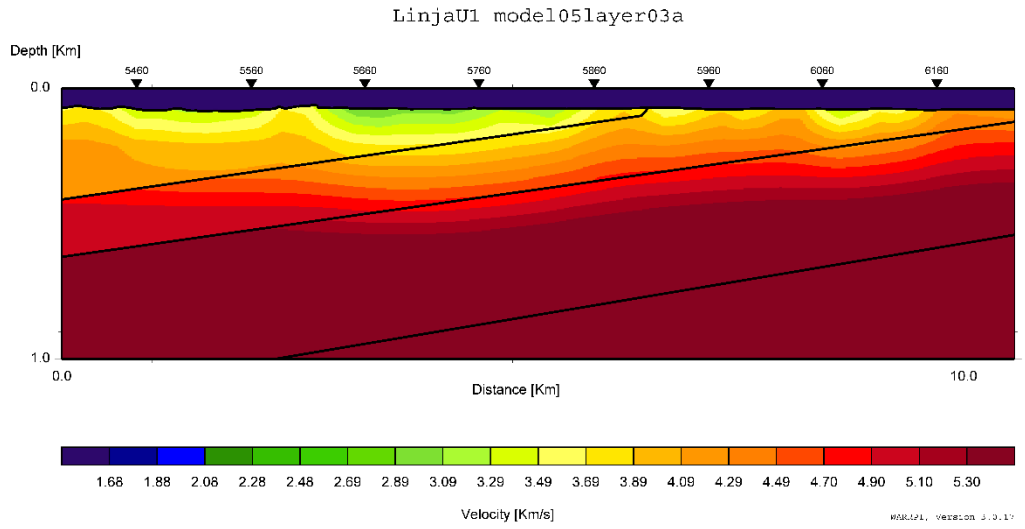

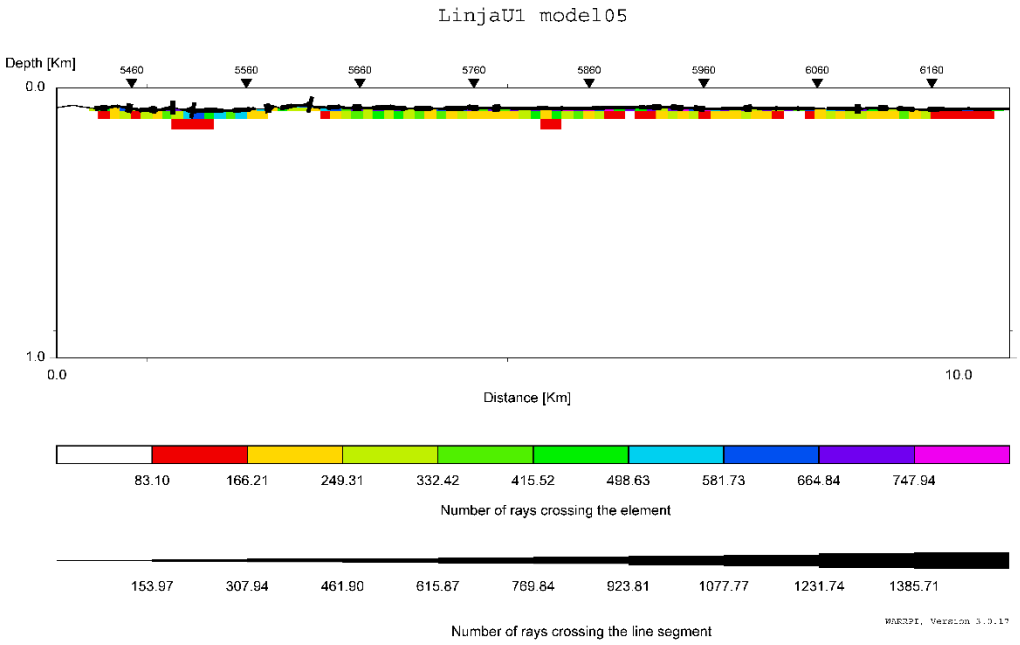
LinjaU1 model05
Depth [Km]
5460
5560
5660
5760
5860
5960
6060
6160
0.0
1.0
0.0
10.0
Distance [Km]
83.10
166.21
249.31
332.42
415.52
498.63
581.73
664.84
747.94
Number of rays crossing the element
153.97
307.94
461.90
615.87
769.84
923.81
1077.77
1231.74
1385.71
Number of rays crossing the line segment

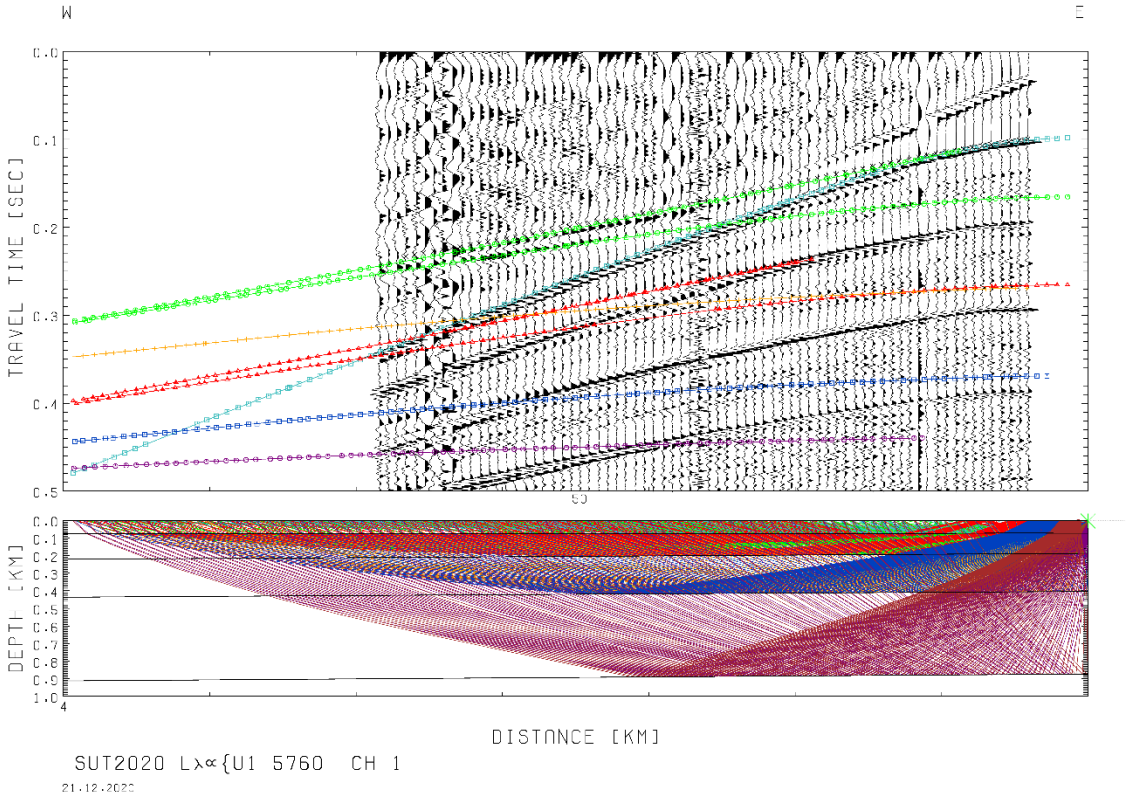
W
E
TRAVEL TIME [SEC]
DEPTH [KM]
DISTANCE [KM]
SUT2020 LλαU1 5760 CH 1

LinjaT1

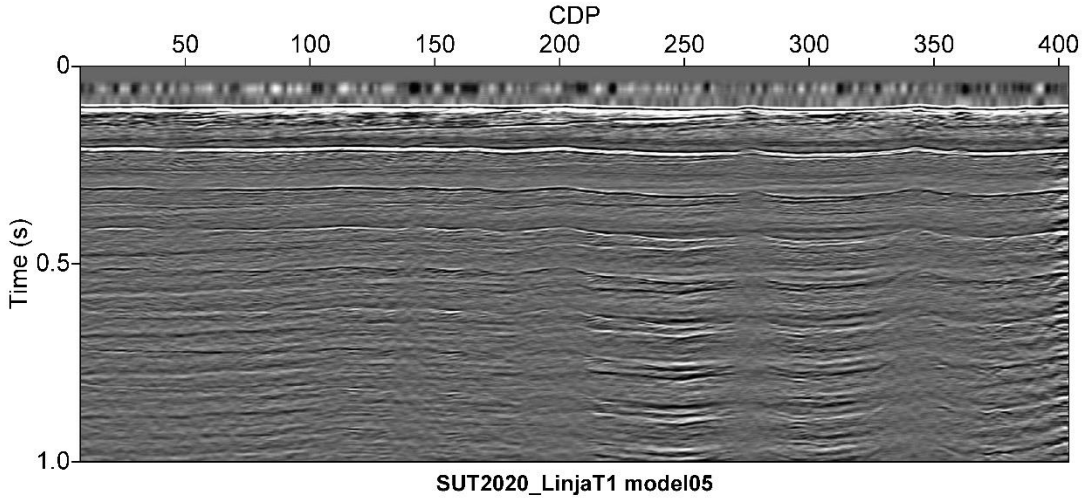
CDP
50
100
150
200
250
300
350
400
0
Time (s)
0.5
1.0
SUT2020_LinjaT1 model05

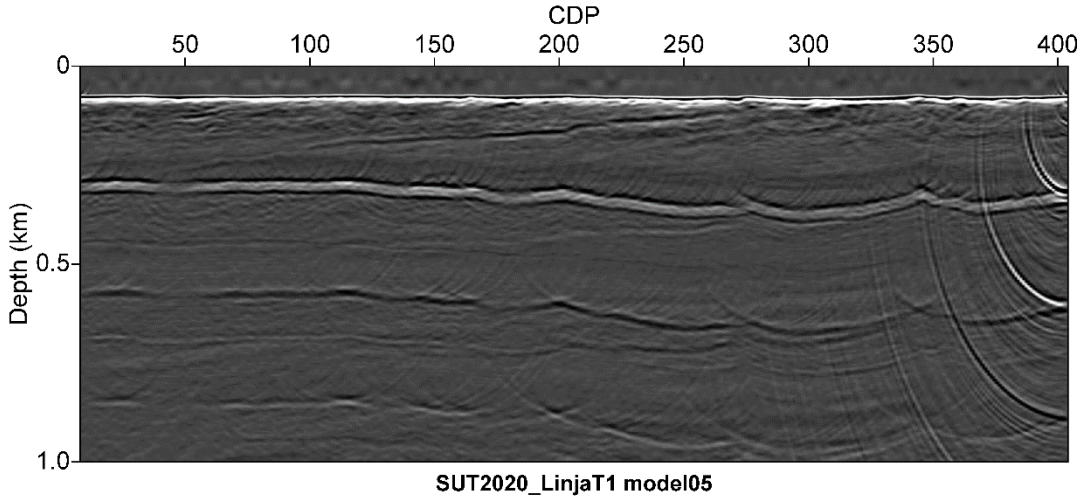
CDP
50
100
150
200
250
300
350
400
0
Depth (km)
0.5
1.0
SUT2020_LinjaT1 model05

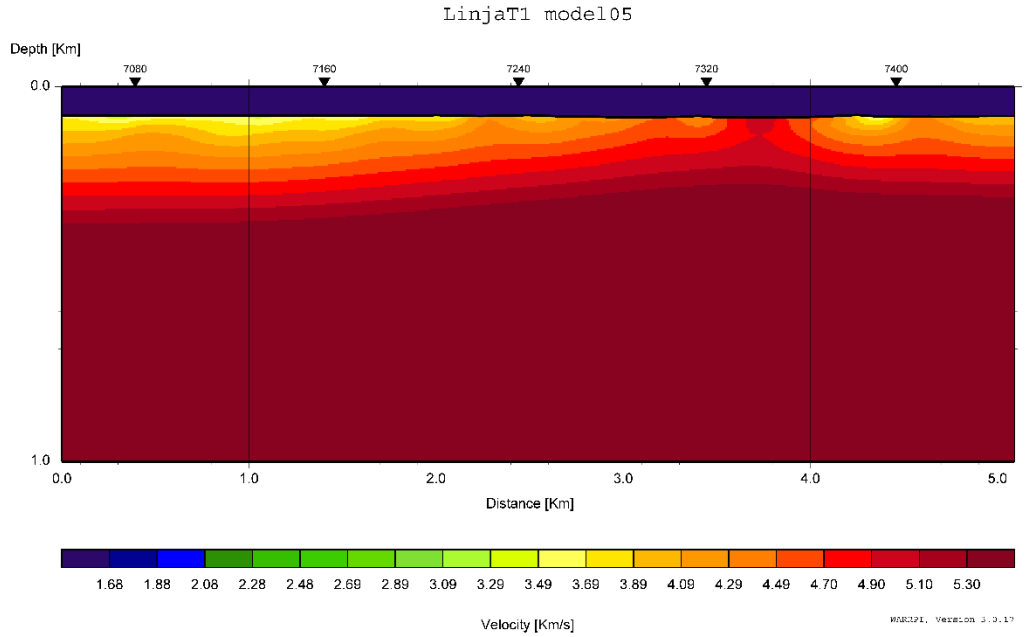
LinjaT1 model05
Depth [Km]
7080
7160
7240
7320
7400
0.0
1.0
0.0
1.0
2.0
3.0
4.0
5.0
Distance [Km]
1.68
1.88
2.08
2.28
2.48
2.69
2.89
3.09
3.29
3.49
3.69
3.89
4.09
4.29
4.49
4.70
4.90
5.10
5.30
Velocity [Km/s]

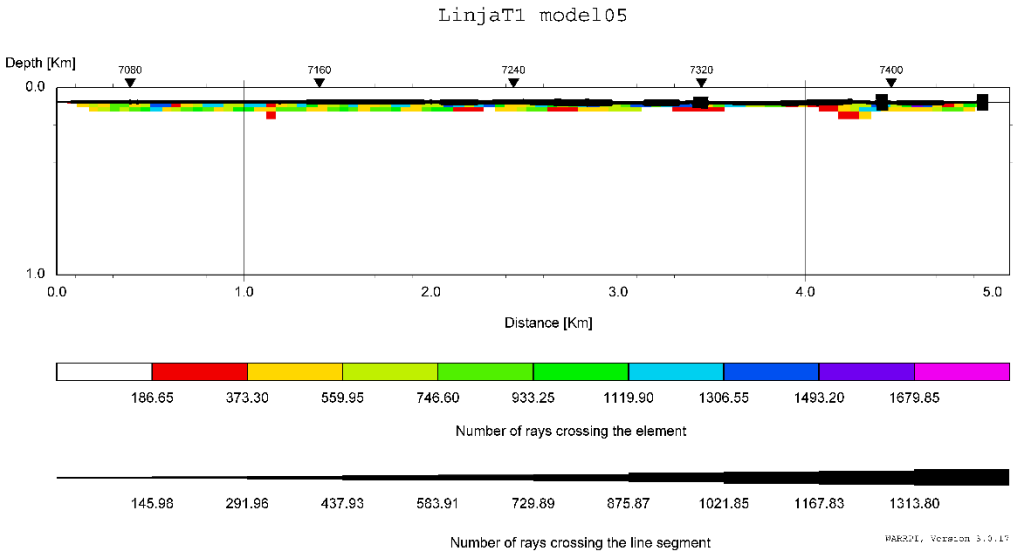
LinjaT1 model05
Depth [Km]
7080
7160
7240
7320
7400
0.0
1.0
0.0
1.0
2.0
3.0
4.0
5.0
Distance [Km]
186.65
373.30
559.95
746.60
933.25
1119.90
1306.55
1493.20
1679.85
Number of rays crossing the element
145.98
291.96
437.93
583.91
729.89
875.87
1021.85
1167.83
1313.80
Number of rays crossing the line segment

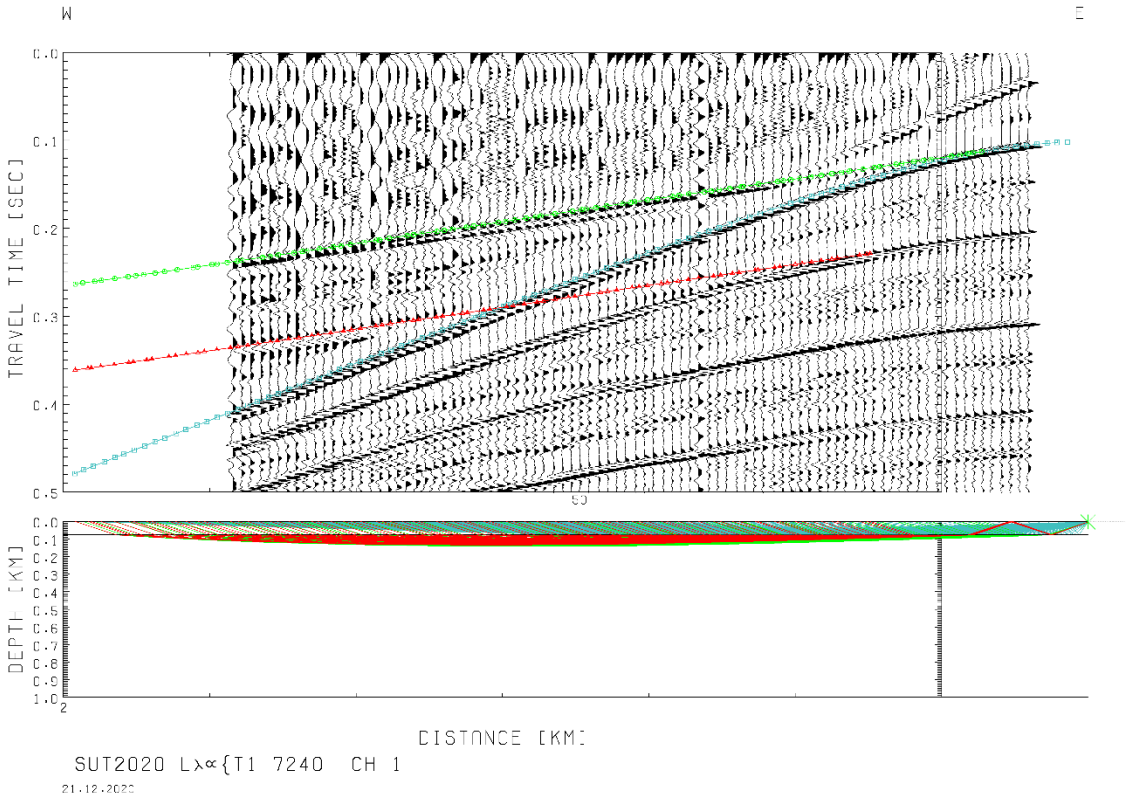
W
E
TRAVEL TIME [SEC]
0.0
0.1
0.2
0.3
0.4
0.5
50
DEPTH [KM]
0.0
0.1
0.2
0.3
0.4
0.5
0.6
0.7
0.8
0.9
1.0
DISTANCE [KM]
SUT2020 LJA{T1 7240 CH 1
21.12.2020

LinjaS1

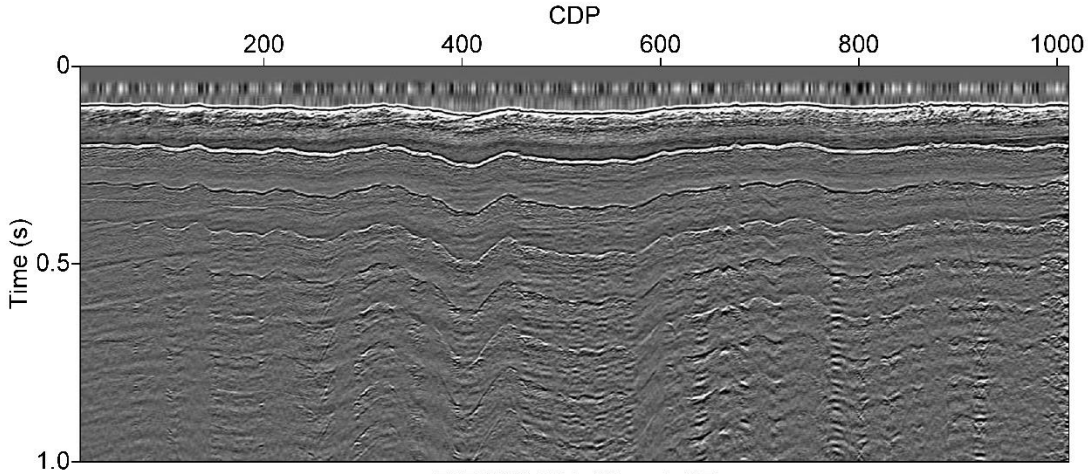

SUT2020_LinjaS1 model05

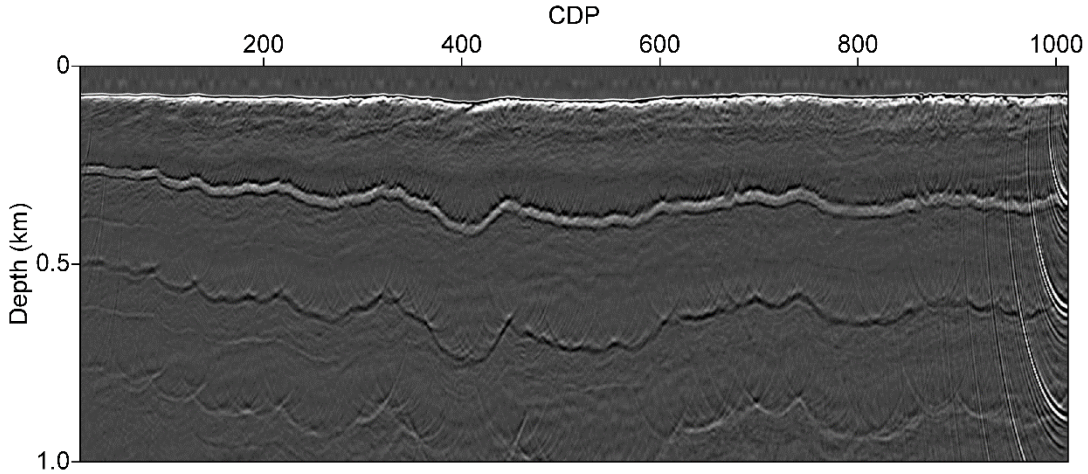

SUT2020_LinjaS1 model05

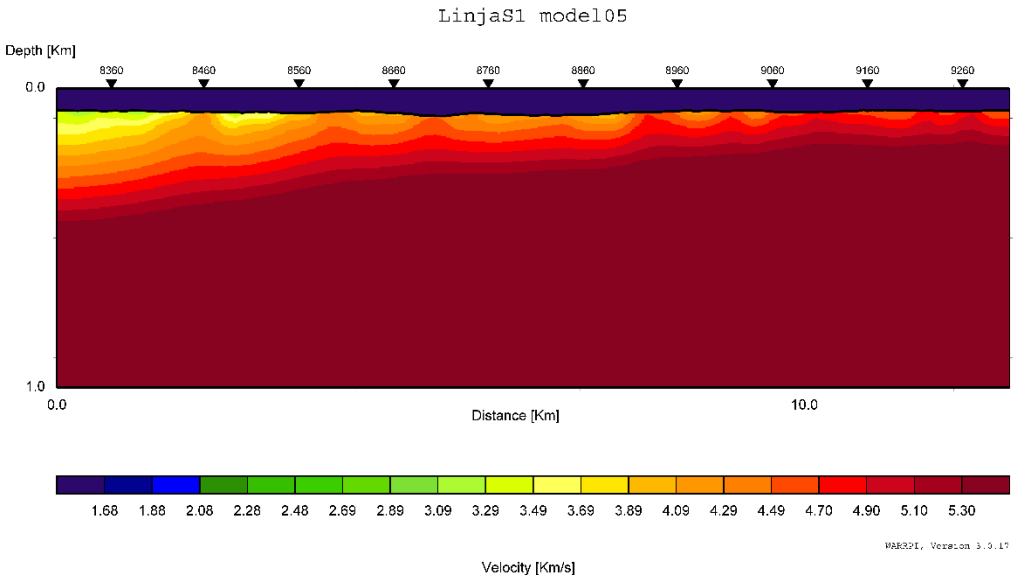

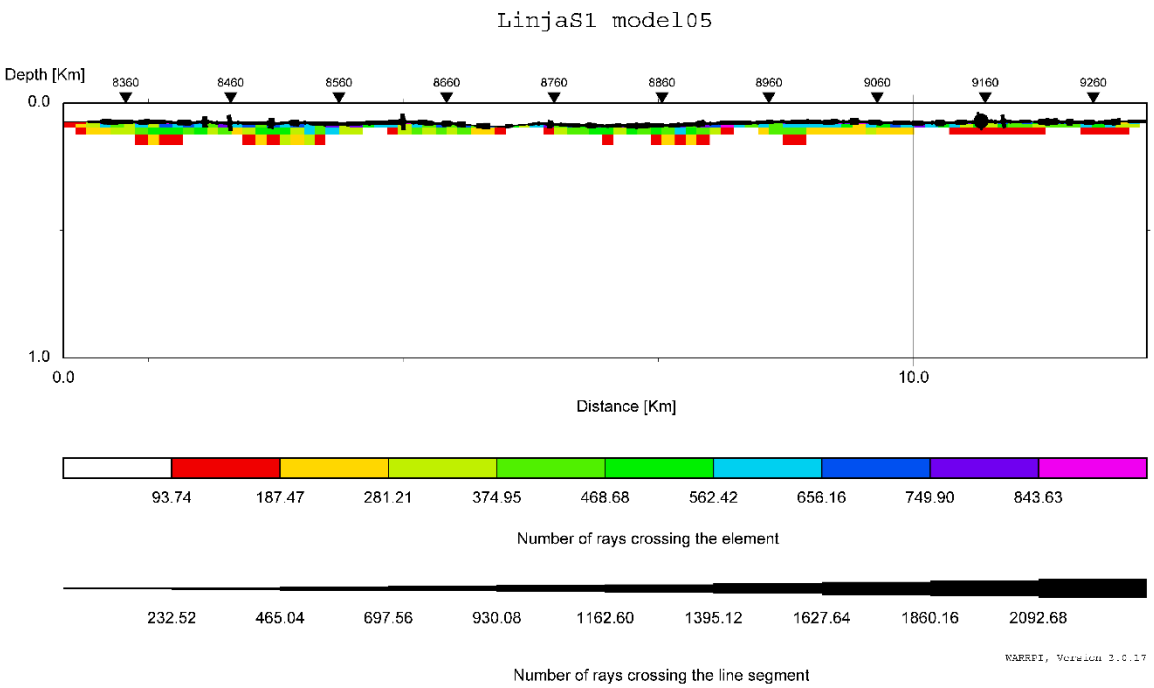
LinjaS1 model05
Depth [Km]
0.0
1.0
8360
8460
8560
8660
8760
8860
8960
9060
9160
9260
0.0
10.0
Distance [Km]
93.74
187.47
281.21
374.95
468.68
562.42
656.16
749.90
843.63
Number of rays crossing the element
232.52
465.04
697.56
930.08
1162.60
1395.12
1627.64
1860.16
2092.68
Number of rays crossing the line segment

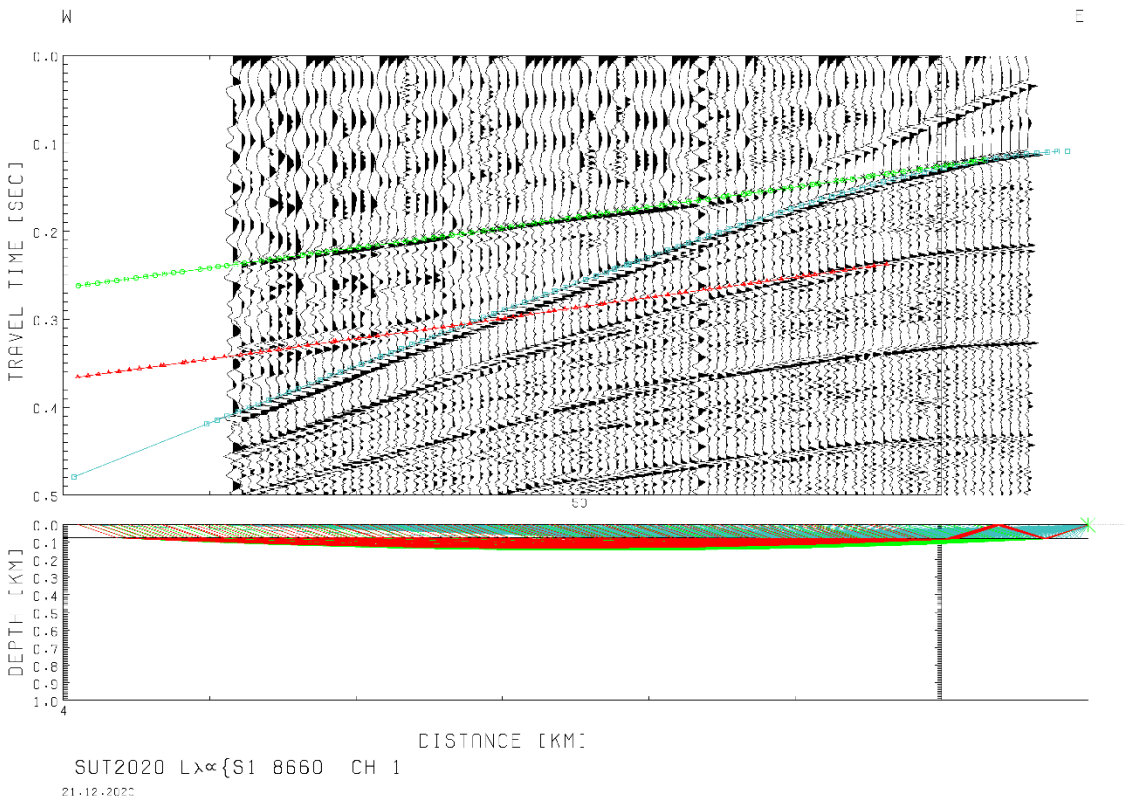
W
E
TRAVEL TIME [SEC]
DEPTH [KM]
DISTANCE [KM]
SUT2020 Lx{S1 8660 CH 1

LinjaG1

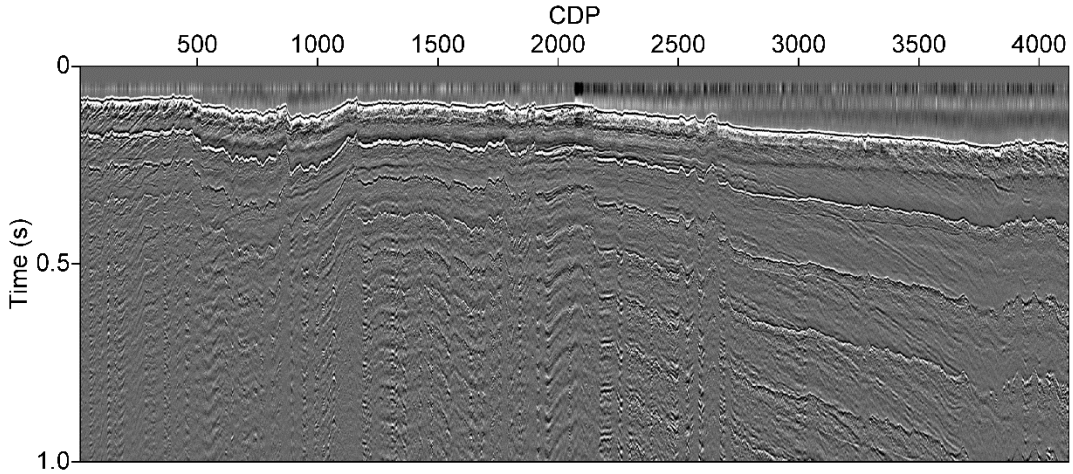

SUT2020_LinjaG1 model09layer01a

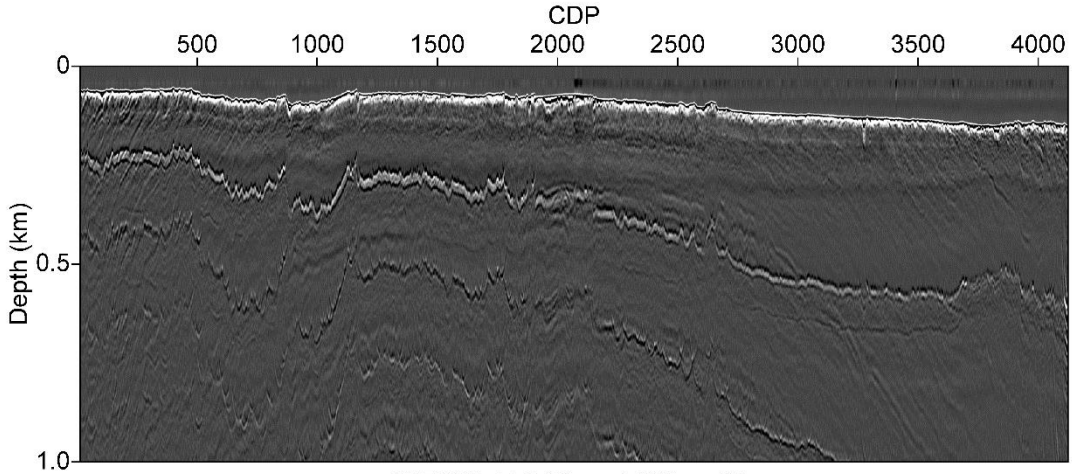

SUT2020_LinjaG1 model09layer01a

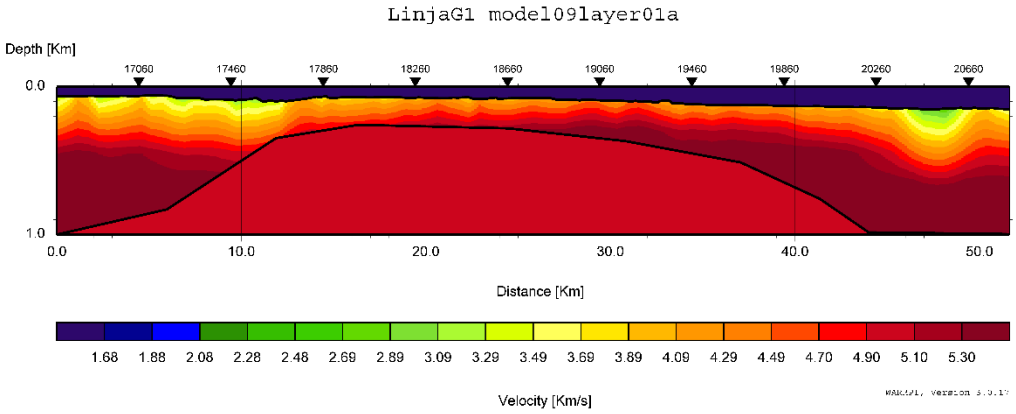

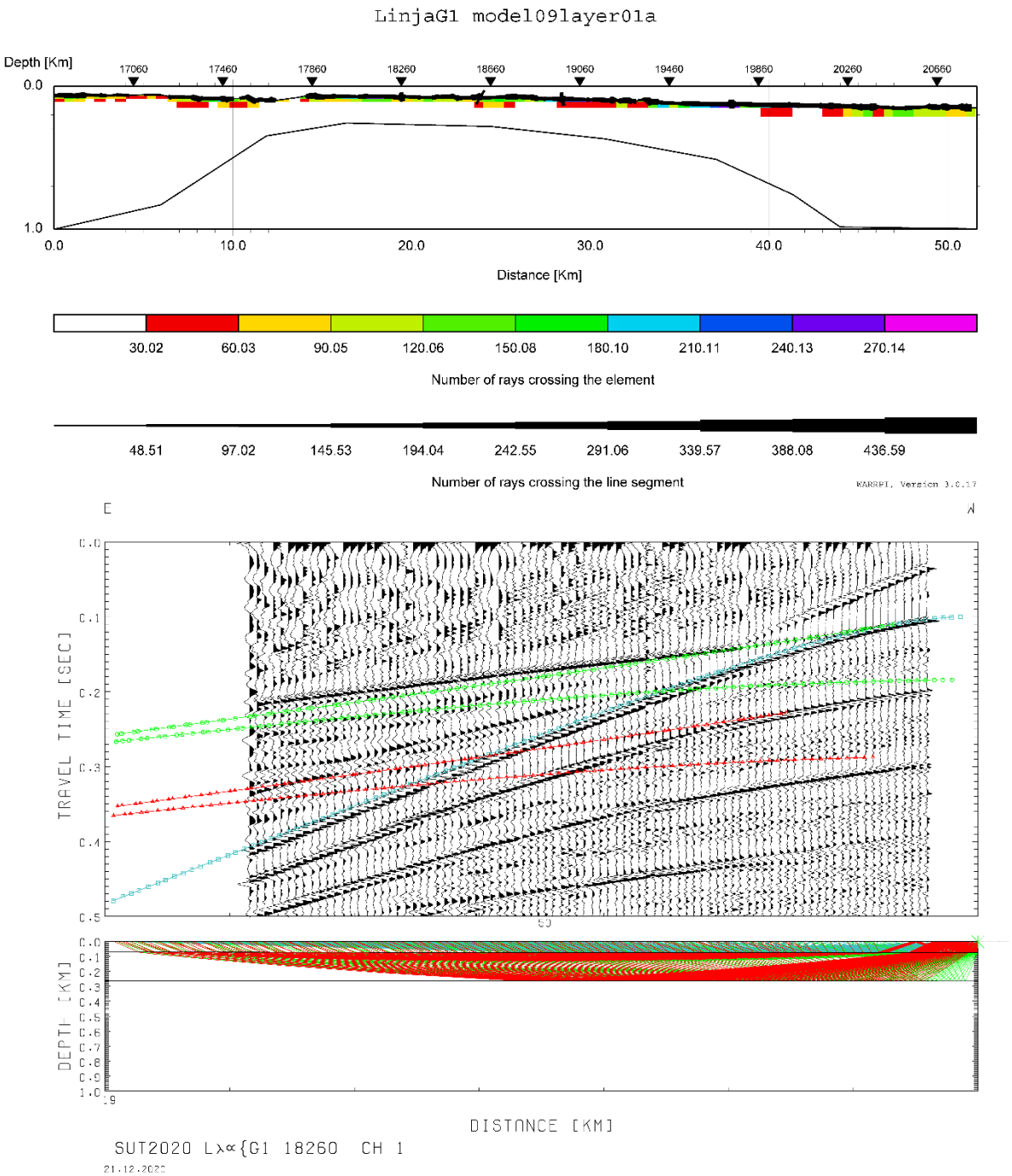
LinjaG1 model09layer01a
Depth [Km]
17060
17460
17860
18260
18660
19060
19460
19860
20260
20660
0.0
1.0
0.0
10.0
20.0
30.0
40.0
50.0
Distance [Km]
30.02
60.03
90.05
120.06
150.08
180.10
210.11
240.13
270.14
Number of rays crossing the element
48.51
97.02
145.53
194.04
242.55
291.06
339.57
388.08
436.59
Number of rays crossing the line segment
TRAVEL TIME [SEC]
DEPTH [KM]
DISTANCE [KM]
SUT2020 L×∝{G1 18260 CH 1

LinjaQ

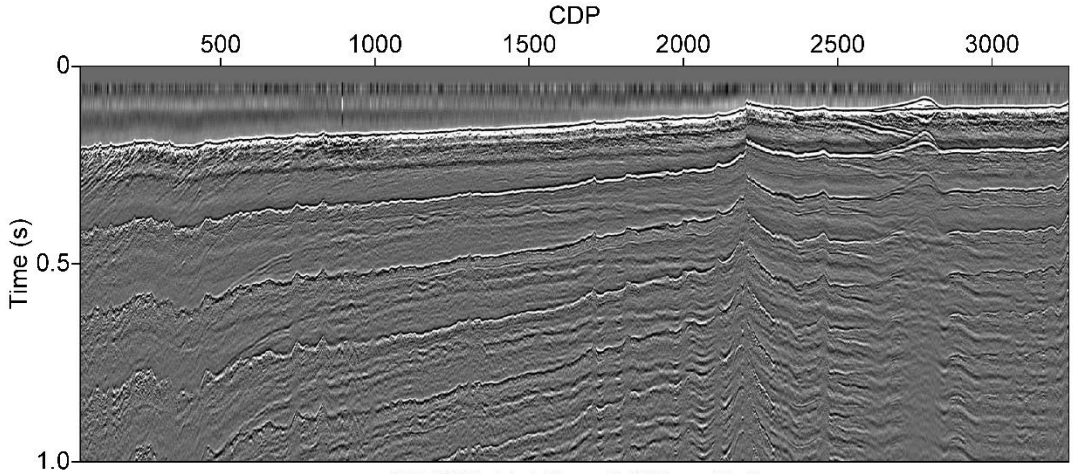

SUT2020_LinjaQ model08layer01a2

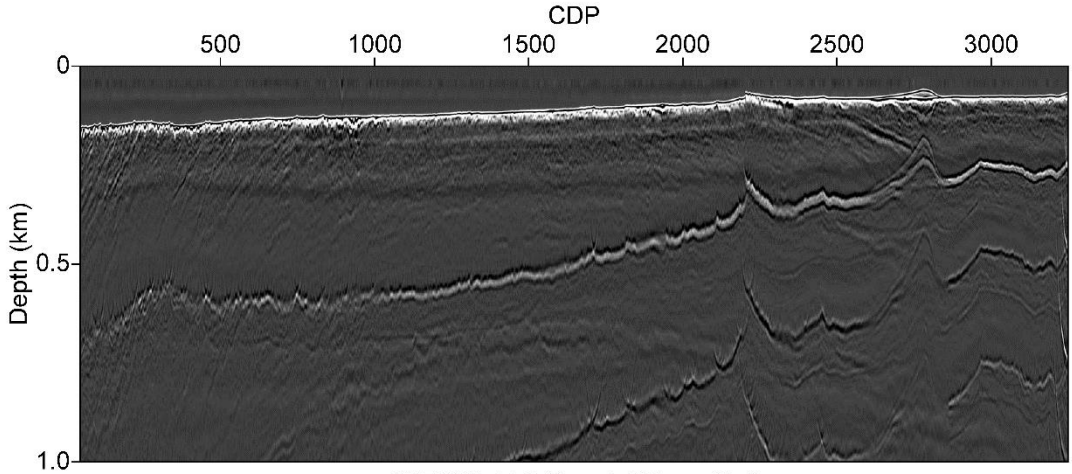

SUT2020_LinjaQ model08layer01a2

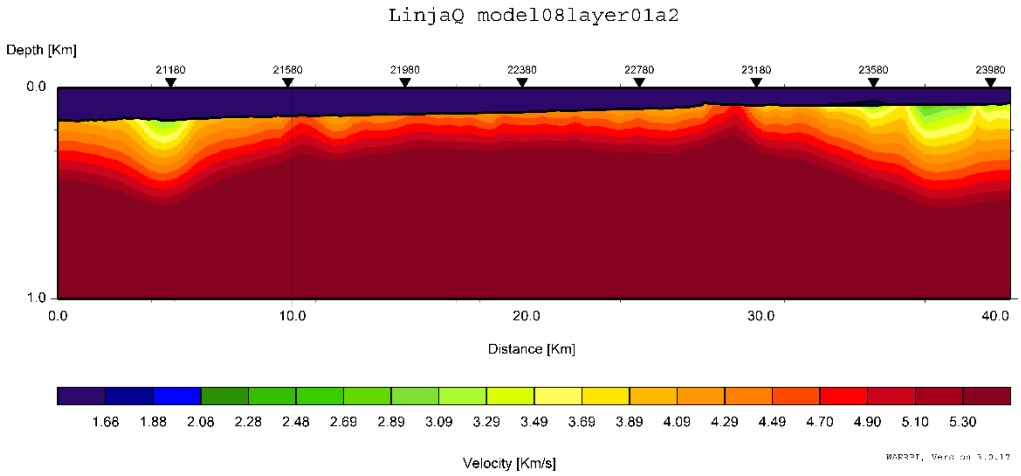

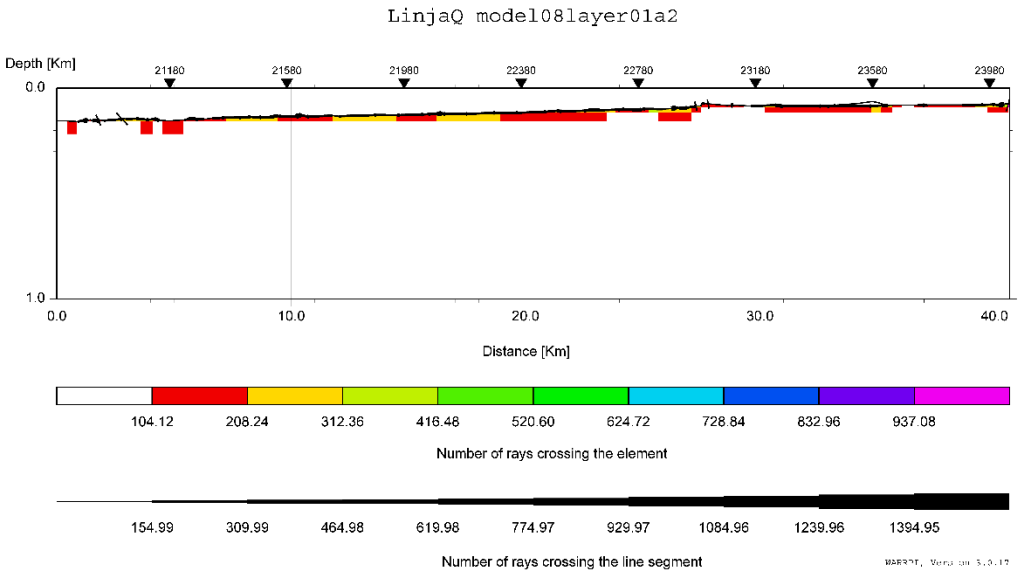
LinjaQ model08layer01a2
Depth [Km]
21180
21580
21980
22380
22780
23180
23580
23980
0.0
1.0
0.0
10.0
20.0
30.0
40.0
Distance [Km]
104.12
208.24
312.36
416.48
520.60
624.72
728.84
832.96
937.08
Number of rays crossing the element
154.99
309.99
464.98
619.98
774.97
929.97
1084.96
1239.96
1394.95
Number of rays crossing the line segment

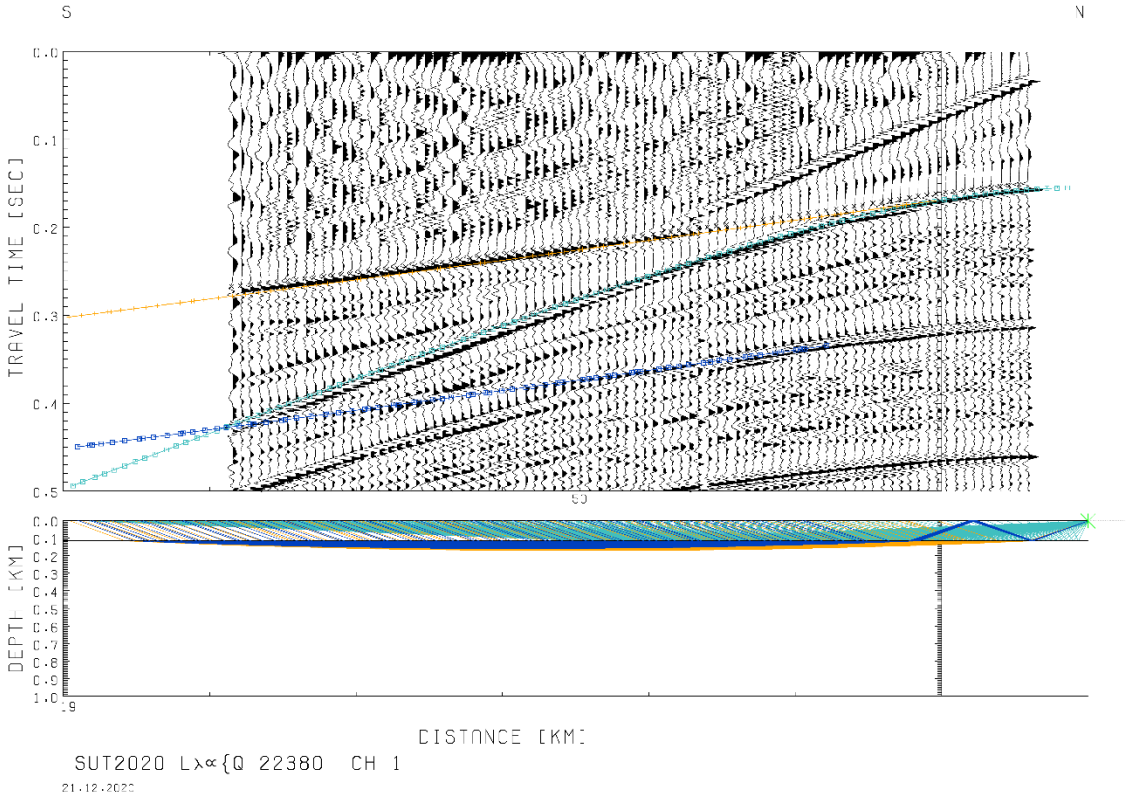
S
N
TRAVEL TIME [SEC]
0.0
0.1
0.2
0.3
0.4
0.5
50
DEPTH [KM]
0.0
0.1
0.2
0.3
0.4
0.5
0.6
0.7
0.8
0.9
1.0
DISTANCE [KM]
SUT2020 LinjaQ 22380 CH 1
21.12.2020

LinjaR

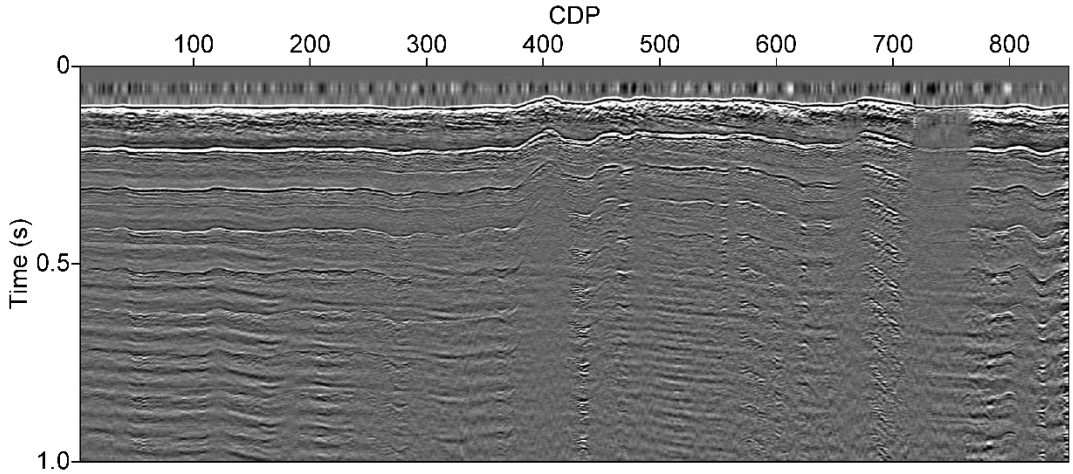

SUT2020_LinjaR model04

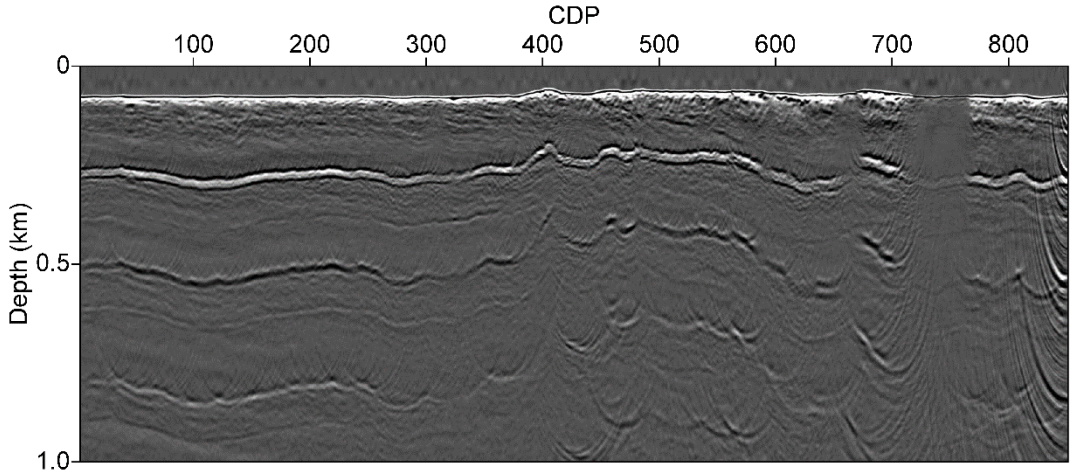

SUT2020_LinjaR model04

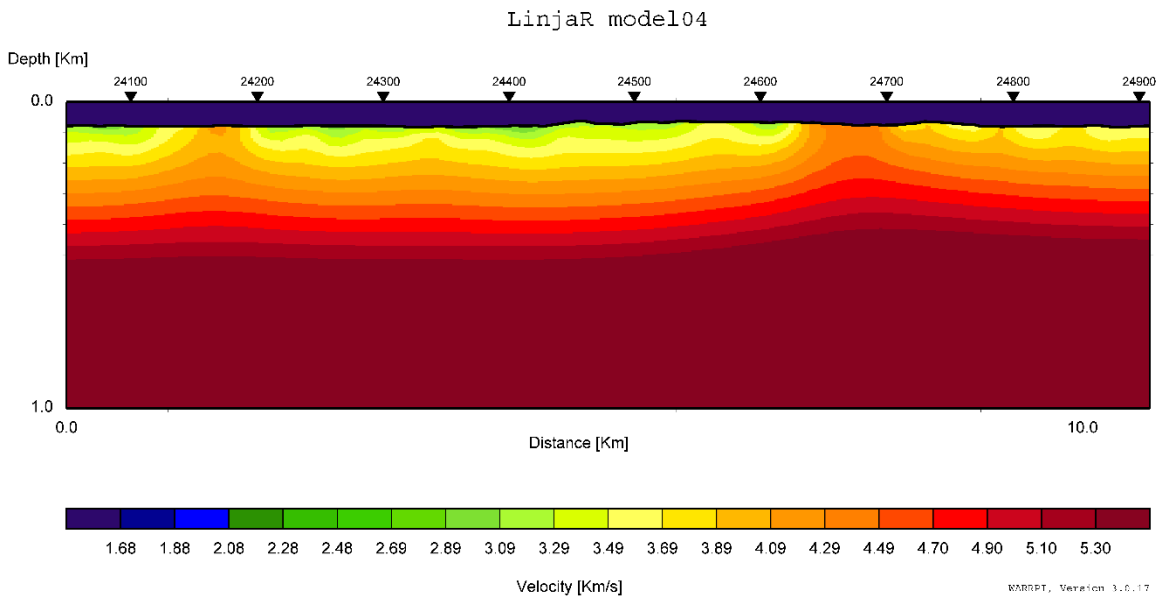

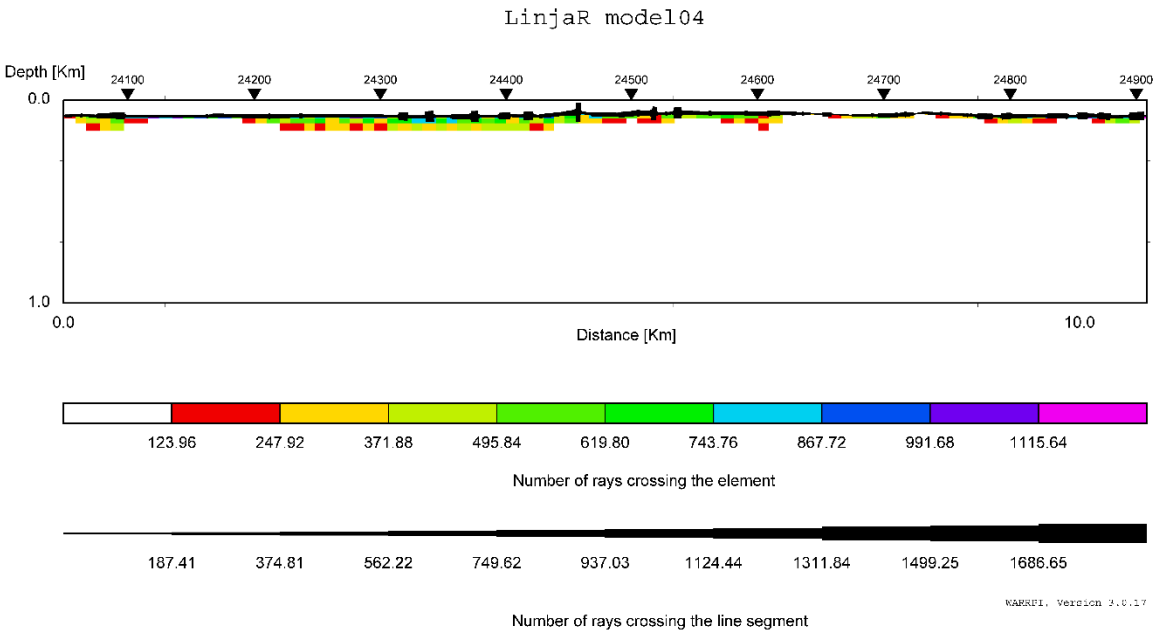
LinjaR model04
Depth [Km]
0.0
1.0
24100
24200
24300
24400
24500
24600
24700
24800
24900
0.0
10.0
Distance [Km]
123.96
247.92
371.88
495.84
619.80
743.76
867.72
991.68
1115.64
Number of rays crossing the element
187.41
374.81
562.22
749.62
937.03
1124.44
1311.84
1499.25
1686.65
Number of rays crossing the line segment

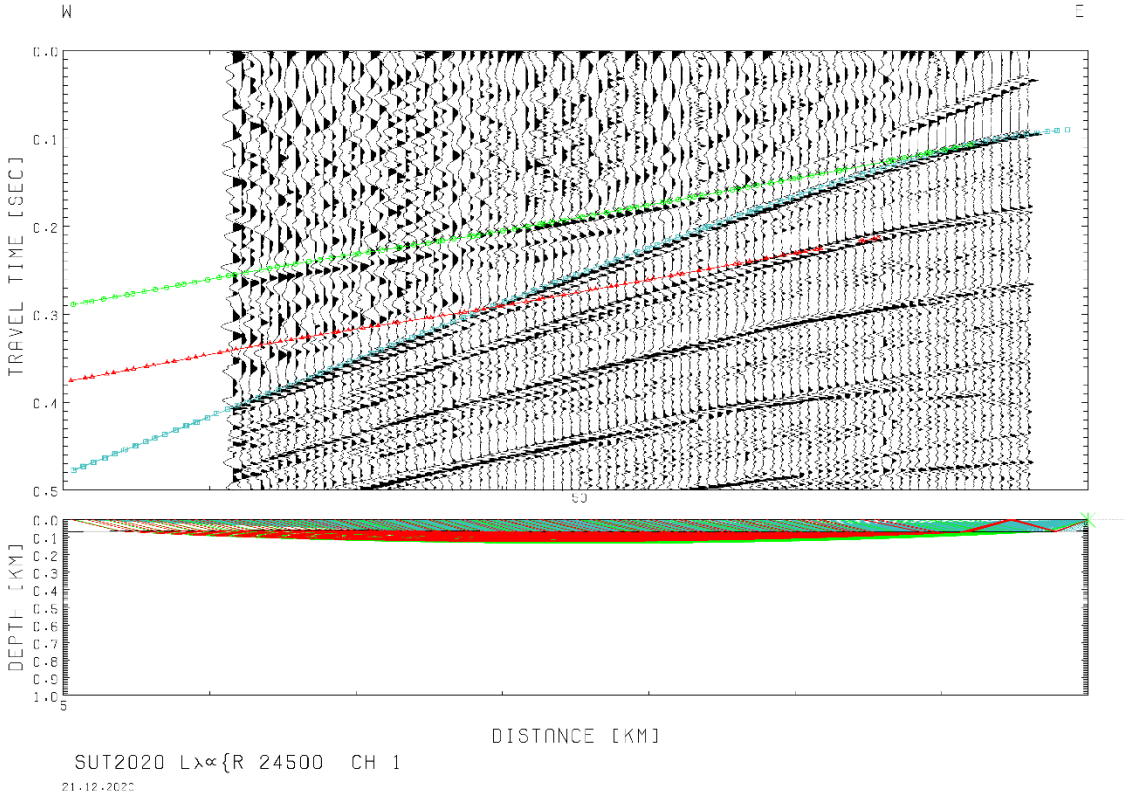
W
E
TRAVEL TIME [SEC]
DEPTH [KM]
DISTANCE [KM]
SUT2020 LλαR 24500 CH 1

LinjaO1

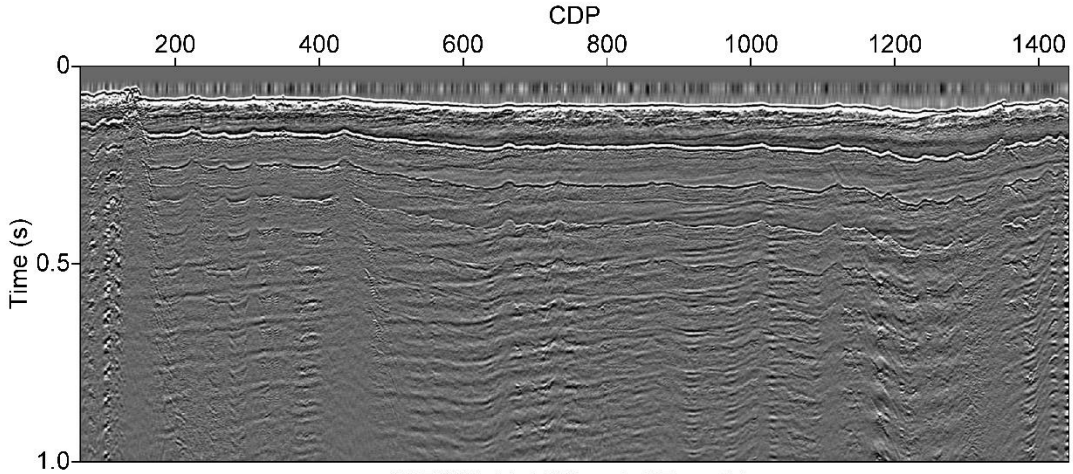

SUT2020_LinjaO1 model07layer04a

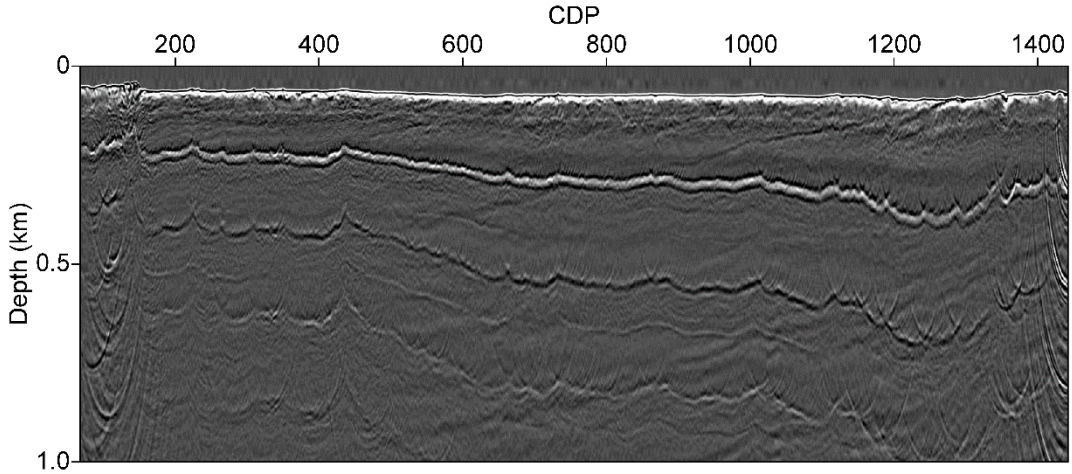

SUT2020_LinjaO1 model07layer04a

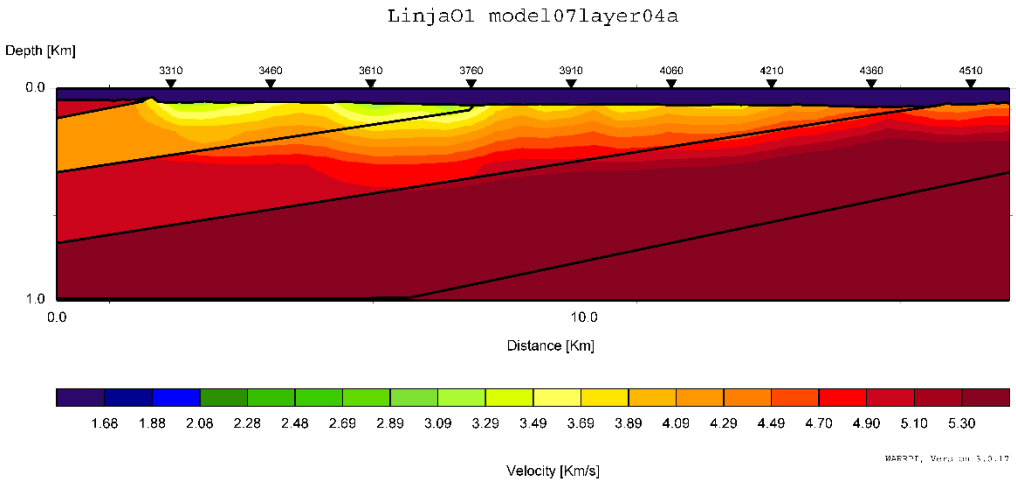

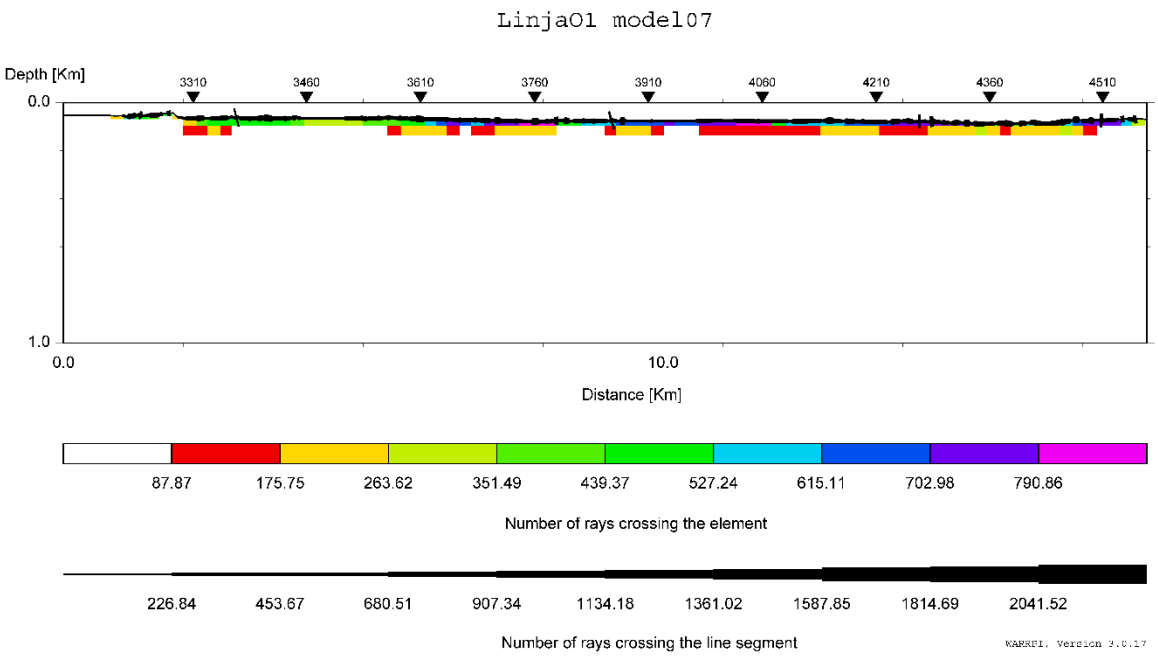
Linja01 model07
Depth [Km]
0.0
1.0
3310
3460
3610
3760
3910
4060
4210
4360
4510
0.0
10.0
Distance [Km]
87.87
175.75
263.62
351.49
439.37
527.24
615.11
702.98
790.86
Number of rays crossing the element
226.84
453.67
680.51
907.34
1134.18
1361.02
1587.85
1814.69
2041.52
Number of rays crossing the line segment

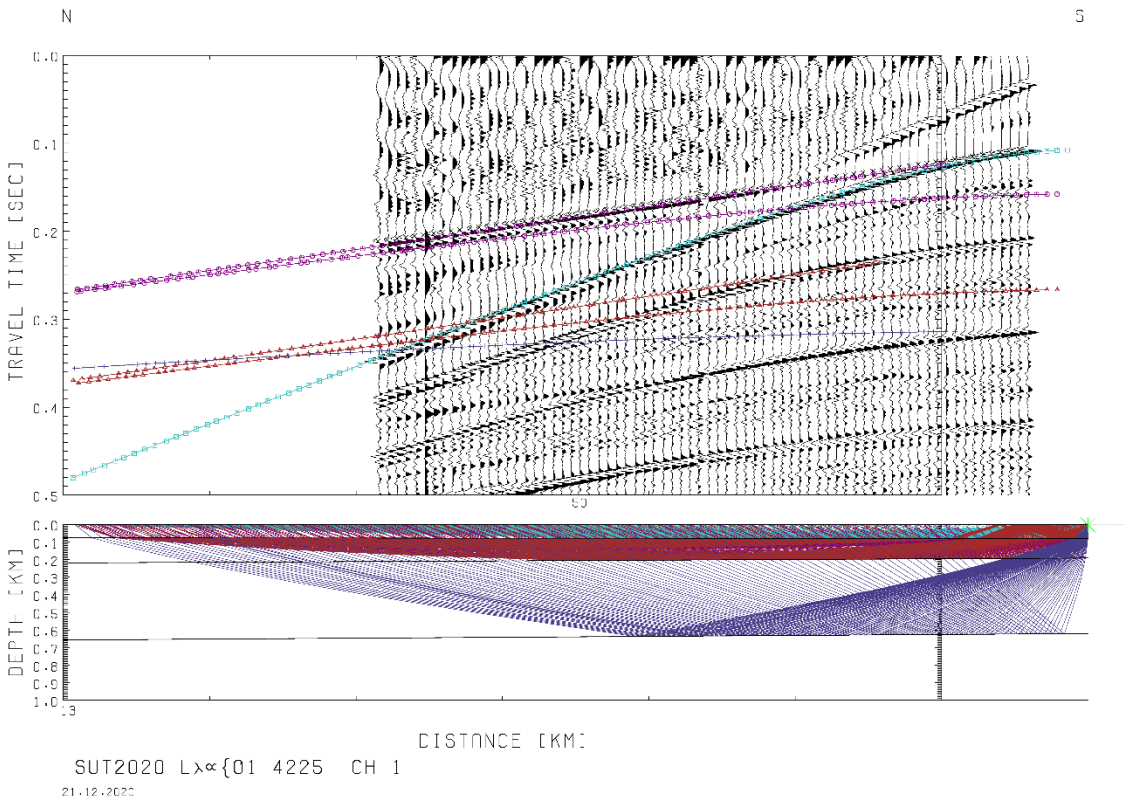
N
S
TRAVEL TIME [SEC]
DEPTH [KM]
DISTANCE [KM]
SUT2020 Lx{01 4225 CH 1

Final comments

The stacked data, depth migrated data, and velocity profiles are loaded into Petrel. Figure 20 and 21 show examples of interpretation that can be tied over several profiles.

The seismic profiles will, together with onshore observations and information from drillholes, form the basis for the geological report for the Suðuroyar tunnel. However, a few very interesting observation from the data will be mentioned here.

Between Sandoy and Skúvoy there is an about 50 m deep sedimentary basin in the approximate location of the planned tunnel profile, while between Skúvoy and Suðuroy there are no indications of significant sedimentary overburden.

The velocity profiles show a velocity distribution along the seabed that corresponds to the expected velocity distribution of the stratigraphic sequence previously derived from velocity logs Vestmanna and Glyvursnes (Petersen, 2011, 2014; Petersen et al., 2013). This could form a basis for further analysis to be used for predicting rock quality along the tunnel profile.

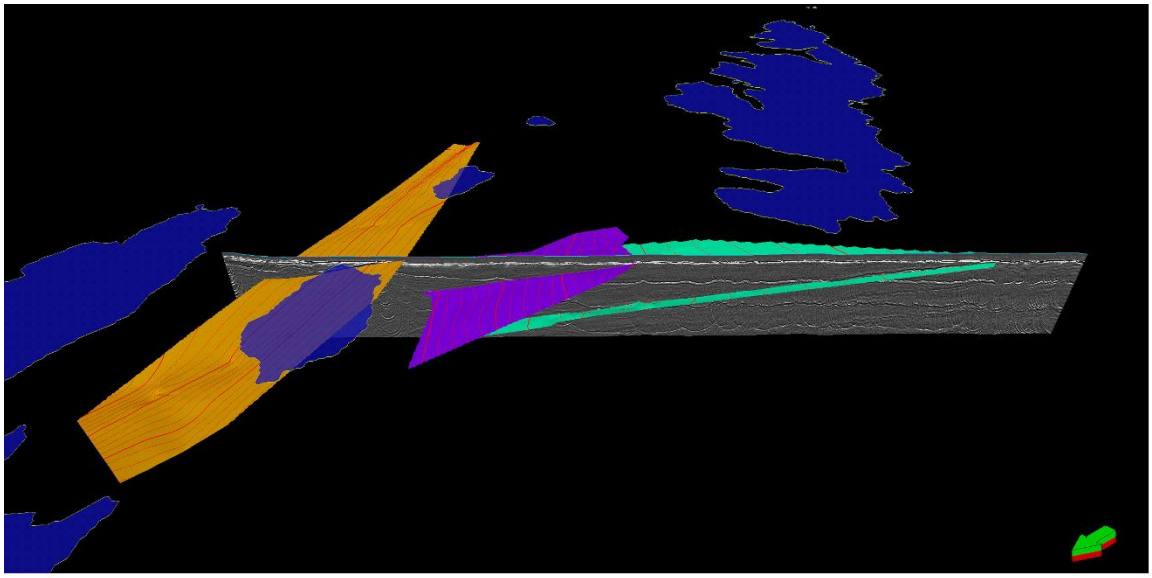

Figure 20. LinjaL with examples of interpretation.

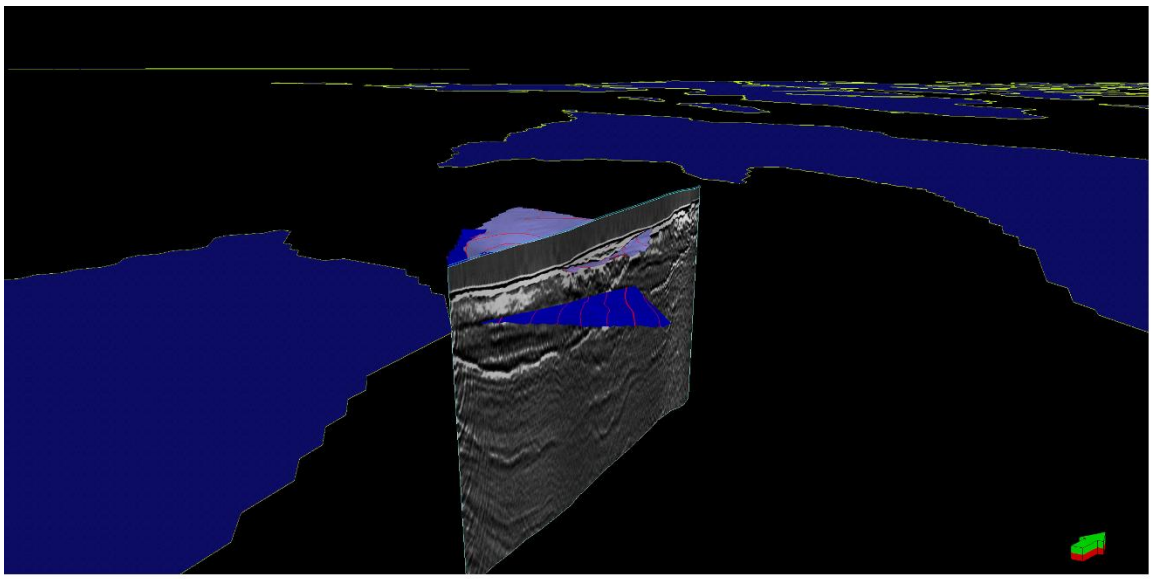

Figure 21. Linjal with examples of interpretation.

Data delivery

Stacked data

Filename	Size
SUT2020_LinjaAmodel04stack.xycdp.twt.sgy	7.7M
SUT2020_LinjaBmodel04layer03astack.xycdp.twt.sgy	3.6M
SUT2020_LinjaC1model04layer05editastack.xycdp.twt.sgy	6.3M
SUT2020_LinjaDmodel03layer06bastack.xycdp.twt.sgy	5.2M
SUT2020_LinjaFmodel05layer02a2stack.xycdp.twt.sgy	24M
SUT2020_LinjaG1model09layer01astack.xycdp.twt.sgy	48M
SUT2020_LinjaHmodel04layer03astack.xycdp.twt.sgy	3.5M
SUT2020_LinjaImodel04layer03astack.xycdp.twt.sgy	3.5M
SUT2020_LinjaJmodel05stack.xycdp.twt.sgy	9.5M
SUT2020_LinjaKmodel05stack.xycdp.twt.sgy	9.7M
SUT2020_LinjaLmodel05layer01a2stack.xycdp.twt.sgy	25M
SUT2020_LinjaMmodel05stack.xycdp.twt.sgy	10M
SUT2020_LinjaO1model07layer04astack.xycdp.twt.sgy	16M
SUT2020_LinjaPmodel04layer05astack.xycdp.twt.sgy	4.2M
SUT2020_LinjaQmodel08layer01a2stack.xycdp.twt.sgy	37M
SUT2020_LinjaRmodel04stack.xycdp.twt.sgy	9.8M
SUT2020_LinjaS1model05stack.xycdp.twt.sgy	12M
SUT2020_LinjaT1model05stack.xycdp.twt.sgy	4.6M
SUT2020_LinjaU1model05layer03astack.xycdp.twt.sgy	9.6M

Depth migrated data

Filename	Size
SUT2020_LinjaAmodel04mig.xycdp.dm.sgy	812K
SUT2020_LinjaBmodel04layer03amig.xycdp.dm.sgy	1.3M
SUT2020_LinjaC1model04layer05editamig.xycdp.dm.sgy	2.3M
SUT2020_LinjaDmodel03layer06bamig.xycdp.dm.sgy	1.9M
SUT2020_LinjaFmodel05layer02a2mig.xycdp.dm.sgy	17M
SUT2020_LinjaG1model09layer01amig.xycdp.dm.sgy	17M
SUT2020_LinjaHmodel04layer03amig.xycdp.dm.sgy	1.3M
SUT2020_LinjaImodel04layer03amig.xycdp.dm.sgy	1.3M
SUT2020_LinjaJmodel05mig.xycdp.dm.sgy	6.5M
SUT2020_LinjaKmodel05mig.xycdp.dm.sgy	6.7M
SUT2020_LinjaLmodel05layer01a2mig.xycdp.dm.sgy	17M
SUT2020_LinjaMmodel05mig.xycdp.dm.sgy	6.8M
SUT2020_LinjaO1model07layer04amig.xycdp.dm.sgy	11M
SUT2020_LinjaPmodel04layer05amig.xycdp.dm.sgy	1.5M
SUT2020_LinjaQmodel08layer01a2mig.xycdp.dm.sgy	26M
SUT2020_LinjaRmodel04mig.xycdp.dm.sgy	6.7M
SUT2020_LinjaS1model05mig.xycdp.dm.sgy	7.9M
SUT2020_LinjaT1model05mig.xycdp.dm.sgy	3.2M
SUT2020_LinjaU1model05layer03amig.xycdp.dm.sgy	6.6M

Velocity models

Filename	Size
SUT2020_LinjaAmodel04vels.xycdp.dm.sgy	812K
SUT2020_LinjaBmodel04layer03avels.xycdp.dm.sgy	1.3M
SUT2020_LinjaC1model04layer05editavels.xycdp.dm.sgy	2.3M
SUT2020_LinjaDmodel03layer06bavels.xycdp.dm.sgy	1.9M
SUT2020_LinjaFmodel05layer02a2vels.xycdp.dm.sgy	17M
SUT2020_LinjaG1model09layer01avels.xycdp.dm.sgy	17M
SUT2020_LinjaHmodel04layer03avels.xycdp.dm.sgy	1.3M
SUT2020_LinjaImodel04layer03avels.xycdp.dm.sgy	1.3M
SUT2020_LinjaJmodel05vels.xycdp.dm.sgy	6.5M
SUT2020_LinjaKmodel05vels.xycdp.dm.sgy	6.7M
SUT2020_LinjaLmodel05layer01a2vels.xycdp.dm.sgy	17M
SUT2020_LinjaMmodel05vels.xycdp.dm.sgy	6.8M
SUT2020_LinjaO1model07layer04avels.xycdp.dm.sgy	11M
SUT2020_LinjaPmodel04layer05avels.xycdp.dm.sgy	1.5M
SUT2020_LinjaQmodel08layer01a2vels.xycdp.dm.sgy	26M
SUT2020_LinjaRmodel04vels.xycdp.dm.sgy	6.7M
SUT2020_LinjaS1model05vels.xycdp.dm.sgy	7.9M
SUT2020_LinjaT1model05vels.xycdp.dm.sgy	3.2M
SUT2020_LinjaU1model05layer03avels.xycdp.dm.sgy	6.6M

Appendix A

Field notes

Date:	13-07-2020	Marine Survey - General Information	Line:	0001 to
Cruise:	Suduroyartunnel	Ship: R/V Magnus Heinason	Location:	Faeroes Islands

GPS antenna		Refpoint ship (midt, agter spejl)		Gyro				Deck cable	Length stretch section	Length section (m)	Length section (m)	Length section (m)	Length section (m)	Length section (m)	Length section (m)	Length section (m)	Length section (m)	Length section (m)	Length section (m)	Length section (m)	Length section (m)
X (m)	4,6	X (m)	0,00	X (m)	0,00			25	50	50	50	50	50	50	50	50	50	50	50	50	50
Y (m)	21	Y (m)	0,00	Y (m)	21,00	Serial no. depth transducer 6,25 m section				5008	5022	5018	5001	5006	5004	5020	5019	5009	5016	5002	5010
Z (m)	0	Z (m)	0,00	Z (m)	0,00	Front/Tail				Front	Front	Front	Tail	Tail	Front	Tail	Tail	Front	Tail	Front	Tail
		Airgun		Streamer		Bird S/N				14610		14514	14510				14497				26567
		SB towpoint		BB towpoint																	
X (m)		X (m)	2,60	X (m)	-2,60	Navigation:				Transformation parameters:											
Y (m)		Y (m)	0,00	Y (m)	0,00	Software:	NaviPac ver 4.2.3			Semimajor axis (m):		6378137	Longitude at Origin		09° 0' 0.0"						
Z (m)		Z (m)	0,00	Z (m)	0,00	Projection:	UTM north, Zone 29			Inverse flattening:		298,2572	Latitude at Orgin		0° 00' 0.0"						
Tow length (m)		Tow length (m)		Tow length (m)		Datum:	WGS84			Scale at Origin		0,9996	False easting (m):		500000						
		-32		-52									False northing (m):		0						

Seismic Energy Source:		Seismic Instruments:		Streamer:	
Type 1:	Sercel GI gun	Type:	Geometrics GeoEel contoller	Type:	Geometrics GeoEel
Serial no. GI-Gun:	44212	Lowcut filter (Hz):	out	Length of tow section (m):	30
Volume G (cu.inch):	45	Lowcut filt. (dB/Oct):	out	Length of live section (m):	50,0
Volume I (cu.inch):	45	Highcut filter (Hz):	anti-alias	No. of live sections:	12
Injector delay	34mS	Highcut filt. (dB/Oct):	anti-alias	No. of channels:	96
Discharge port	603_120, Medium	Gain Setting (dB):	0	No. of channels/live section:	8
Delay	50 mS	Sample Rate (ms):	1	channel interval (m):	6.25 m
Pressure (bar):	120	Record Length (ms):	3000	No. of hydrophones/channel:	8
Planned depth (m):	3	No of recording chs:	96	Hydrophone type	Geopoint
		Software version	5.844	Planned depth (m):	3
		No of auxilliary chs:	4	Vib/Stretch section	25
		Nearfield hydrophone	Aux 2	Length from Tail GPS to last ch (m)	25
		Data format	Seg-D		

Remarks:

Airgun and streamer positions from Remote GPS, with RTK, stored in SEG-D header
Streamer depth scanned on every shot.
Events set to trigger every 12.5 m
Ch 37 virker ikke

Airgun positions calculated in NaviPac as drag from the BB towpoint
Streamer depth scanned on every shot.
Events set to trigger every 12.5 meter

Serial string from NaviPac to SEG-D header, "Time, Event, X, Y (airgun), X, Y (tail bouy), X, Y vessel pos".
navi event: start byte 142 i6
airgun utm x : start byte 148 f9.2
airgun utm y : start byte 158 f10.2

References

Petersen, U. K. (2011). Horizontal and vertical velocity distribution of basalt flows, located in the Enni Formation at Glyvursnes, obtained from refraction seismic analysis *Report* (Vol. Sindri C46-49-01). Tórshavn: Jarðfeingi.

Petersen, U. K. (2014). *Propagation and scattering of reflection seismic waves in a basalt succession.* (PhD thesis), University of the Faroe Islands, Tórshavn. (NVDRit 2014:01) doi: 10.13140/RG.2.1.1133.1927

Petersen, U. K. (2015). The Sandoy subsea tunnel: Seismic processing report; Report to P/F Eystur- og Sandoyartunlar (Vol. 2). Tórshavn: Jarðfeingi.

Petersen, U. K. (2016). The high resolution marine seismic survey 2007; The Skálafjarðar subsea tunnel: Seismic processing report (Vol. 1). Tórshavn: Jarðfeingi.

Petersen, U. K., Brown, R. J., & Andersen, M. S. (2013). P-wave velocity distribution in basalt flows of the Enni Formation in the Faroe Islands from refraction seismic analysis. *Geophysical Prospecting, 61*, 168–186. doi: 10.1111/j.1365-2478.2012.01065.x

Petersen, U. K., Brown, R. J., & Andersen, M. S. (2015). *Geophysical aspects of basalt geology and identification of intrabasaltic horizons.* Paper presented at the Faroe Islands Exploration Conference: Proceedings of the 4th Conference, Tórshavn, Faroe Islands. doi: 10.13140/RG.2.1.2387.9765

JARÐFEINGI

Jóannesar Paturssonargøta 32-34

100 Tórshavn

Føroyar